structure and evolution of soap-like foams

Marco Mancini

ECOLE DOCTORALE SCIENCES ET INGENIERIE
De l'Université de Cergy-Pontoise

THESE

Présentée pour obtenir le grade de docteur de l'université de Cergy-Pontoise

Spécialité: Physique Théorique

Structure and Evolution of Soap-Like Foams

par

Marco Mancini
Laboratoire de Physique Théorique et Modélisation (UMR 8089)

le 13 Juillet 2005

Devant le jury composé de:

Prof. Rivier Nicolas	Président
Prof. Denis Weaire	Rapporteur
Prof. Renaud Delannay	Rapporteur
M. Christophe Oguey	Directeur de thèse
Prof. François Dunlop	Directeur de thèse
Prof. Jean-Marc di Meglio	Examinateur

Abstract

Starting from the laws which characterize the pseudo–equilibrium of two and three–dimensional liquid dry foams, we study theoretically some specific problems concerning: the contact of a foam with a solid boundary, the properties of invariance of the equilibrium equations, the geometrical consequences of the equilibrium on a group of bubbles and the coarsening. The main tool which we use to study foams is the geometry of the bubbles implied by the equilibrium.

Considering the pattern formed by a liquid foam in contact with a solid surface, it can can be regarded as a two–dimensional foam on the surface. We derive the equilibrium equations for this 2D foam where the solid surface is curved and smooth, generalising the standard case of flat Hele–Shaw cells. The equilibrium conditions at the vertices in 2D, at the edges in 3D, are invariant by conformal transformations. Considering foams confined in thin interstices between two non parallel plates, normal incidence and Laplace's law lead to an approximate equation relating the plate profile to a conformal map. We solve this equation in the constant pressures setting for mappings corresponding to the logarithm and power laws. In the case of constant volume, we compare our theoretical result with the available experimental data, making some prediction about the pressure field. These results are given in:

- M. Mancini and C. Oguey, *Foams in contact with solid boundaries: Equilibrium conditions and conformal invariance*, Eur. J. Phys. E, **17**, 119-128 (2005).

- M. Mancini and C. Oguey, *Equilibrium conditions and symmetries for foams in contact with solid surfaces*, Colloids and Surfaces A: Physicochemical and Engineering Aspects, **263**, 33-38 (2005).

Considering a three–sided bubble in equilibrated 2D flat dry foam, we furnish the proof that replacing this bubbles by the prolongation of the films meeting on it, the obtained foam is also equilibrated (star–triangle equivalence). This property is verified also in the case of non–standard foams, where the line tension can change from a film to another. Star–triangle equivalence implies that the topological change T2(3), during gas diffusion, is a continuous process. Moreover,

$\curlywedge\!-\!\triangle$ equivalence implies as corollary the *decoration* theorem of Weaire. $\curlywedge\!-\!\triangle$ is proved in:

- M. Mancini and C. Oguey, *Star–Triangle equivalence in two–dimensional soap froths*, Phil. Mag. Lett. **83**, 10, 643 (2003).

We have proved star–triangle equivalence also in the case of 3D spherical foams. As spherical foam is usually a good approximation for vanishing bubbles, this implies that this phenomenon can be considered as continuous.

The text contains some other unpublished works. We provide the equilibration of a two–bubbles cluster and we give the exact solutions of von Neumann's equations for this cluster. This we allows to give an equation for the variation of the perimeter for a cluster made of an arbitrary number of bubbles. The evolution of the two–bubble cluster is resolved also in three dimensions.

In the case of a two–dimensional foam defined on a surface embedded in the 3D–space we find again the generalization of von Neumann's law.

Contents

Introduction

Je n'y pouvais rien. D'ailleurs,
il faut bien que cela arrive tôt
ou tard, qu'on vous classe.
L-F Céline.

To speak about foam is not very simple. Although anyone has an idea of what foam is, to give a coherent and unique definition of foam is already a problem. For example, shaving cream and bread, though they are very different products, are both foams. The most general definition of foam could be that which defines the foam as a binary system formed by two immiscible phases, called *dispersed* phase and the *continuous* phase. The dispersed phase takes up regions of the space, the bubbles, which are enclosed by the continuous phase. This latter has a volume fraction much smaller than the dispersed phase. Around the bubbles, the continuous phase forms a skeleton of communicating tubes. A foam can be regarded either as a discrete aggregate of bubbles or as connected network of films. The two points of view are complementary and, depending on the considered problems, one of the two views it used. Depending on the materials which are used for the two phases, different types of foams are obtained. The main typologies of foams are shown in the table 1. Although aqueous foams are

FOAM/PHASES	continuous	dispersed
Aqueous	liquid	gas
Solid	solid	gas
Liq/Liq	liquid	liquid

Table 1: Typologies of foams.

the most common type of foams (most people come in contact with foams on a daily basis; foams are commonly formed from washing clothing, dishes, hair, and in other ways) other typology of foams exist. In non–aqueous foams, the continuous phase could consist of highly viscous fluids or a solid (solid foams). An example of solid foams (aluminium foam) is shown in figure 1. In others cases

the dispersed phases could be another liquid (liquid/liquid foams). Although there are differences between aqueous and non–aqueous foams, ideally the same basic theories should apply to both types.

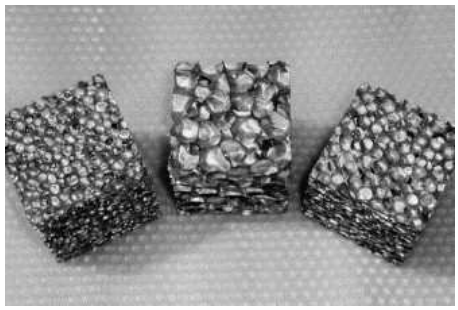

Figure 1: Alluminum foam.

Many examples of foams are found in nature: the magma foam (aqueous foam) in the magma chambers, which can lead to explosive volcanic eruptions, the skeleton of a sponge (solid foam) or the sea foam.

In the last decades, the study of foams has been strongly intensified. This increasing interest in foams is due prevalently to the fact that the applications in modern industrial processes involving foams have grown dramatically. Foams are used:

- In the oil industry, in enhanced oil recovery and drilling.
- In chemical engineering, to separate impurities (foam flotation and filtration).
- To create materials, by solidification of liquid foams, used for insulation and construction (polymer foams).
- In fire–fighting.
- In the personal care industry.
- In textile and paper processing.
- In the food industry.
- Insulation systems.
- Aerospace industry.

The success of the foams in these applications is due mainly to the ability to coat surfaces without immediately running away and cover a big volume minimizing the drying. For some references see [WH99, PE96].

In this thesis we will treat meanly aqueous foams (or liquid foam or soap foams). In soap foams, the dispersed phase is a gas which forms some regions, called *bubbles* or cells, separated one from the other by the dispersed phase which is a liquid. Liquid foams are broadly divided into 'wet' and 'dry', depending on the proportion of liquid contained in them. In wet foams (where the liquid volume fraction is typically between 10% and 20%) the bubbles are approximately spherical while, in dry foams (where the volume fraction of liquid is less than 10%), the bubbles are more polyhedral in shape. In dry foams, the thin films forming the faces of the roughly polyhedral bubbles are called lamellae. A film consists of a thin layer of liquid interposed between two gas/liquid interfaces. The "tubes" of liquid at the junctions of these films are called *Plateau borders*. The vertices where typically four Plateau borders meet are called *nodes*. An example of foam is given in figure 2, in the top part of the photo the foam is dry: the liquid is drained toward the bottom part by the gravity. In the bottom part, the bubbles have spherical shapes, more liquid is present and the foam is wet.

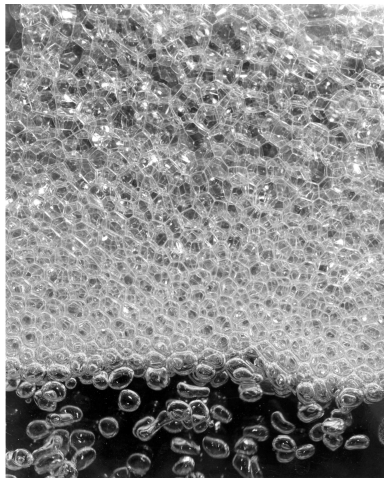

Figure 2: Example of aqueous foam: dry foam (top) and wet foam (bottom).

The existence of foams is due to the fact that when two non–miscible fluids are in contact, the contribution of this contact to the energy of the system is proportional to the area of the contact surface (surface energy). The proportionality factor is called the *surface tension*. If some energy is furnished to the system, the exceeding energy can be trapped in the form of surface energy and the contact surface between the phases increases. There are many ways in which foams can be produced, including:

- the nucleation of gas bubbles in a liquid which is supersaturated;
- shaking or beating a liquid;
- blowing gas through a thin nozzle into a liquid;
- blowing gas into a liquid through a porous plug.

From the point of view of thermodynamics, foams are metastable systems and evolve spontaneously toward their destruction, coming back in a state where there is only a single surface of contact between the phases. Since foams are characterized by great surface energy, they evolve naturally toward state of lower energy, reducing in this way the contact surface and dissipating the exceeding energy as thermal energy. The disappearance of the liquid foams occurs by three fundamental phenomena:

- The coarsening or disproportionation. Driven by pressure gradient between the bubbles, the gas diffuses through the films. The gas flows out from small bubbles, which have greater pressure, toward big bubbles (with small pressure). So big bubbles grow and small bubbles disappear.
- The coalescence. When a film break, the two bubbles which are separated by this film form a single bubble. The collapse of a film implies the instability on the structure of the local equilibrium of neighbouring bubbles. This instability can cause other film ruptures. So, avalanches of film ruptures can occur [BCT$^+$95, VLDB01, VL01].
- In presence of gravity, the liquid of the continuous phase, which is heavier than the gas, is drained toward the bottom of the foam. This process causes a reduction of the thickness of the films and so, it can cause the coalescence of the film and increase the gas diffusion.

Although foams are unstable and they are inevitably destined to disappear, their life time can be considerably increased by adding some surface–active agents to the continuous phase. These substances, called *surfactants*, reduce the surface tension of the interfaces between the two phases. In this way the energetic gap between the "foam state" and "non–foam state" is reduced too and the foam is more stable. More importantly, the surfactants stabilise the thin films against rupture. A molecule of a surfactant is amphiphilic: it has both a hydrophobic and a hydrophilic part. The hydrophobic part often has an organic structure, while the hydrophilic part contains a group which either has charges which separate when dissolved in water or is polar. At sufficiently high bulk concentrations, the surfactant molecules associate with each other in the bulk and form micelles. These are "balls" of surfactant molecules arranged in such a way that the hydrophobic "tails" are completely surrounded by hydrophilic "heads", see figure

3(a). Surfactant molecules prefer to be present at an interface, rather than remaining in the bulk. They arrange themselves so that the tail groups are in contact with the air, while keeping the head groups within the liquid, see figure 3(b). Adsorption of surfactant in this manner reduces the surface tension of the interface.

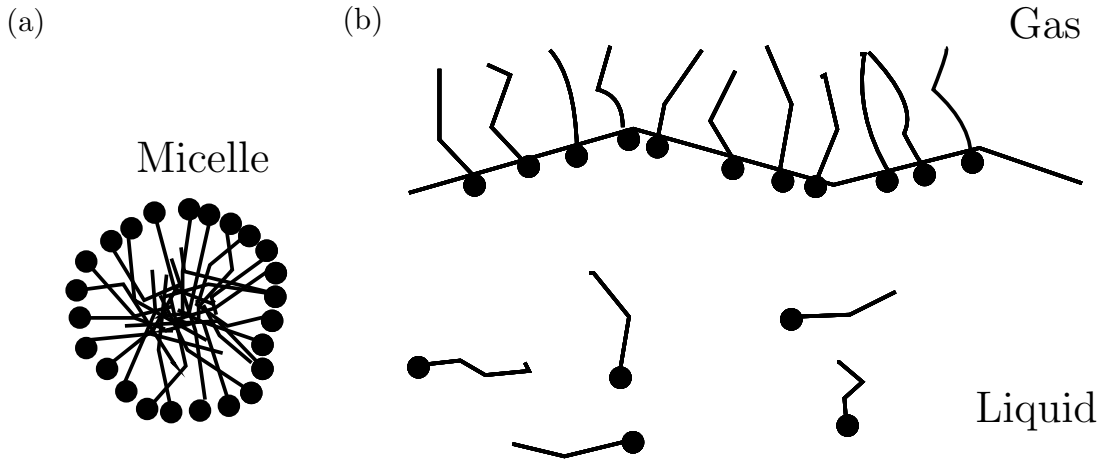

Figure 3: Surfactant molecules (a) forming a micelle and (b) at a free surface of contact.

Although coalescence, gas diffusion and drainage can be reduced, they can not be eliminated. Making experiments at zero gravity (in space or by zero gravity flies) the drainage of the liquid can be neglected. Diffusion can be reduced by choosing a gas with a very small dilution in the liquid.

These phenomena are present in the aqueous foams whereas they do not occur in solid foam at room temperature. This makes solid foams stable with respect to the time, however metastable in the energy.

Chapter 1

Three–Dimensional Ideal Dry Soap Foams

As we said in the introduction, a liquid foam is called dry when it has little liquid (the volume fraction ϕ of the continuous phase is smaller than 0.1). Almost all the foam volume is taken by gas cells and the bubbles have a polyhedral shape. The thickness of the films is so small, with respect to the linear size of the bubble, that it can be neglected. So, the liquid contained in the films is approximately zero and all the liquid is present only at the interstitial regions between the bubbles where the films meet (Plateau borders and nodes). We will call the foam *ideal dry* when the foam is very dry (in the limit where the liquid fraction tends to zero), then the Plateau border can be considered as lines and the nodes where they meet as points. Although ideal dry foams are only a theoretical model of real foams, they make the problem easier to study: the assumption of zero liquid gives rise to some properties which are observed, with a good approximation, also when little liquid is present.

When three–dimensional dry foams are created, by increasing the surface energy of the immiscible gas–liquid system, they achieve very quickly the mechanical equilibrium, which is a relative minimum of the surface energy of the foam. A dry foam reaches mechanical equilibrium on time–scales of the order of $10^{-6} - 10^{-3} s$ [SJG05, WH99], depending on the viscosity of the fluid. In reality the equilibrium is not even reached because the foam continually evolves according to the coarsening process. As typical coarsening time–scales are of the order of $10 - 10^{3} s$ [WH99], diffusion and equilibration are often considered as decoupled processes and equilibration as a instantaneous process. In the following we suppose at each point in time the foam can be considered in mechanical equilibrium. This equilibrium state then further relaxes through gas diffusion (we do not consider drainage and film breakage).

At equilibrium, the foam has some important properties which characterize

this state. These properties, known as *Plateau's laws*, were observed experimentally by Plateau [Pla73], the mathematical proof was given by J.Taylor [Tay76]. Supposing that the surface tension γ is constant and equal for all the films, Plateau's laws for very dry foams are:

- The films can intersect only three at a time on a Plateau border, and must do so at 120^o.
- At the vetices, or nodes, no more than four borders may meet, and this tetrahedral vertex is perfectly symmetric. The angle formed by two borders at the nodes is $\theta_M = \cos^{-1}(-1/3)$ (Maraldi angle).
- The pressure drop across a film, composed by two liquid/gas interfaces, is proportional to the mean curvature of the film H:

$$\Delta P = 2\gamma H\,. \tag{1.1}$$

  The mean curvature of a surface is the mean value between the maximal and the minimal sectional curvature of the surface (for more details, see section 3.1). γ is the surface tension of the film.

The fact that the films meet three at a time at Plateau borders forming angles of $2\pi/3$ can be proved simply by considering an orthogonal section of a border (figure 1.1). As the energy is proportional to the surface, $E = \gamma S$, the force per unit of length acting on the border is given by $\gamma\mathbf{b}$ where $\mathbf{b}$ is the unit vector normal to the border and tangent to the film (the co–normal vector). It is obvious that the mechanical equilibrium is attained when the angles formed by the co–normal vectors are all $2\pi/3$.

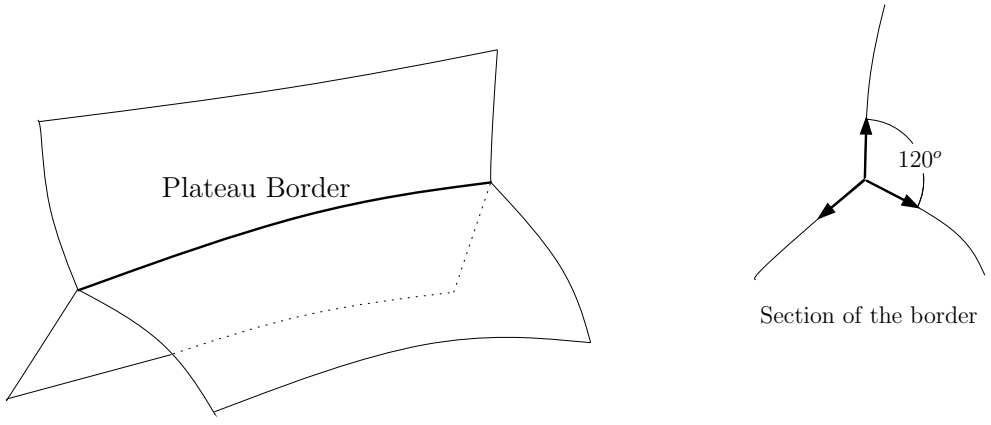

Figure 1.1: Perspective view and cross–section of a Plateau border in a 3D ideal dry foam.

The three–connection property follows from the fact that borders with higher connections are not minimal. It can be understood by a simple direct calculus

considering four parallel fixed lines connected by films. So, the configuration which minimizes the area of the films is not that one where four films meet in a border but that one where five films meet in two connected borders. For example, let's suppose that the cross section of the four lines is the square of unitary side centred in the origin. When the films, starting from the lines, meet in a unique border, the total area of the films is $A_{1\times4} = 2\sqrt{2}l$, where l is the length of the lines. When they form two connected borders the total area is $A_{2\times3} = (1+\sqrt{3})l < A_{1\times4}$ (see figure 1.2).

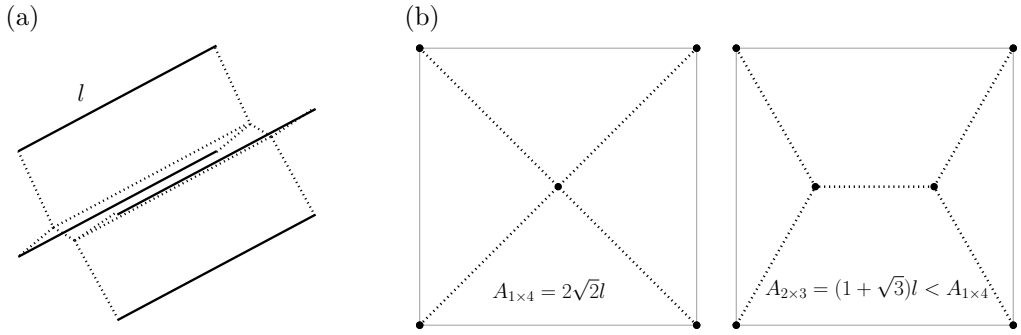

Figure 1.2: Simple example showing that minimal borders are threefold: b) section of the four parallel lines structure shown in a).

The last property of equilibrated foams is Young–Laplace's law applied to two liquid–gas interfaces which constitute a film. Young–Laplace's expresses the balance of the pressure difference across an interface, ΔP, and the force of surface tension acting upon an element of the surface: $\Delta P = 2\gamma H$. The proof of (1.1) is straightforward for the case of a single spherical bubble of radius r where $H = 1/r$ [Mor98]. The minimum of the enthalpy function of the single bubble system, expressing the minimum of the surface energy under the constraint that the volume of the bubble, V_0, is constant, gives the mechanical equilibrium. The enthalpy function is:

$$h(r) = \gamma A(r) - \Delta P(V(r) - V_0) = 4\gamma\pi r^2 - \Delta P(\frac{4\pi}{3}r^3 - V_0)\,.$$

Imposing the variation of the enthalpy equal to zero, one obtains:

$$\delta h = (8\gamma\pi r - 4\pi\Delta P r^2)\delta r = 0\,,$$

then

$$\Delta P = 2\gamma\frac{1}{r} = 2\gamma H\,.$$

Plateau's laws can be written in the short form:

$$\sum_{i=1,3}\gamma\,\mathbf{b}_i = 0\,, \quad \text{at Plateau borders}\,; \tag{1.2}$$

$$\sum_{i=1,3} \gamma\, k_i = 0\,. \tag{1.3}$$

Equation (1.2) states that the sum of the three co-normal vectors to the films at any Plateau border is zero. In equation (1.3), k_i, for $i = 1, 2, 3$, is the curvature of the films meeting on a Plateau border: Laplace's law implies that the sum of the curvatures around any closed loop of bubbles is zero.

Incompressibility of the Bubbles

Another property of equilibrated foams is that the bubbles can be assumed incompressible. In fact the compressibility of the gas within the bubbles is negligible with respect to the effect of the surface tension. Let's consider a bubble of radius R. The compressibility $1/k$ of the gas, considered as a perfect gas, within the bubble is given by:

$$\frac{1}{k} = -\frac{1}{V}\frac{\partial V}{\partial P} = \frac{1}{P_0} \approx 10^{-5} J^{-1} m^3$$

where P_0 is the pressure of the gas, typically of the order of the ambient pressure. The effect due to the surface tension can be calculated using the same formula where P has to be replaced with the pressure drop ΔP on the film and using Laplace relation (2.2):

$$\frac{1}{k_\gamma} = -\frac{1}{V}\frac{\partial V}{\partial \Delta P} = \frac{3}{\Delta P} = \frac{3R}{\gamma}.$$

Typical values for γ and R are $\gamma = 10^{-2} J m^{-2}$ and $R = 1cm$, then $\frac{1}{k_\gamma} \approx J^{-1} m^3 >> \frac{1}{k}$.

Non–Ideal Foams

When the foam is dry but not dry ideal the volume of the liquid at Plateau borders and nodes is no longer negligible. Whereas the thickness of the films can still be treated as infinitesimal, Plateau border is a channel of finite width and its cross section can be modelized as a concave triangle (figure 1.3). In this case the foam is constituted by a network of tubes which pack the bubbles of gas and there are no general stability rules for the multiplicity of the intersections of the films at Plateau borders and at nodes.

The liquid within the borders, applying Laplace's equation (1.1) to the concave gas/liquid interfaces at the borders, has a pressure P_B smaller than the gas in the bubbles. As the liquid of the continuous phase is connected by the network of borders and films, the pressure of the liquid (borders and films) has to be constant and equal to P_B. Furthermore, when a border joins an adjacent film, the surface of the film is joined smoothly, so, the vector normal to the surface is the same on both sides of the intersection [WH99].

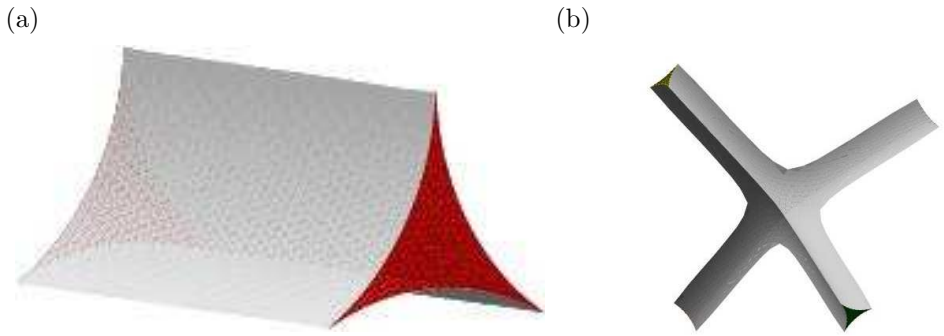

Figure 1.3: Dry non–ideal foam: a) cross–section of a Plateau border, b) node where four border meet.

1.1 Disjoining Pressure, Non–Standard Foams

We have to note that in reality the thickness of the films is never zero. To see that, let us apply Laplace's law at both the gas/liquid interfaces across a film to find the liquid pressure P_F within a film. We can see easily that the pressure within the film, P_F, is the mean of the pressures of the two gas pressures in the adjacent bubbles:

$$\begin{cases} P_1 - P_F = \gamma H \\ P_F - P_2 = \gamma H \end{cases} \Longrightarrow P_F = \frac{P_1 + P_2}{2}.$$

This is not consistent with the equality of the pressure within all the liquid with the pressure P_B prevailing in the Plateau border and smaller than the gas pressure in the bubbles. In fact, if P_F was greater than P_B, then the liquid would drain rapidly from the films into the Plateau borders and so the films would burst. This paradox is resolved if it is considered that when the thickness of the films become small, the molecular forces (e.g., van der Waals, electrostatic, steric etc.), arising from the interaction of the two interfaces, come into play. These give rise to a force which balances the normal component of the overpressure tensor acting on the film [DCM87]. When the thickness of the film is very small, this force is repulsive and prevents the films from shrinking to zero thickness. This force per unit of area, which acts perpendicular to the interfaces, is called the *disjoining pressure* Π:

$$P_F = P_B + \Pi \tag{1.4}$$

Although the surface tensions γ in the foam are considered constant this is not always the case. This is a consequence of the fact that, in a foam, films with different thickness can coexist and that the surface tension depends on the film thickness h, $\gamma = \gamma(h)$. To see that we can use the fact that the disjoining pressure

can be defined in terms of thermodynamic variables [Ber99]:

$$\Pi(h) = -\frac{1}{A}\left(\frac{\partial G}{\partial h}\right)_{T,P,A,N_i}, \tag{1.5}$$

where $G(T, P, A, N_i, h)$ is the Gibbs free energy of a film and T, P, A and N_i are the temperature, the overall pressure, the area and the mole numbers of the i-th component, respectively. In the case of a flat film, at constant temperature and chemical potential of the i-th component, equation (1.5) gives rise to [Ber99, PE96]:

$$\left(\frac{\partial \gamma}{\partial h}\right)_{T,\mu_i} = -\Pi\,. \tag{1.6}$$

Integration of equation (1.6) then yields an expression that relates the surface tension of the film interfaces to the disjoining pressure isotherm,

$$\gamma(h) = \gamma(\infty) - \int_{\Pi(h)}^{0} h\,\mathrm{d}\Pi\,. \tag{1.7}$$

A schematic disjoining pressure isotherm $\Pi(h)$ for a single planar isolated soap film is shown in figure 1.4. The behaviour of $\Pi(h)$ is non–monotonical. For a

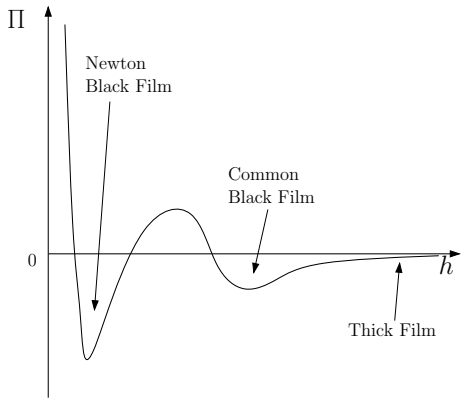

Figure 1.4: Schematic disjoining pressure isotherm Π in soap films vs. the thickness h.

thick film, as $h \to \infty$, the disjoining pressure goes to zero. Then $\gamma(h) \to \gamma_\infty = \gamma$, where γ is twice the usual surface tension of the bulk liquid/gas interface. So,

$$\gamma(h) = \gamma - \int_{\Pi(h)}^{0} h\,\mathrm{d}\Pi\,. \tag{1.8}$$

From (1.8) the surface tension depends on the considered branch in the disjoining pressure isotherm (fig. 1.4). The films, with same disjoining pressure

but different thicknesses and film tensions, can therefore be in thermodynamic equilibrium.

In a foam, one can therefore expect to get films with different thicknesses for the same applied capillary pressure P_B, as showed by [HDPF$^+$00].

The existence of foams where different surface tensions coexist allows us to define the *non–standard* foams. Non–standard foams are models of foams where each film can have a different value of surface tension. The equilibrium equations for non–standard foams differ from Plateau's laws (1.2,1.3) in the fact that now γ is not the same for any film [Mou97]:

$$\sum_{i=1,3} \gamma_i \, \mathbf{b}_i = 0 \,, \quad \text{at Plateau borders} \,; \tag{1.9}$$

$$\sum_{i=1,3} \gamma_i \, k_i = 0 \,. \tag{1.10}$$

Chapter 2

Two Dimensional Foams

Two dimensional systems are very important in physics. By their relative simplicity, they often permit to understand some properties of a specific problem which, in higher dimensions, can result very difficult to study. Moreover $2D$ systems are not only theoretical toys, in fact they can often be realized in experiments or taken, with a very good approximation, as models for some physical problems. However, not all the properties of a $2D$ systems can be extended to a higher dimensional case and a thorough analysis is necessary before any generalization.

Soap–like foams are one of these systems for which the study of the two–dimensional problem has given important results in the comprehension for the analogous higher dimensional systems. $2D$ foams, defined theoretically, can have more experimental realizations where a $3D$ foam is constrained to be quasi two–dimensional (Hele–Shaw cell, Langmuir mono–layer, Bragg raft).

2.1 2D Foams: Definition and Equilibrium

In this section we give the definition of ideal two–dimensional foams. It does not pretend to be the exact mathematical definition which could be too complicated for our purposes, we give the equivalent "physical" definition which is light and more intuitive.

A two–dimensional foam is a partition of the plane in cells (bubbles) of gas separated by liquid interfaces (films) having a tension line. Except when specified, we will refer, as for 3D foams, to these as to *dry* 2D foams. Foams are dry if the *liquid fraction* is small. The liquid fraction is the ratio between the liquid area and the total area (gas plus liquid). As in a 3D dry foam the films are thin, they can be idealized as simple lines. With this assumption all the liquid present in the foam is concentrated in a small region at the intersection of the films, the vertices. Physically, in the experimental realization of 2D foams (section 3.6), two–dimensional vertexes and films correspond, respectively, to orthogonal

sections of three–dimensional Plateau borders and films; the 3D nodes are not present in 2D: 2D foams are a monolayer of bubbles with cylindrical symmetry. 2D dry foams are the two–dimensional analogous of the 3D dry foams.

A 2D foam is ideal if the liquid stays only in one or zero dimensional subspaces of the plane (respectively the edges and the vertexes) with zero area. In other words, the films and the vertexes are respectively lines and points. This corresponds to take the limit where the liquid fraction ϕ tends to zero. In practice, in physical experiments, the dryness of the foam is limited by the stability of the films: typically, in soap foams it can go down to one or two percent [Gra02]. In table 2.1 and figure 2.1 the different definitions are shown. For wet foams, the maximum value of ϕ in table 2.1 corresponds to the *wet foam limit* where the bubbles come apart[WH99]. In this limit the bubbles are circular and the system is not any more jammed (it is no longer considered as a foam). In table 2.1 $\phi = 0.16$ was obtained from numerical simulation of a polydisperse foam. This value, calculated for a hexagonal honeycomb foam, gives $\phi = 0.093$ (by a simple straight calculation).

2D foam	Liquid fraction	Films thick.	Vertexes area
ideal	$\phi \to 0$	0	0
dry	$\phi << 1$	0	$\neq 0$
wet	$\phi < 0.16$	$\neq 0$	$\neq 0$

Table 2.1: Different regimes of 2D foams.

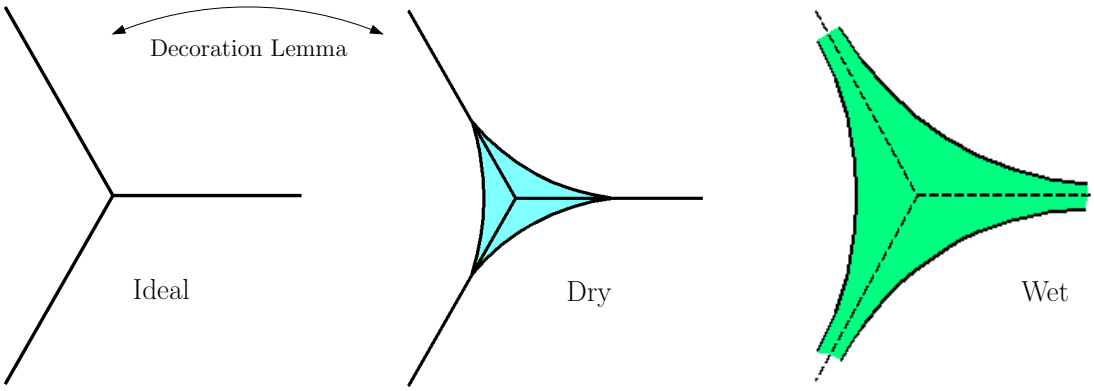

Figure 2.1: Example of Ideal, Dry and Wet vertex and films.

The equilibrium of 2D foams is defined for ideal 2D foams. The equilibrium of dry foams is defined by using a very wonderful property of 2D foams: the

decoration theorem [Wea99, WH99]. This theorem implies that it is possible to add to an equilibrated 2D ideal foam a small quantity of liquid without changing the equilibrium. So the decoration theorem permits to treat dry foams as if they were ideal and so it makes the problem much easier (see fig.2.1).

Later, we will find again the decoration theorem (theorem 6.1) as a corollary of the star–triangle equivalence (chapter 6) which is one of the main results of this thesis.

Let's consider for the moment that the gas diffusion between the bubbles is switched off (zero porosity). The bubbles have constant area: as for 3D foams, the bubbles can be considered incompressible (sec.1). Moreover, let's suppose that no external force field is applied on the foam, then the only forces which act in the foam are the line tension forces under a constant area constraint.
For a constant line tension in the foam, the *energy* of a 2D foam is the total length of the films L multiplied the tension line γ:

$$E_{2D} = \gamma L = \gamma \sum_i l_i \,, \tag{2.1}$$

where i varies on all the films of the foam and l_i is the length of a film. Given a fixed set of bubble areas, a 2D foams is termed *equilibrated* if its structure is a local minimum for the energy function. As in the 3D case, no global minimum is required for the definition of equilibrated foam. This implies that the equilibrium states are only metastable.

How many possible states of equilibrium exist for a 2D foam of fixed bubble area set is unknown. The number of configurations, or different neighbourhood relations between bubbles, could be a good candidate to this role but to establish which topologies are possible or not is not simple. In the trivial cases of cluster constituted of two or three bubbles, there is only one equilibrium state (only one configuration). For four bubbles the problem is not resolved. It depends on the values of the areas; in fact some configurations could be impossible at equilibrium.

Equilibrium properties of 2D foams can be deduced directly from three–dimensional ones (equations (1.1), (1.2) and (1.3)). Here we will rewrite the equilibrium laws for 2D foams recalling their origins. For the rigorous proof of these equilibrium laws, see [Tay76]. The equilibrium states (as for 3D foams, they are metastable) are the local minima of the energy. Equivalently, the variation of the energy is zero and the sum of the forces acting on any film or vertex is zero. The sum of the forces on a film, pressure forces and line tensions, is zero when the Laplace–Young's equation (1.1) is verified:

$$\Delta P = \gamma k \,. \tag{2.2}$$

This equation relates the pressure drop ΔP between the two bubbles separated by the considered film, the tension line γ and the curvature k of the film. As the

films are lines and since, at equilibrium, the pressure inside each bubble must be constant, (2.2) implies that the films are circular arcs.

The equilibrium at vertexes, observed for the first time by Plateau, implies that the films meet three by three at a vertex at angles of $2\pi/3$ (120°). The value of the angles is a immediate consequence of the fact that, at the vertex, the force exerted by any film is tangent to the film line, in the direction outgoing from the vertex, and it has the line tension γ as modulus. Then, at equilibrium, these three vectors have to form an equilateral triangle.

The three–connection property depends on the fact that 2D vertexes are orthogonal sections of 3D borders. It can be shown to be minimal by a simple direct calculus where four fixed points are connected by films, analogously to the example of figure 1.2-b).

We have to note that in the case of wet 2D foams the stability of a threefold vertex is not guaranteed any more. Theoretical and numerical studies on the stability of the two threefold vertexes (or single fourfold vertex) attached to four fixed points are made in [WP96, FW92a, BM98]. In these works the films are lines again but some liquid is present at the vertexes. The stability of the two possible configurations is studied as function of the liquid fraction (configuration 1×4 is stable for $\phi > 0.04$).

The last equilibrium property concerns the contact of the foam with a fixed smooth wall: at the contact of the film with a rigid wall, at equilibrium, the vector tangent to the film is orthogonal to the wall. This property, valid in the case of dry foam where the films are lines and in non–wetting conditions, derives from Young's law:

$$\gamma \cos\theta + \gamma_1 - \gamma_2 = 0\,, \tag{2.3}$$

θ is the angle between the tangent to the film and the wall and γ_1 and γ_2 are the line tensions of the interfaces between the two fluids on both sides of the film and the wall. In normal foams the fluids are the same, so $\gamma_1 = \gamma_2$ and (2.3) implies that $\theta = \frac{\pi}{2}$. Then, when a 2D foam is equilibrated, the films are arcs of circle which meet three by three at the vertexes and the angles between the films are $2\pi/3$. The curvature of the films is given by (2.2). A film between two equal pressure bubbles is considered to be an arc of a circle with infinite radius. A typical vertex is shown in figure 2.2.

Before we conclude this section we want to rewrite, as in 3D, the equilibrium equations in the form that we will use afterward:

$$\textstyle\sum_{i=1}^{3} \gamma\, \boldsymbol{\tau}_i = 0 \quad \text{at } \mathbf{v}, \tag{2.4}$$

$$\textstyle\sum_{i=1}^{3} \gamma\, k_i = 0 \tag{2.5}$$

where $i = 1, 2, 3$ label the circular films meeting at a vertex $\mathbf{v}$. $\boldsymbol{\tau}_i$ and k_i are the

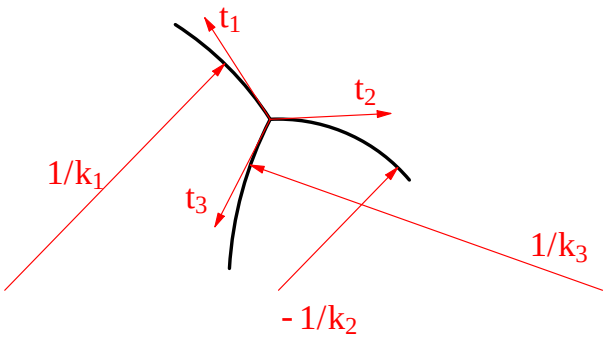

Figure 2.2: Typical vertex of a 2D equilibrated foam.

tangent vector and the curvature of the film i. Equation (2.5) is a consequence of (2.2): the sum of pressure drops on a closed path of bubbles is zero.

2.1.1 Topological Changes

As we said in the previous chapter for 3D foams, also 2D foams are doomed to disappear because of the coarsening and film burst (which we will neglect in the following). Supposing the gravity orthogonal to the plane of the foam, in two dimensions, differently from 3D, the drainage does not cause a gradient of liquid fraction on the plane. Furthermore, by suitable experimental set–up, the effects of the gravity on the drainage of liquid are negligible (see section 3.6). During their evolution, 2D foams (and 3D foams) can change their relations of neighbouring between the bubbles and pass from an equilibrium state to another.

These phenomena, very frequent in the evolution of foams, are called *topological changes*. The term "topological" derives from the changes in the relations of adjacency. There are two elementary topological changes:

- T1) It doesn't change the number of bubbles, it changes the neighbourhoods: see figure 2.3. In general, the energy (and perimeter) of the foam changes discontinuously when a T1 occurs.

- T2(3)) Is the disappearance of a bubble. When the area of a bubble goes to zero, then the number of bubbles changes. We will prove that at a T2(3) the energy of the foam varies continuously (sec. 5.6).

Although the existence of vanishing cells with number of sides larger than three is observed (T3(4) and T3(5) [GGS87]), when the time–scale of observed phenomena (like coarsening) is large with respect to the time–scale of the topological processes, they can be considered as compounded by T1 and T2(3).

In low viscosity regime, as in topological change processes the foam leaves the

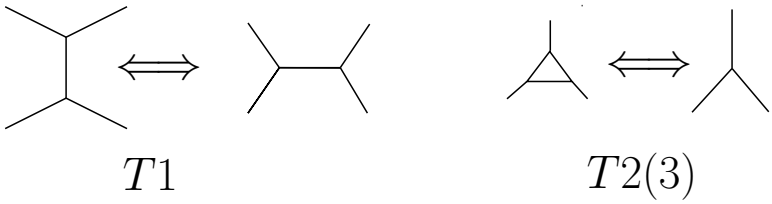

Figure 2.3: T1 and T2(3).

local equilibrium state to go into another, the time–scale of these processes is very small with respect to the time–scale of coarsening.

2.2 Minimization Problem (in 2D and 3D)

At equilibrium 2D foams can be represented by a planar graph $\mathcal{G} = (V, E)$ of connectivity 3, with vertex set V and edge set E, given as arcs of circle which verify equations (2.4) and (2.5). If a cluster of n bubbles of fixed area $\mathbf{a} = \{a_1, a_2 \dots a_n\}$ is given, where the $(n+1)$-th bubble is considered as the exterior of the cluster (the plane minus the cluster), the relation between the area set $\mathbf{a}$ and $\mathcal{G}$ is unknown. If the foam is not equilibrated, the problem to know what neighbourhood relations between the bubbles will be chosen at equilibrium is not resolved. Anyone of the possible configurations is possible *a priori* if the bubbles' areas are not considered. When the areas of the bubbles are taken into account the number of possible configurations, which are local minimum of the energy, is smaller.

The problem of the minimization of a set of bubbles of given area is a problem studied by many mathematicians and it requires sophisticated tools as geometric measure theory [Mor00]. In 2000 the conjecture that the unique stable configuration, which minimizes a two–bubble cluster in 3D, is the standard double–bubble (fig. 2.4) was proved by Hutchings *et al* [HMRR00].

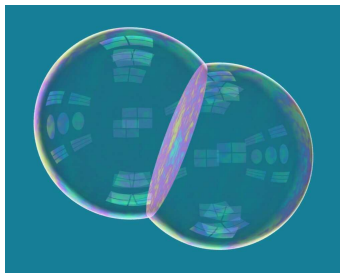

Figure 2.4: Standard double–bubble configuration in 3D.

In two dimensions, Foisy[FAB$^+$93] and Wichiramala *et al*[Wic02] proved re-

spectively that the standard double and triple–bubble uniquely minimize perimeter in the plane for any two and three given areas (fig. 2.5-a and 2.5-b, respectively).

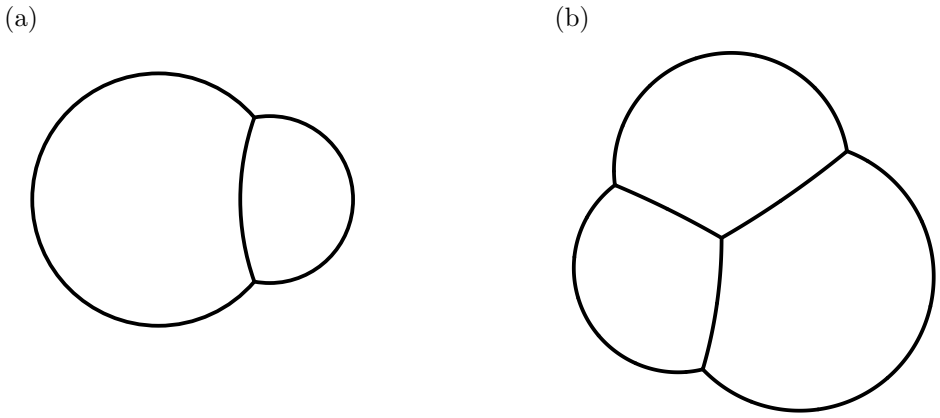

Figure 2.5: Standard double–bubble (a) and triple–bubble (b).

More recently, Cañete and Ritore [CR04] proved that the unique least–perimeter way of partitioning the unit 2–dimensional disk into three regions of prescribed areas is by means of the standard graph described in figure 2.6. For a number

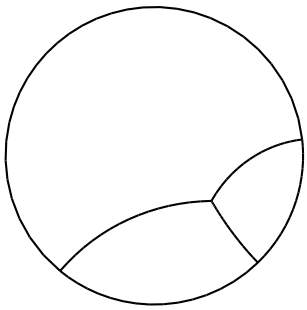

Figure 2.6: Standard graph which separates the unit 2D disk into three regions. (Reproduced by kind permission of Antonio Cañete.)

of bubbles greater than three the problem is open except for the particular case where the 2D foam is composed of an infinite number of bubbles of the same area. In 2001 Hales proved that the configuration where all the bubbles are hexagonal (honeycomb structure) is the absolute minimum of the energy for this foam [Hal01]. Also physicists considered the minimization problem. At the end of the last century, Lord Kelvin [Kel87] created a tetrakaidecahedron; a structure with six planar quadrilateral faces and eight non–planar faces, all with curved edges (fig. 2.7-a). He showed that it both tessellates space and minimises surface area for a given volume. More recently, Weaire and Phelan [WP94] found that

such cells were present within real foams. They also noted, that in practice the most common films in a foam are pentagonal. They constructed a collection of eight polyhedral bubbles which contains many pentagonal faces, fills space, and also has fractionally less surface than a Kelvin cell (0.3%). In Weaire–Phelan's packing (fig. 2.7-b), two irregular pentagonal dodecahedra (12-sided) and six tetrakaidecahedra (14-sided) form a translation unit with a lattice periodicity which is simple cubic. In two dimensions, some works showed numerically and

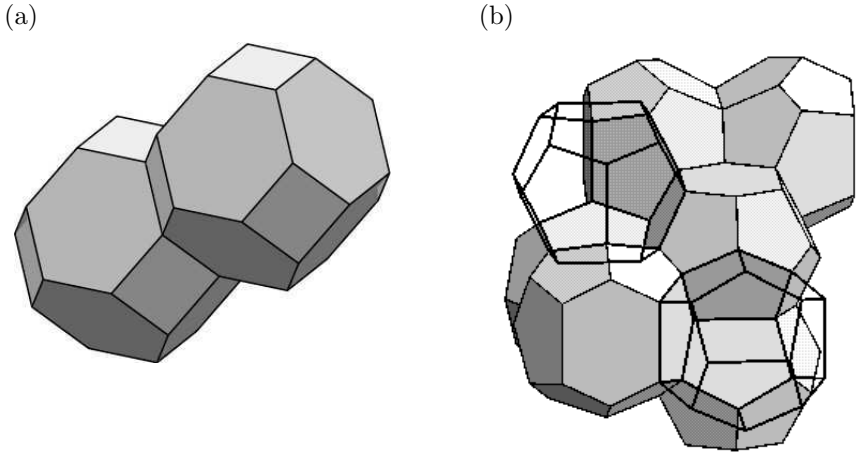

Figure 2.7: a) Two cells of a Kelvin's foam. b) Weaire–Phelan's packing. The dodecahedra is shown as wire frames, and the tetrakaidecahedra as solid. The dodecahedra do not touch each other, but are entirely surrounded by tetrakaidecahedra.

analytically that a finite monodisperse 2D foam behaves like a crystal rather than a liquid [VF01, FR01, CGV$^+$03, CG03, HM05]. The minimal energy is achieved when its outer boundary respects the underlying hexagonal lattice, rather than by introducing internal defect pairs (bubbles with 5 and 7 edges) and reducing its boundary energy. It was found that the inside of the cluster must be close to the honeycomb, and that the minimum energy configuration (for a large number of bubbles) is given by the closest possible configuration to a regular honeycomb–like structure.

2.3 Two Bubbles: a Simple Minimization

Let us consider a cluster of two bubbles $\mathcal{C}$. We do not require that the cluster is equilibrated but we suppose that it is a small variation of the standard double–bubble cluster (fig. 2.5-a):

- Each bubble is in contact with the other by only a film,
- Each bubble is in contact with the outside by only a film,

- The films are circular arc,
- The films meet three at time.

We suppose that the area of the two bubbles is fixed and given by the vector $\mathbf{a} = (a_1, a_2)$. As $\mathcal{C}$ is bounded by arcs of circles, there is a symmetry axis where the centres of curvature of the films pass [Mou97] (see also pag. 20); we identify it with the x-axis (fig2.8). By our hypothesis, $\mathcal{C} = \mathcal{C}[\mathbf{y}]$ is described by four variables: $\mathbf{y} = \{R_{13}, R_{23}, R_{21}, y\}$, respectively the three radii of curvature of the films and the distance from the vertex to the symmetry axis. The variables are assumed to vary in suitable intervals. We suppose here that $R_{13} > R_{23}$ (or $a_1 > a_2$).

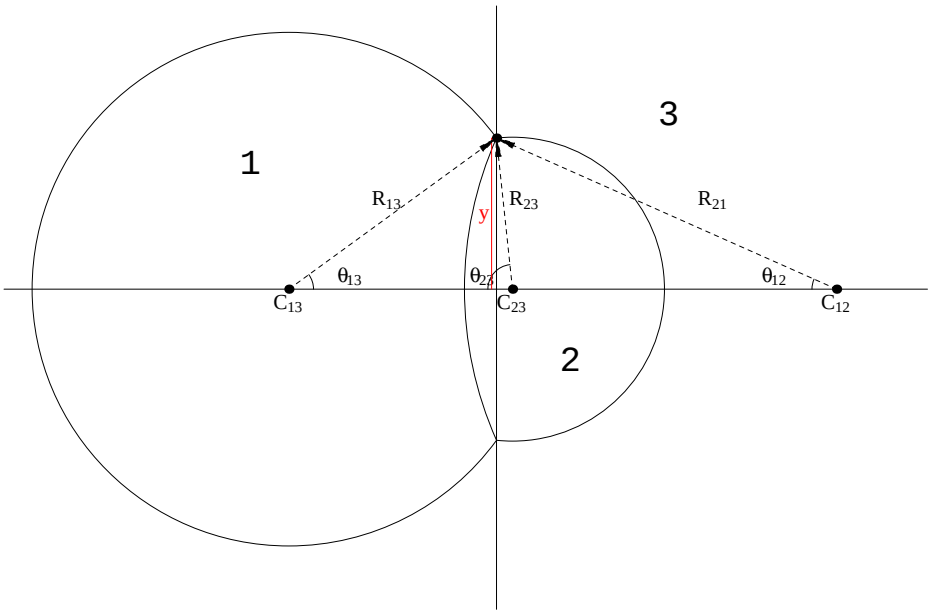

Figure 2.8: Cluster of two bubbles.

The other parameters depend on the first ones by geometrics considerations (fig2.8):

$$\begin{cases} \theta_{13} = \arcsin(y/R_{13}), \\ \theta_{23} = \arcsin(y/R_{23}), \\ \theta_{12} = \arcsin(y/R_{21}). \end{cases} \tag{2.6}$$

The expressions of the cell areas $\mathbf{s}[\mathbf{y}] = (s_1[\mathbf{y}], s_2[\mathbf{y}])$ spanned by the two cells and of the total perimeter $P[\mathbf{y}]$ as functions of the free parameters are:

$$\begin{aligned} s_1[\mathbf{y}] = &\quad R_{13}^2 f(\pi - \theta_{13}) - R_{21}^2 f(\theta_{12}), \\ s_2[\mathbf{y}] = &\quad R_{23}^2 f(\pi - \theta_{23}) + R_{21}^2 f(\theta_{12}), \\ L[\mathbf{y}] = &\quad 2\left(R_{13}(\pi - \theta_{13}) + R_{23}(\pi - \theta_{23}) + R_{21}\theta_{12}\right), \end{aligned}$$

where $f(x) \equiv \frac{1}{2}(2x - \sin(2x))$.
To find again the equilibrium laws (2.4) and (2.5) we have to impose that the energy of the cluster is stationary under the constraint that the bubble areas are constant $\mathbf{s}[\mathbf{y}] = \mathbf{a}$. So, we define the *Enthalpy* function:

$$G\left[\mathcal{C}[\mathbf{y}], \boldsymbol{\lambda}; \mathbf{a}\right] = \gamma L[\mathbf{y}] + \boldsymbol{\lambda} \cdot (\mathbf{a} - \mathbf{s}[\mathbf{y}]) \tag{2.7}$$

where $\boldsymbol{\lambda} \in \mathbb{R}^2$ are the Lagrange's multipliers to impose $\mathbf{s}[\mathbf{y}] = \mathbf{a}$.

The minimum of $G[\mathcal{C}[\mathbf{y}], \boldsymbol{\lambda}; \mathbf{a}]$ is the minimum of the perimeter $L[\mathbf{y}]$ over all possible $\mathcal{C}[\mathbf{y}]$'s. Imposing that

$$\begin{cases} \nabla_{\mathbf{y}} G[\mathcal{C}[\mathbf{y}], \boldsymbol{\lambda}; \mathbf{a}] = 0, \\ \nabla_{\boldsymbol{\lambda}} G[\mathcal{C}[\mathbf{y}], \boldsymbol{\lambda}; \mathbf{a}] = 0, \end{cases}$$

we find:

$$\begin{cases} \boldsymbol{\lambda} = \gamma(\frac{1}{R_{13}}, \frac{1}{R_{23}}), \\ \frac{1}{R_{21}} = \frac{1}{R_{23}} - \frac{1}{R_{13}}, \\ cos(\theta_{12}) - cos(\theta_{13}) - cos(\theta_{23}) = 0, \\ \mathbf{s}[\mathcal{C}] = \mathbf{a}. \end{cases}$$

The first equation implies that λ_i is the pressure difference between the bubble i and the exterior one (this is the genuine Laplace law (2.2) that in this way is obtained again). The second equation corresponds to equation (2.5). By the third equation, using expressions (2.6), we obtain:

$$\begin{aligned} \theta_{13} &= \tfrac{\Pi}{3} - \theta_{12}, \\ \theta_{23} &= \tfrac{\Pi}{3} + \theta_{12}, \end{aligned} \tag{2.8}$$

this corresponds, with a little geometry, to Plateau's law (2.4). We do not prove that the found configuration is a minimum (the proof could by very complicated and we have already the proof by [FAB+93]).

The degrees of freedom of the equilibrated double–bubble cluster are only two (up to the three Euclidian degrees of freedom) and they correspond to the components of $\mathbf{a}$. Replacing equilibrium conditions in the areas and energy (E=γL) expressions, we can write these as function of the other two variables (y and θ_{12}):

$$\mathbf{a} = y^2 \left(g(-\theta_{12}), g(\theta_{12})\right), \tag{2.9}$$

$$\boldsymbol{\lambda} = \frac{\gamma}{y \sin(\theta_{12})} \left(\sin(\frac{\Pi}{3} - \theta_{12}), \sin(\frac{\Pi}{3} + \theta_{12})\right), \tag{2.10}$$

$$E = \gamma L = 2\boldsymbol{\lambda} \cdot \mathbf{a}, \tag{2.11}$$

where

$$g(x) = \frac{f(\frac{2\pi}{3} - x)}{\sin^2(\frac{2\pi}{3} - x))} + \frac{f(x)}{\sin^2(x)}\,.$$

Inverting the expressions (2.9) would determinate the corresponding values of y and θ_{12} as functions of $\mathbf{a}$, so it would express any geometrical parameter of an equilibrated foam by the only two independents physical variables: the area of the internal bubbles. The components of $\boldsymbol{\lambda}$ are the pressure of the bubbles with respect to the pressure p_0 external to the cluster: $\lambda_i = p_i - p_0$.

Let us consider now a one–parameter variation (the time) of the bubble areas $\mathbf{a}(t)$ such that the system can be considered at any time at equilibrium and the topology of the cluster does not change (in thermodynamics this variation corresponds to a quasi–static transformation). Let $\mathbf{y} \in \mathbb{R}^4$ be the variables describing $\mathcal{C}$. The enthalpy function is

$$G\left[\mathbf{y}, \boldsymbol{\lambda}; \mathbf{a}\right] = \gamma L(\mathbf{y}) + \boldsymbol{\lambda} \cdot (\mathbf{a} - \mathbf{s}(\mathbf{y})),$$

where $\mathbf{a}$ is a parameter in G. We assume that G has a non degenerate local minimum at $(\mathbf{y}_0, \boldsymbol{\lambda}_0)$ determined by

$$\nabla_{\mathbf{y}} G\left[\mathbf{y}_0, \boldsymbol{\lambda}_0; \mathbf{a}\right] = 0 \Rightarrow \quad \gamma \nabla_{\mathbf{y}} L(\mathbf{y}_0) - \textstyle\sum_{i=1}^{2} \lambda_{0i} \nabla_{\mathbf{y}} s_i(\mathbf{y}_0) = 0, \tag{2.12}$$

$$\nabla_{\boldsymbol{\lambda}} G\left[\mathbf{y}_0, \boldsymbol{\lambda}_0; \mathbf{a}\right] = 0 \Rightarrow \quad \mathbf{s}(\mathbf{y}_0) = \mathbf{a}. \tag{2.13}$$

$\mathcal{C}[\mathbf{y}_0] = \mathcal{C}[\mathbf{y}_0(\mathbf{a})]$ corresponds to the standard double–bubble configuration, which verifies the equations (2.2), (2.4) and (2.5). As during the variation we suppose that the equilibrium is preserved, equations (2.12-2.13) are verified for any value of $\mathbf{a}(t)$ in some time interval (t_0, t_1)). This time interval is bounded by a change of the topology of the two–bubble configuration, for example the disappearing of a bubble.

Let $\mathbf{a}(t + dt)$, $\mathbf{a}(t)$ be the area vectors of the two bubbles for any $t \in (t_0, t_1)$ and $\mathbf{y}(t)$, $\mathbf{y}(t + dt)$ the corresponding value of the variables at the minimum of G, then

$$\begin{aligned} L(\mathbf{y}(t + dt) - L(\mathbf{y}(t)) = & \ \textstyle\sum_{i=1}^{2} \frac{\partial L}{\partial y_i}(\mathbf{y}(t)) \frac{dy_i}{dt}(t) dt = \\ = & \ \textstyle\sum_{i=1}^{2} \frac{1}{\gamma} \left(\boldsymbol{\lambda}(t) \cdot \frac{\partial \mathbf{s}}{\partial y_i}(\mathbf{y}(t)) \right) \frac{dy_i}{dt}(t) dt = \\ = & \ \frac{1}{\gamma} \left(\boldsymbol{\lambda}(t) \cdot \dot{\mathbf{a}}(t) \right) dt \end{aligned}$$

where equations (2.12) and (2.13) have been used. Dividing by dt and taking the limit $dt \to 0$ we obtain:

$$\frac{dE}{dt} = \boldsymbol{\lambda}(t) \cdot \dot{\mathbf{a}}(t). \tag{2.14}$$

Remark. Let us note that the proof of equation (2.14) does not depend upon the number of bubbles and the dimension of space: it is a consequence of the fact that, varying t, the cluster is always in a configuration which is a minimum of the enthalpy. It can be extended easily to a cluster of n bubbles by enlarging $\mathbf{y}$

to a suitable phase space. A differential formulation of this equation appears also in [CR04]. Considering a cluster of n bubbles, where the diffusion is switched off, and the area of a bubble, for example the bubble i, is varied slowly, keeping constant the other and leaving the cluster equilibrated at each time. Equation (2.14) can be used to prove that, when the pressure in bubble i, p_i is equal to external pressure p_0: $\lambda_i = p_i - p_0$, then the energy of the cluster is stationary. In fact:

$$\frac{dE}{da_i} = \boldsymbol{\lambda} \cdot \frac{d\mathbf{a}}{da_i} = \lambda_i \,.$$

This property was proved by Teixeira and Fortes [TF05].

Also equation (2.11) is valid for any number of bubbles F. In D dimensions, it generalises as:

$$E_D = \gamma A_D = \frac{D}{D-1} \boldsymbol{\lambda} \cdot \mathbf{V}_D. \tag{2.15}$$

A_D is the D-dimensional total area of the bubbles and $\mathbf{V}_D \in \mathbb{R}^F$ is the volume vector (its components are the D-dimensional volumes of the bubbles). The proof of (2.15) is obtained by considering the enthalpy under dilatations, $A_D \to \delta^{D-1} A_D$, $V_D \to \delta^D V_D$ [AV00, GJJF01].

2.4 2D Foams at Equilibrium (Properties)

Let us consider a two–dimensional foam cluster of F bubbles in a local minimum of the energy. Supposing that the films don't burst and the diffusion of the gas through the films is switched off, the foam persists in this metastable state where: the areas of the bubbles are constant and Plateau's laws (2.4-2.5) are verified. The curvatures of the films are constant and linked to the bubble pressures by Laplace's equation (2.2). For a given configuration of a 2D finite cluster of F bubbles, embedded in a gas at pressure p_{F+1} and given areas of each of its bubbles, Plateau's laws yield a number of equations equal to the number of unknowns [FT01]. There may be a unique solution, but multiple solutions are of course possible [WCG02]. Furthermore, in certain area ranges there may be no solutions. We list here some propieties of equilibrated 2D foams which derive from equilibrium laws.

Centres on a Stright Line

Moukarzel has proved that for any 2D equilibrated foam the equilibrium properties imply that the centres of the circular arcs, representing the films, meeting at the same vertex, are one the same line [Mou97]. Here we re-derive this property directly from equilibrium equations (1.9) and (1.10) applied at a vertex. Let us consider a general vertex which films are labelled by $1, 2, 3$ as in fig.2.2. We fix the

vertex at the origin of the complex plane $\mathbb{C}$. In complex notation the equilibrium equations are:

$$\gamma_1\tau_1 + \gamma_2\tau_2 + \gamma_3\tau_3 = 0, \tag{2.16}$$

$$\tfrac{\gamma_1}{R_1} - \tfrac{\gamma_2}{R_2} + \tfrac{\gamma_3}{R_3} = 0, \tag{2.17}$$

where R_i and γ_i are, respectively, the positive radius and the surface tension of the films. The centres of curvature C_i, for $i = 1, 2, 3$, are:

$$C_1 = R_1 e^{i\pi/2}\tau_1, \quad C_2 = R_2 e^{-i\pi/2}\tau_2, \quad C_3 = R_3 e^{i\pi/2}\tau_3\,.$$

Using equilibrium equation, it is simply verified that the difference between two of centres is proportional, by a real factor, to the difference between other two centres. Then the three centres corresponding to a vertex are on a line. For example, using (2.16), the vector

$$C_1 - C_2 = e^{i\pi/2}(R_1\tau_1 + R_2\tau_2)$$

can be re-written as

$$C_1 - C_2 = e^{i\pi/2}\left((R_1 - \frac{\gamma_1}{\gamma_2}R_2)\tau_1 - R_2\frac{\gamma_3}{\gamma_2}\tau_3\right),$$

then, eliminating R_2 by (2.17), we find:

$$C_1 - C_2 = \frac{\gamma_3 R_1}{\gamma_3 R_1 + \gamma_1 R_3} e^{i\pi/2}(R_1\tau_1 - R_3\tau_3) = \frac{\gamma_3 R_1}{\gamma_3 R_1 + \gamma_1 R_3}(C_1 - C_3)$$

. □

Number of Edges per Bubble

First, let us note that the three–connection property implies that $V = \frac{2}{3}E$, where V and E are respectively the number of vertices and edges in the foam. Moreover, the number of bubbles, edges and vertices are related by Euler's theorem of topology for cellular structure (see [WH99, Gla89], for example) :

$$F - E + V = \chi(g) = 2 - g, \tag{2.18}$$

where χ is the *Euler characteristic* and it is a topological invariant of the space in which the cellular structure (in this case the 2D foam) is defined. g is the *genus* of the embedding space. In the case of a flat 2D foam, $\chi = 1$[1] and (2.18) implies that:

$$E = 3(F - 1), \qquad V = 2(F - 1)\,. \tag{2.19}$$

[1]Here, the outside of the F-bubble cluster is not considered as a bubble. If, on the contrary, the outside is considered as a bubble then $\chi = 2$.

Euler's theorem (2.18) and the three–connectivity imply that the average number of edges per cell $\langle n \rangle$ is given by:

$$\langle n \rangle = \frac{2E}{F+1} = 6\frac{F-1}{F+1} \quad \text{and } \langle n \rangle = 6, \text{ for } F \to \infty. \tag{2.20}$$

Pressure

By (2.2), all the E curvatures of the films are determined by the pressure p_i, for $i = 1, \ldots, F$, on any bubble. If $k_{ij} = -k_{ji}$ is the curvature of the film ij between bubbles i and j then:

$$k_{ij} = p_i - p_j, \quad \forall\ 1 \leq i \leq F+1, \tag{2.21}$$

Where p_{F+1} is the outside pressure. If $p_i > p_j$ the curvature of the film ij is positive and the centre of curvature of the bubbles is toward bubble i. If $p_i = p_j$, the curvature of the film is zero, its radius is infinite and it is a straight line. Frequently, the additive constant is chosen equal to the outside pressure, rescaling the pressure of any bubbles by $p_i \to p_i/p_{F+1}$. If the cluster is connected and F of the E curvature k_{ij} are given, using equation (2.5), it is possible to determine the pressure p_i of any bubble up to an additive constant.

Invariance under Moebius Transformations

The equilibrium equations of 2D foams are invariant under Moebius (or linear fractional or homographic) transformation [Mou97, Wea99, MO03]. Given $a\,, b\,, c$ and $d \in \mathbb{C}$, conformal mappings of the form

$$w = f(z) = \frac{az+b}{cz+d}\,, \quad \text{where} \quad ad - bc \neq 0\,, \tag{2.22}$$

are called Moebius transformations. This transformation can be extended to the entire extended complex plane $\mathbb{C}^* = \mathbb{C} \cup \{\infty\}$ by defining $f(-d/c) = \infty$ and $f(\infty) = a/c$. A linear fractional transformation is a composition of translations, rotations, dilatations, and inversions [Neh52]. Linear fractional transformations send circles and lines to circles or lines and preserve the angles. From these properties, identifying $\mathbb{R}^2$ with $\mathbb{C}^*$, it follows that the equilibrium equations of 2D flat foams, eqs. (2.2), (2.4) and (2.5), are left invariant by Moebius transformations. In other words, if $\mathcal{F}$ is the graph formed by the three–connected films (which are circular arcs) of an equilibrated 2D foam, then the 2D foam, whose graph $\mathcal{F}'$ is the image of $\mathcal{F}$ by a Moebius transformation, is also equilibrated.

Associating to any Moebius transformation (2.22) the matrix whose elements are the parameters (a, b, c, d) of the transformation:

$$\begin{pmatrix} a & b \\ c & d \end{pmatrix},$$

it results that Moebius transformations are a representation $\mathrm{SL}(2,\mathbb{C})/\{1,-1\}$ on $\mathbb{C}$.

2.5 A set of Coordinates

We see that for any 2D equilibrated foam the equilibrium implis that the centres of the films, meeting at the same vertex, are one the same line [Mou97] (see previous section, pag.20). Using these results we construct a set of coordinates for the study of equlibrated foams. Given an equilibrated cluster of F bubbles, knowing the value of F curvatures (and so, the pressures of the bubbles with respect to the outside pressure), this set of coordinates permits to describe the cluster (edges, vertices) modulo global Euclidean transformations.

Let us consider a vertex $\mathbf{v}_x$, with $x \equiv \{ijk\}$, of an equilibrated 2D foam. At $\mathbf{v}_x$, the films of curvatures k_{ij}, k_{jk}, k_{ki}, separating bubbles i, j and k, meet. Let us suppose for example that the pressures of the bubbles are $p_k < p_i < p_j$. We treat later the special cases where two or three pressures have the same value. Properties (2.2) and (2.5) imply that k_{ik}, k_{jk} and $k_{ji} = k_{jk} - k_{ik}$ are positive.

Let $\mathbf{n}_x$ be the unit vector corresponding to the direction of the line containing the centres $\mathbf{C}_{ij}$, $\mathbf{C}_{jk}$ and $\mathbf{C}_{ki}$ of the films[2]:

$$\mathbf{n}_x = \frac{\mathbf{C}_{ik} - \mathbf{C}_{jk}}{\parallel \mathbf{C}_{ik} - \mathbf{C}_{jk} \parallel}, \qquad p_k < p_i < p_j. \tag{2.23}$$

In other words, the direction of the centres' line $\mathbf{n}_x$ goes from the bubble with greatest pressure to the bubbles with smaller pressure (in this case: $p_k < p_i < p_j$, then $\mathbf{n}_x$ is directed from bubble j to i).

We define $\mathbf{O}_x$ the orthogonal projection of the vertex $\mathbf{v}_x$ on the line $\mathbf{n}_x$, θ_x as the angle $\widehat{\mathbf{v}_x\mathbf{C}_{ij}\mathbf{O}_x}$. and $C'_{\alpha\beta}(x)$ by

$$\mathbf{C}_{\alpha\beta} = \mathbf{O}_x + \mathbf{n}_x C'_{\alpha\beta}(x) \qquad \forall\, \alpha,\beta \in x \quad \alpha \neq \beta\,; \tag{2.24}$$

$C'_{\alpha\beta}(x)$ is the local coordinate of the centre $\mathbf{C}_{\alpha\beta}$ on the line associated to $\mathbf{v}_x$. The local coordinates are completly determined by the curvatures (or pressures):

$$p_k < p_i < p_j \quad \begin{cases} C'_{ik}(x) = \frac{1}{k_{ik}} \cos(\frac{\pi}{3} - \theta_x), \\ C'_{jk}(x) = \frac{1}{k_{kj}} \cos(\frac{\pi}{3} + \theta_x), \\ C'_{ij}(x) = \frac{1}{k_{ij}} \cos(\theta_x) \\ \quad \text{and} \quad \theta_x = \arctan\left(\sqrt{3}\frac{k_{ji}}{k_{ik}+k_{jk}}\right) = \arctan\left(\sqrt{3}\frac{p_j - p_i}{p_i + p_j - 2p_k}\right), \end{cases} \tag{2.25}$$

[2]The centres are symmetrically defined: $\mathbf{C}_{ki} = \mathbf{C}_{ik}$.

Where $0 \leq \theta_x \leq \frac{Pi}{3}$. Replacing the curvatures by the pressures of the bubbles, the local coordinates are (setting $\gamma = 1$):

$$p_k < p_i < p_j \quad \begin{cases} C'_{ik}(x) = \frac{1}{p_k - p_i} \frac{(p_i+p_k)-2p_j}{2\sqrt{m_x}}, \\ C'_{jk}(x) = \frac{1}{p_j - p_k} \frac{(p_j+p_k)-2p_i}{2\sqrt{m_x}}, \\ C'_{ij}(x) = \frac{1}{p_i - p_j} \frac{(p_i+p_j)-2p_k}{2\sqrt{m_x}} \\ \quad \text{and} \quad m_x \equiv (p_i^2 + p_j^2 + p_k^2 - p_i p_j - p_j p_k - p_k p_i)\,. \end{cases} \tag{2.26}$$

m_x is a positive quantity for any value of the pressures p_i, p_j and p_k (which are supposed different). In fact

$$2m_x = (k_{ij})^2 + (k_{jk})^2 + (k_{ki})^2 \geq 0\,.$$

Let us consider now the whole cluster. Moreover we suppose that the pressures of the bubbles are known and that no two closed bubbles have the same pressure. Each film touches two vertices, so the centres of curvature of any film can be written in terms of the local coordinates related to the two vertices that the film touches. For example, let $\{ijk\}$ and $\{ijl\}$ be two vertices joined by the film ij which separetes bubbles i and j. Then

$$\mathbf{C}_{ij} = \mathbf{O}_{\{ijk\}} + \mathbf{n}_{\{ijk\}} C'_{ij}(\{ijk\}) = \mathbf{O}_{\{ijl\}} + \mathbf{n}_{\{ijl\}} C'_{ij}(\{ijl\})\,, \tag{2.27}$$

$$\text{or} \qquad \mathbf{O}_{\{ijk\}} - \mathbf{O}_{\{ijl\}} + \mathbf{n}_{\{ijk\}} C'_{ij}(\{ijk\}) - \mathbf{n}_{\{ijl\}} C'_{ij}(\{ijl\}) = 0 \tag{2.28}$$

Equation (2.28) has to be verified for all the E edges of the foam. So we have a linear system of E vectorial equations ($2E$ scalar eqs.) in the $3V$ unknown quantities $\mathbf{n}_x$ (unit vector) and $\mathbf{O}_x$ (vector). The system of equations defined by (2.28) is clearly invariant under global Euclidean transformations.

In the case where two pressures are equal, for example $p_i = p_j$, the film ij has zero curvature ($k_{ij} = 0$) and it is a straight line (infinite radius of curvature). By (2.5) it results that $k_{jk} = k_{ik}$. Taking the limit of 2.25 where $k_{ij} \to 0$, we obtain:

$$p_k < p_i = p_j = p \quad \begin{cases} \theta_x = 0, \\ C'_{ik}(x) = \frac{1}{2(p-p_k)}, C'_{jk}(x) = \frac{1}{2(p_k-p)}, \\ C'_{ij}(x) = \infty\,. \end{cases} \tag{2.29}$$

So, when two bubbles meeting at a vertex have the same pressure, different from the third one, the vertex and the centers of the two curved films form an equilateral triangle of edge equal to the radius of the curved edges.

In the case where the pressures of three bubbles meeting at a vertex are equal, the curvatures of the films are all zero. The local coordinates relative to this vertex are indefinite and the line containing the centres can not be defined.

This case has to be treated separately and the missing equations in the system (2.28), corresponding to the three straight edges, can be replaced by imposing the symmetry of the vertex. We do not treat this case here. At present we are working on a program which, starting from the pressure vector and topology, of the cluster, will be able to build the corresponding equilibrated cluster (see figure 2.9).

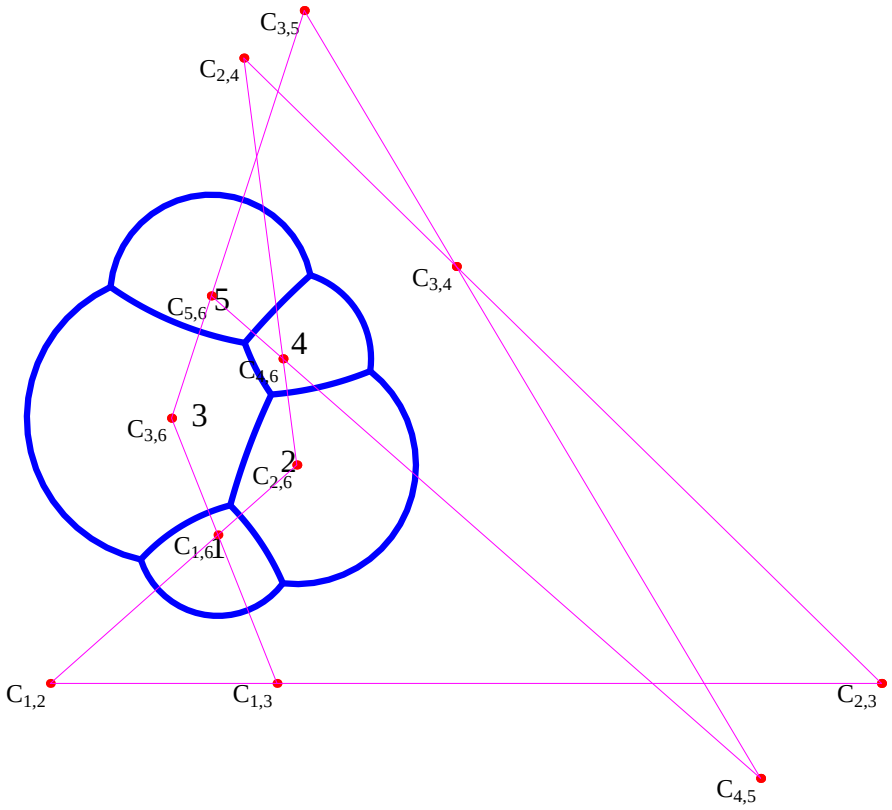

Figure 2.9: Vertex lines and centres of curvature of the films in a simple cluster. Let us note that some centres, as for example $\mathbf{C}_{3,6}$, $\mathbf{C}_{4,6}$ $\mathbf{C}_{3,4}$, are aligned also if there is not an associate vertex. This property is treated in chapter 5.

Chapter 3

Foams in Contact with a Solid Wall

Although soap foams can be theoretically considered as isolated systems, in any experimental set-up or application foams are usually in contact with some solid wall. For instance, dish washing, shaving cream, container decontamination, penetration and dispersion through porous media like rocks, etc., involve contacts with solid surfaces.

The contact of the foam with the boundary surface gives rise to a 2D pattern on the contact surface. Experimentally two–dimensional soap foams can be obtained looking at the traces of the films on one of two parallel glass plates which trap the foam (Hele–Shaw cell) [WH99, CDK04]. Reinelt, Boltenhagen and Rivier studied, using equilibrium and symmetry properties, the shapes of the film trace of an equilibrated 3D foam in a cylindrical tube [RBR01]. Drenckhan, Weaire and Cox, analysed the pattern formed by a monodisperse foam sandwiched between two non–parallel plates (non–conventional Hele–Shaw cell) showing that it looks like the image of a hexagonal honeycomb two–dimensional foam through a conformal transformation which depends on the form of the plates [DWC04]. We look at this problem in the next chapter.

Let us consider a very common experiment where a three–dimensional foam (dry, in the limit where the liquid fraction tends to zero) is in contact with a glass surface, or somewhat similar transparent and rigid material [MS05, RBR01, DWC04, CDK04]. Let us suppose the surface rigid, clean and smooth, allowing the foam's films to slide and so, to achieve equilibrium. Regarding the shape formed on the surface by the films which are in contact with it, we could ask if there exist some equilibrium laws for this figure and, in the affirmative case, what these laws are. The answer is affirmative. The three–dimensional equilibrium equations, (1.2) and (1.3), and Young's relation for the contact angle imply equilibrium laws for the vertex on the surface where three films meet (two–

dimensional vertex in the tangent plane).

In the case where each film is in normal incidence with the rigid surface, the equilibrium equations are similar to Plateau's laws (2.4) and (2.5) for two–dimensional foams, except that, in this case equation (2.5) is valid only at vertices and the films are not longer circular arcs. At equilibrium, at any vertex on the surface, the sum of the unit tangent vectors to the films and the sums of the geodesic curvatures of the films are zero. The geodesic curvature of a film on the surface is the projection, on the plane tangent to the surface, of the curvature vector of the film. These equations are invariant for analytical transfomations. These properties of equilbrium are proved in [MO05b] and the invariance under analytical transfomations is showed in [MO05a].

In this chapter, after a small review of the elementary differential geometry which we use in the proofs, the contact of a film with a smooth rigid surface is studied and the normal incidence of the film with a solid boundary, in the case of standard foam, is shown. Successively, the equilibrium equations at the surface and their invariance for analytical transformations are proved. The example of the Hele–Shaw cell, used to realize 2D foams experimentally, is given. In section 3.4, we give some extensions dealing with the cases where the surface tension along the solid varies from cell to cell, so that the contact angle is not $\pi/2$.

3.1 Some Geometrical Tools

In this section we give some definitions and properties of the geometrical quantities which we use in the rest of the chapter. Good references to this section are found in several books [Mor98, DFN92, Spi79]. We give the definitions of a curve in space and its *curvature vector*. Let $\boldsymbol{\phi} : [t_1, t_2] \to \mathbb{R}^3$, $t \mapsto \boldsymbol{\phi}(t)$, be a parameterized curve and $\boldsymbol{\tau} = \dot{\boldsymbol{\phi}}/|\dot{\boldsymbol{\phi}}|$ its unit tangent vector. The curvature vector $\boldsymbol{\kappa}$ is defined as the rate of change of $\boldsymbol{\tau}$ with respect to arc length s:

$$\boldsymbol{\kappa} = \frac{\mathrm{d}\boldsymbol{\tau}}{\mathrm{d}s} = \frac{\dot{\boldsymbol{\tau}}}{|\dot{\boldsymbol{\phi}}|} \,. \tag{3.1}$$

$\boldsymbol{\kappa}$ is orthogonal to the tangent vector $\boldsymbol{\tau}$ and its modulus $\kappa = |\boldsymbol{\kappa}|$ is the scalar curvature; it gives the rate of turning of $\boldsymbol{\tau}$. Let $\mathcal{S}$ be a surface embedded in $\mathbb{R}^3$. On $\mathcal{S}$ we make the following assumptions:

- $\mathcal{S}$ is, locally, the graph of a function with continuous second derivatives (C^2).
- If $\mathbf{p} \in \mathcal{S}$ is a point of the surface, the *tangent plane* of all tangent vectors to $\mathcal{S}$ at $\mathbf{p}$ is denoted by $T_p\mathcal{S}$.
- The normal vector to $\mathcal{S}$ at $\mathbf{p}$ is denoted by $\mathbf{n}$.

Considering the planes containing $\mathbf{n}$ through $\mathbf{p}$, these intersect the surface $\mathcal{S}$ forming curves. Each one of these planes is determined by $\mathbf{n}$ and a unit vector in the tangent plane $\mathbf{a} \in T_p\mathcal{S}$. The curvature of such curves must be a multiple of $\mathbf{n}$:

$$\boldsymbol{\kappa} = k_n(\mathbf{a}, \mathcal{S})\, \mathbf{n}\,, \tag{3.2}$$

where $k_n(\mathbf{a}, \mathcal{S}) = \pm\kappa$ is the signed scalar curvature (the sign depends on the choice of $\mathbf{n}$). In fact, at $\mathbf{p}$, the curvature vector of the curve, obtained by the intersection of such a plane with $\mathcal{S}$, is orthogonal to $\mathbf{a}$, thus proportional to $\mathbf{n}$. $k_n(\mathbf{a}, \mathcal{S}) = \pm\kappa$ is also called the *sectional curvature* of $\mathcal{S}$ in the direction $\mathbf{a}$ at $\mathbf{p}$.

Spanning all possible such planes, the directions $\mathbf{v}_1$ and $\mathbf{v}_2$, where $\kappa = \lambda_1$, λ_2 takes the maximum and minimum value, are called the *principal directions* (λ_1, and λ_2, are the *principal curvatures*) of $\mathcal{S}$ at $\mathbf{p}$. Let us see now some properties of these vectors.

Up to second order around $\mathbf{p}$ the surface $\mathcal{S}$ is the graph of a quadratic form $q(\mathbf{a}, \mathbf{a})$ defined in the tangent plane T_pS with ordinate axis parallel to $\mathbf{n}$. The corresponding symmetric bi–linear form defines the curvature (linear) operator Q by $q(\mathbf{a}, \mathbf{b}) = \mathbf{a} \cdot Q\mathbf{b}$ for all $\mathbf{a}, \mathbf{b}$ in $T_p\mathcal{S}$. If at $\mathbf{p}$, the surface $\mathcal{S}$ is parallel to the x, y-plane, the operator Q corresponds to the Hessian of the function which is, locally, the graph of $\mathcal{S}$.

Since Q is symmetric, it is diagonalizable. It results that the principal directions $\mathbf{v}_1$ and $\mathbf{v}_2$, when $\lambda_1 \neq \lambda_2$, are the eigenvectors of Q and they form an orthogonal basis of $T_p\mathcal{S}$. The *mean curvature* H and the *Gaussian curvature* G of $\mathcal{S}$ at $\mathbf{p}$ are defined, respectively as half the trace and as the determinant of Q at $\mathbf{p}$:

$$\mathrm{H} = \frac{1}{2}\mathrm{tr}\, Q = \frac{\lambda_1 + \lambda_2}{2}\,, \tag{3.3}$$

$$\mathrm{G} = \det Q = \lambda_1\lambda_2\,. \tag{3.4}$$

The bi–linear form $q(\mathbf{a}, \mathbf{b})$ is called the *second fundamental form*. Let $(u^1, u^2) \mapsto \mathbf{x}(u^1, u^2)$ be a local parameterization (or coordinates) of $\mathcal{S}$, where $\mathbf{x} : A \subset \mathbb{R}^2 \to \mathcal{S}$ is a diffeomorphism between a domain $\mathcal{A}$ in the u^1, u^2-plane and the surface. The first and the second fundamental forms are usually defined as

$$\mathrm{I}: \quad \mathbf{x}_i du^i \cdot \mathbf{x}_j du^j = g_{ij}\, du^i du^j \quad \Rightarrow g_{ij} = \mathbf{x}_i \cdot \mathbf{x}_j\,; \tag{3.5}$$

$$\mathrm{II}: \quad q(\mathbf{x}_i du^i, \mathbf{x}_j du^j) = q_{ij}\, du^i du^j \quad \Rightarrow q_{ij} = \mathbf{x}_{ij} \cdot \mathbf{n}\,, \tag{3.6}$$

where $\mathbf{x}_i = \partial\mathbf{x}/\partial u^i$, $i, j = 1, 2$ and summation is implicitly assumed over repeated indices. g_{ij} and q_{ij} are the matrices associed respectively to I and II with respect to the basis (x_1, x_2). The vectors $\mathbf{x}_i$ are in the tangent plane $T_p\mathcal{S}$. If Q^i_j denotes the matrix defined by $Q\mathbf{x}_i = \mathbf{x}_j Q^j_i$, then $q_{ij} = \mathbf{x}_i \cdot Q\mathbf{x}_j = g_{ik}Q^k_j$ or, as 2×2 matrices,

$$Q = g^{-1}q. \tag{3.7}$$

The identity $\mathbf{n}\cdot\mathbf{a}=0$ for all $\mathbf{a}$ in T_pS implies $\mathbf{n}_i=\partial\mathbf{n}/\partial u^i=-\mathbf{x}_jQ_i^j$.

While II is linked to the curvature of a curve on the surface, the first fundamental form I is the *metric* induced by the restriction of the scalar product of $\mathbb{R}^3$. It is symmetrical and positive definite and it is related to measurements inside the surface. Given a curve in $\mathcal{S}$ with coordinates $u(t)=(u^1(t),u^2(t))$, the arc length of this curve is given by:

$$l=\int_{t_0}^{t_1}|\dot{\mathbf{x}}|\,\mathrm{d}t=\int_{t_0}^{t_1}|\mathbf{x}_i\dot{u}^i|\,\mathrm{d}t=\int_{t_0}^{t_1}\sqrt{g_{ij}\dot{u}^i\dot{u}^j}\,\mathrm{d}t\,. \tag{3.8}$$

So the infinitesimal arc length, in eq.(3.1), is given by $\mathrm{d}s^2=g_{ij}\dot{u}^i\dot{u}^j$. Moreover it is related to the area of a domain U on $\mathcal{S}$:

$$A(U)=\int_U dA=\iint_U\sqrt{g}\,du^1du^2\,, \tag{3.9}$$

where

$$\sqrt{g}=\sqrt{\det g}=\sqrt{g_{11}g_{22}-g_{12}^2}=(\mathbf{x}_1^2\mathbf{x}_2^2-(\mathbf{x}_1\cdot\mathbf{x}_2)^2)^{1/2}\,. \tag{3.10}$$

The sectional curvature, eq. (3.2), of S in the direction $\boldsymbol{\tau}\in T_pS$ is [DFN92]:

$$k_n(\boldsymbol{\tau},S)=\frac{\mathrm{II}(\boldsymbol{\tau},\boldsymbol{\tau})}{\mathrm{I}(\boldsymbol{\tau},\boldsymbol{\tau})}=\frac{q_{ij}\,du^idu^j}{g_{ij}\,du^idu^j}=\boldsymbol{\tau}\cdot Q\boldsymbol{\tau}. \tag{3.11}$$

The eigenvalues λ_i, for $i=1,2$, of Q are the eigenvalues of the second fundamental form with respect to the metric, in fact:

$$\det(Q-\lambda_i\mathbb{1})=\det(q-\lambda_ig)=\lambda^2-\lambda\,\mathrm{tr}\,Q+\det Q=\lambda_i^2-2H\lambda_i+G=0\,. \tag{3.12}$$

In the last equality, definitions (3.3-3.4) and the property of 2×2 matrices determinant are used. So, completing $\boldsymbol{\tau}$ into an orthonormal basis $(\boldsymbol{\tau},\boldsymbol{\tau}^\perp)$ of $T_p\mathcal{S}$ and calling α the angle between $\mathbf{v}_1$ and $\boldsymbol{\tau}$, the change of coordinates between orthogonal basis implies (Euler's Theorem):

$$k_n(\boldsymbol{\tau},S)=\boldsymbol{\tau}\cdot Q\boldsymbol{\tau}=\lambda_1\cos^2\alpha+\lambda_2\sin^2\alpha, \tag{3.13}$$

or, since λ_1,λ_2 are the solutions of the characteristic equation (3.12):

$$k_n(\boldsymbol{\tau},S)=H+(H^2-G)^{1/2}\cos(2\alpha)\,. \tag{3.14}$$

Moreover, recalling the invariance of the trace by similarity:

$$2H=\lambda_1+\lambda_2=\boldsymbol{\tau}\cdot Q\boldsymbol{\tau}+\boldsymbol{\tau}^\perp\cdot Q\boldsymbol{\tau}^\perp=k_n(\boldsymbol{\tau},S)+k_n(\boldsymbol{\tau}^\perp,S) \tag{3.15}$$

for any orthonormal pair $(\boldsymbol{\tau},\boldsymbol{\tau}^\perp)$ of tangent vectors.

We write also another expression for H, which we will use in the next chapter. Writing the trace of Q by equation (3.7):

$$2H = \operatorname{tr} Q = g^{ij} q_{ij} = \frac{1}{\det g} \left(|\mathbf{x}_1|^2 \, \mathbf{x}_{22} - 2(\mathbf{x}_1 \cdot \mathbf{x}_2) \, \mathbf{x}_{12} + |\mathbf{x}_2|^2 \, \mathbf{x}_{11} \right) \cdot \mathbf{n} \,, \tag{3.16}$$

where g^{ij} is the inverse of g_{ij}:

$$g^{-1} = \frac{1}{\det g} \begin{pmatrix} g_{22} & -g_{12} \\ -g_{12} & g_{11} \end{pmatrix} . \tag{3.17}$$

When a curve $\boldsymbol{\phi}$ (parameterized by arc length s) is embedded in a surface S, its tangent vector $\dot{\boldsymbol{\phi}}(s)$ is, of course, in the tangent plane $T_{\boldsymbol{\phi}(s)}\mathcal{S}$. Its curvature vector $\mathbf{k} = \ddot{\boldsymbol{\phi}}(s)$, always perpendicular to the curve, may be decomposed into

$$\mathbf{k} = \mathbf{k}_g + \mathbf{k}_n = k_g(\boldsymbol{\phi}, S) \, \mathbf{n} \wedge \dot{\boldsymbol{\phi}} + k_n(\boldsymbol{\phi}, S) \, \mathbf{n} \,, \tag{3.18}$$

where $\mathbf{b}(\boldsymbol{\phi}, \mathcal{S}) = \mathbf{n} \wedge \dot{\boldsymbol{\phi}}$ is the co–normal to $\mathcal{S}$ in $\boldsymbol{\phi}(s)$; it is the unit vector in the tangent plane, orthogonal to $\dot{\boldsymbol{\phi}}(s)$. The component $k_g(\boldsymbol{\phi}, S)$ tangent to the surface is the *geodesic curvature* of $\boldsymbol{\phi}$ in S; the other is the normal curvature $k_n(\boldsymbol{\phi}, S)$ which coincides with the sectional curvature of S in the direction $\dot{\boldsymbol{\phi}}$: $k_n(\dot{\boldsymbol{\phi}}, S)$.

3.2 Contact with a Boundary

When a liquid is deposited on a solid substrate (or liquid) it spreads on to the solid surface, wetting it differently depending on the mutual properties of the liquid, the substrate and the surrounding gas. The wetting is called *total* if the liquid is strongly attracted by the solid and a liquid film (*the wetting film*) covers the entire surface.

If the wetting is not total it is called *partial* (or non–wetting). The three phases meet in a line (*triple line*). At the triple line, the liquid–gas interface forms an angle θ with the solid surface (figure 3.1), obeying Young's relation [dGBWQ02]:

$$\gamma \cos\theta = \gamma_{SG} - \gamma_{SL} \,. \tag{3.19}$$

The *contact angle* is related to the surface tension of the three interfaces ($G/S/L$: γ, γ_{SG} and γ_{SL}).
Equation (3.19) is obtained by projecting the forces at equilibrium on the solid surface.

Young's equation is valid also when the liquid L is replaced by another gas G′ and the interface between the gases is a thin film. In the limit where its thickness tends to zero, then

$$\gamma \cos\theta = \gamma_1 - \gamma_2 \,, \tag{3.20}$$

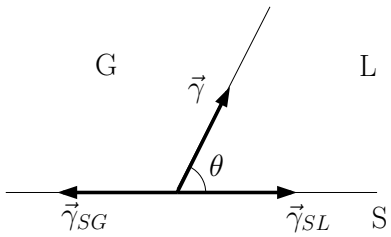

Figure 3.1: Contact angle θ at the triple line (vertical section).

where γ_1 and γ_2 are the surface tensions of the two gas–solid interfaces. Usually, in the case of foams, the bubbles contain the same gas so that $\gamma_1 = \gamma_2$ and $\cos\theta = 0$. This condition of *normal incidence* is typical of soap froth; it is also valid when the soap solution wets the solid surface, provided the wetting films on both sides have similar surface tension.

3.3 Equilibrium Conditions at a Boundary

Here, we derive equilibrium equations, analogous to Plateau's laws, valid for the 2D foam formed by the contacts of the films of a dry 3D foam with the solid boundary. The main assumptions are the equilibrium of the foam and the normal incidence condition with the boundary which is a solid smooth surface. We relax also the hypothesis of constant surface tensions for the foam, (non–standard foams, section 1.1), and we find the equilibrium equations at a boundary in this more general case.

Let us consider an equilibrated dry 3D foam which is in contact with a solid surface $\mathcal{S}$. $\mathcal{S}$ may be curved, but must be solid and smooth to prevent film pinning by irregularities and ensure relaxation to equilibrium. Contact with non rigid walls such as elastic membranes or an interface with another fluid medium must be treated differently; in a number of cases, at least for statics, flexible surfaces may be included as part of the foam with a surface tension differing from the rest of the foam. Smoothness rules out corners, wedges as well as dirty or fractal surfaces. Usually, the films are pinned by such irregularities.

At each edge of the foam, the equilibrium implies the laws (eqs. (1.9) and (1.10)):

$$\sum_{j=1}^{3} \gamma_j \mathbf{b}_j = 0\,, \tag{3.21}$$

$$\sum_{j=1}^{3} \gamma_j H_j = 0\,, \tag{3.22}$$

A Plateau border is a line $\boldsymbol{\psi}$ at the junction of three films $\mathcal{F}_j$, $j = 1, 2, 3$. We call this a *triple*. These films and border are in contact with $\mathcal{S}$. The contact of each film $\mathcal{F}_j$ gives rise to a line $\boldsymbol{\phi}_j$ in S; these three lines emanate from a vertex

p of the 2D foam that is the contact of the border $\boldsymbol{\psi}$ with $\mathcal{S}$ (fig. 3.2). Unless otherwise specified, all the curves are parameterized by arc length s with $s = 0$ at **p**. Then, for any curve $\boldsymbol{\phi}$, $\boldsymbol{\tau} = \dot{\boldsymbol{\phi}} = \frac{d}{ds}\boldsymbol{\phi}$ is the unit vector field tangent to $\boldsymbol{\phi}$.

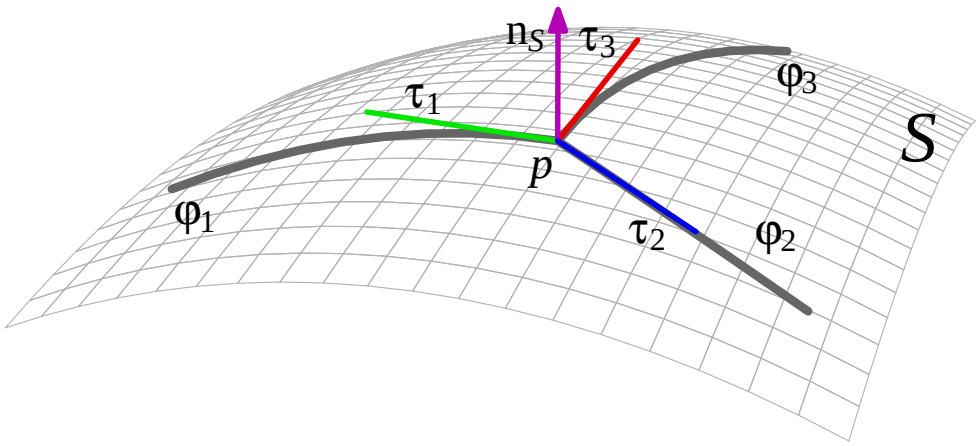

Figure 3.2: The neighbourhood of a vertex **p** of a 2D foam: three films and a Plateau border meet at **p** on the solid surface $\mathcal{S}$.

Assume normal incidence on $\mathcal{S}$ as implied by equilibrium for real soap froth on clean surfaces. Then
At **p**, *common to* $\mathcal{F}_1$, $\mathcal{F}_2$, $\mathcal{F}_3$ *and* $\mathcal{S}$, *the following equations are verified:*

$$\sum_{j=1}^{3} \gamma_j \boldsymbol{\tau}_j = 0, \tag{3.23}$$

$$\sum_{j=1}^{3} \gamma_j k_g(\boldsymbol{\phi}_j, \mathcal{S}) = 0, \tag{3.24}$$

where $k_g(\boldsymbol{\phi}_j, \mathcal{S})$ *is the geodesic curvature of* $\boldsymbol{\phi}_j$ *in* $\mathcal{S}$.

When all the film tensions are equal, $\gamma_j = \gamma$, the triangles representing the vector sums in (3.21) and (3.23) are equilateral and the Plateau angles are $2\pi/3$.

For the proofs of (3.21) and (3.22), we use two lemmas. The following lemmas are valid in full generality. The normal incidence assumption will only be used to prove the main equations (3.23), (3.24).

Lemma 3.1. *Let $\mathcal{F}, \mathcal{S}$ be two smooth embedded surfaces nowhere tangent to each other, intersecting transversely on a line $\boldsymbol{\phi}$. Then the geodesic and normal curvatures satisfy the following relation at any intersection point $\mathbf{x}$:*

$$\begin{pmatrix} k_g(\boldsymbol{\phi}, \mathcal{S}) \\ k_n(\boldsymbol{\phi}, \mathcal{S}) \end{pmatrix} = \begin{pmatrix} \cos\theta & -\sin\theta \\ \sin\theta & \cos\theta \end{pmatrix} \begin{pmatrix} k_g(\boldsymbol{\phi}, \mathcal{F}) \\ k_n(\boldsymbol{\phi}, \mathcal{F}) \end{pmatrix} \tag{3.25}$$

where θ is the angle between the two surfaces at $\mathbf{x}$.

On an edge $\boldsymbol{\psi}$, the tangent vector $\dot{\boldsymbol{\psi}}$, the unit normal $\mathbf{n}_j$ (short for $\mathbf{n}_{\mathcal{F}_j}$) and the co–normal $\mathbf{b}_j$ form an orthonormal basis for each i. The circular sign convention implies the following:

Lemma 3.2. *On a Plateau border $\boldsymbol{\psi}$ the first equilibrium equation (3.21) is equivalent to*

$$\sum_{j=1}^{3} \gamma_j \mathbf{n}_j = 0. \tag{3.26}$$

In turn, (3.26) implies

$$\textstyle\sum_{j=1}^{3} \gamma_j k_n(\boldsymbol{\psi}, \mathcal{F}_j) = 0\,, \tag{3.27}$$

$$\textstyle\sum_{j=1}^{3} \gamma_j k_g(\boldsymbol{\psi}, \mathcal{F}_j) = 0\,. \tag{3.28}$$

Moreover the pair (3.27), (3.28) is equivalent to (3.26) at all points where $\boldsymbol{\psi}$ is curved.

Proof of Lemma 3.1

In the plane perpendicular to $\boldsymbol{\phi}$ at $\mathbf{x}$, the two orthonormal bases $(\mathbf{n}_F, \mathbf{n}_F \wedge \dot{\boldsymbol{\phi}})$ and $(\mathbf{n}_S, \mathbf{n}_S \wedge \dot{\boldsymbol{\phi}})$ are rotated by θ with respect to each other. Equation (3.25) is the coordinate change formula applied to the curvature vector $\mathbf{k}$ (section 3.1). □

Proof of Lemma 3.2

The vector product of (3.21) with $\dot{\boldsymbol{\psi}}$ gives (3.26).

One gets (3.27) and (3.28) by taking the scalar product of (3.26) with, respectively, the curvature vector $\mathbf{k} = \ddot{\boldsymbol{\psi}}$ and $\dot{\boldsymbol{\psi}} \wedge \mathbf{k}$ and applying the definitions of normal and geodesic curvatures (3.18). When $\mathbf{k} \neq 0$, the reciprocal is also guaranteed because $(\mathbf{k}, \dot{\boldsymbol{\psi}} \wedge \mathbf{k})$ constitutes an orthogonal basis of the plane perpendicular to $\dot{\boldsymbol{\psi}}$ where the vectors in (3.26) are always confined. □

Proof of equation (3.23)

Because of normal incidence, the tangent $\dot{\boldsymbol{\phi}}_j(0)$ coincides with the co–normal $\mathbf{b}_j \equiv \mathbf{b}(\boldsymbol{\psi}, \mathcal{F}_j)$ at $\mathbf{p}$. Thus (3.23) is just a rewriting of (3.21). □

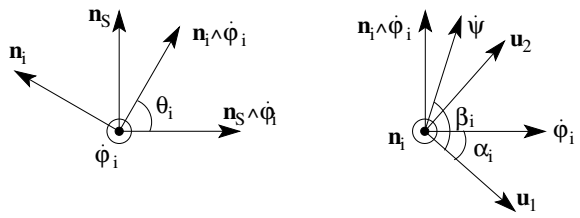

Figure 3.3: Relevant vectors in $\dot{\boldsymbol{\phi}}_j^{\perp}$ (left) and in $T_p\mathcal{F}_j$ (right).

Proof of equation (3.24)

By normal incidence again, $\dot{\boldsymbol{\psi}}$ and $\dot{\boldsymbol{\phi}}_j$ form an orthonormal basis in the tangent plane $T_p\mathcal{F}_j$. Therefore, as trace of the curvature operator (3.15),

$$H_j = \frac{1}{2}\left(k_n(\boldsymbol{\phi}_j, \mathcal{F}_j) + k_n(\boldsymbol{\psi}, \mathcal{F}_j)\right).$$

The linear combination with coefficients γ_j yields

$$\sum_{j=1}^{3} 2\gamma_j H_j = \sum_j \gamma_j k_n(\boldsymbol{\phi}_j, \mathcal{F}_j) + \sum_j \gamma_j k_n(\boldsymbol{\psi}, \mathcal{F}_j).$$

The left hand side is zero by Laplace (3.22). The last term on the right vanishes by (3.27). Normal incidence, (3.25) with $|\theta| = \pi/2$, gives $k_g(\boldsymbol{\phi}_j, \mathcal{S}) = -k_n(\boldsymbol{\phi}_j, \mathcal{F}_j)$ and concludes. □

3.4 Bubble–Glass contact with Different Surface Tensions

When the surface tension along the solid surface differs from cell to cell, the incidence is not normal anymore. Let us treat this case.

Consider, again, an equilibrated triple $(\boldsymbol{\psi}, \mathcal{F}_1, \mathcal{F}_2, \mathcal{F}_3)$ Each of the contact angles $\theta_j = \angle(\mathbf{n}_j, \mathbf{n}_S), j = 1, 2, 3$, satisfies Young's law (3.20), the force balance projected tangentially into the surface. The component along the normal axis $\mathbf{n}_S$ involves the normal reaction of the glass, which is an additional unknown.

If $\boldsymbol{\phi}_j$ is the contact curve $\mathcal{F}_j \cap \mathcal{S}$, $\dot{\boldsymbol{\phi}}_j$ is normal to both $\mathbf{n}_j$ and $\mathbf{n}_S$ (fig. 3.3), so that

$$\mathbf{n}_S \cdot \mathbf{n}_j = \cos\theta_j, \qquad \mathbf{n}_S \wedge \mathbf{n}_j = \dot{\boldsymbol{\phi}}_j \sin(\theta_j). \tag{3.29}$$

The following equations follow from taking the dot and cross products of $\mathbf{n}_S$ with Plateau's law (3.26):

$$\textstyle\sum_{j=1}^{3} \gamma_j \cos(\theta_j) = 0, \tag{3.30}$$

$$\textstyle\sum_{j=1}^{3} \gamma_j \dot{\boldsymbol{\phi}}_j \sin(\theta_j) = 0. \tag{3.31}$$

Regarding the curvatures, we shall prove the following: at the triple point $\mathbf{p} = \boldsymbol{\psi} \cap \mathcal{S}$,

$$\sum_j \gamma_j \left[k_n(\boldsymbol{\phi}_j, \mathcal{S}) \cos\theta_j - k_g(\boldsymbol{\phi}_j, \mathcal{S}) \sin\theta_j\right] = \sum_j \gamma_j (H_j^2 - G_j)^{1/2} \cos(2\alpha_j). \tag{3.32}$$

It involves the angle $\alpha_j = \angle(\mathbf{u}_1(\mathcal{F}_j), \dot{\boldsymbol{\phi}}_j)$ between the curve $\boldsymbol{\phi}_j$ and the first principal direction of $\mathcal{F}_j$.

Equations (3.31), (3.32) are the analogous of (3.23), (3.24). In the present case where the films are not perpendicular to the solid surface, the equations in the boundary do not decouple from the full problem of the 3D foam.

Let us derive now the equilibrium equation (3.32).

Let $(\mathbf{u}_1, \mathbf{u}_2) = (\mathbf{u}_1(\mathcal{F}_j), \mathbf{u}_2(\mathcal{F}_j))$ be the principal directions of $\mathcal{F}_j$. We use the following angles: $\alpha_j = \angle(\mathbf{u}_1, \dot{\boldsymbol{\phi}}_j)$, $\beta_j = \angle(\mathbf{u}_1, \dot{\boldsymbol{\psi}})$, $\theta_j = \angle(\mathbf{n}_S, \mathbf{n}_j)$;

$$\begin{pmatrix} \dot{\boldsymbol{\phi}}_j & \dot{\boldsymbol{\psi}} \end{pmatrix} = \begin{pmatrix} \mathbf{u}_1 & \mathbf{u}_2 \end{pmatrix} \begin{pmatrix} \cos\alpha_j & \cos\beta_j \\ \sin\alpha_j & \sin\beta_j \end{pmatrix}. \tag{3.33}$$

As both $\boldsymbol{\phi}_j$ and $\boldsymbol{\psi}$ are curves in $\mathcal{F}_j$, equation (3.14) reads

$$k_n(\dot{\boldsymbol{\phi}}_j, \mathcal{F}_j) = H_j + (H_j^2 - G_j)^{1/2} \cos(2\alpha_j), \tag{3.34}$$

$$k_n(\dot{\boldsymbol{\psi}}, \mathcal{F}_j) = H_j + (H_j^2 - G_j)^{1/2} \cos(2\beta_j). \tag{3.35}$$

Putting the coefficients γ_j and summing (3.34, 3.35) over the triple around $\boldsymbol{\psi}$ gives

$$\sum_j \gamma_j k_n(\dot{\boldsymbol{\phi}}_j, \mathcal{F}_j) = \sum_j \gamma_j (H_j^2 - G_j)^{1/2} \cos(2\alpha_j), \tag{3.36}$$

$$\sum_j \gamma_j k_n(\dot{\boldsymbol{\psi}}, \mathcal{F}_j) = \sum_j \gamma_j (H_j^2 - G_j)^{1/2} \cos(2\beta_j) = 0. \tag{3.37}$$

The second vanishes by (3.27). In the first, (3.25) allows to express the left hand side in terms of curvatures in $\mathcal{S}$:

$$\textstyle\sum_j \gamma_j \left[k_n(\boldsymbol{\phi}_j, \mathcal{S}) \cos\theta_j - k_g(\boldsymbol{\phi}_j, \mathcal{S}) \sin\theta_j\right] = \sum_j \gamma_j (H_j^2 - G_j)^{1/2} \cos(2\alpha_j). \tag{3.38}$$

This is (3.32). □

The equations for the case of normal incidence follow from the general ones. Indeed, $|\theta_j| = \pi/2 = |\beta_j - \alpha_j|$ implies $\cos(2\beta_j) = -\cos(2\alpha_j)$; then, in (3.32), the $\cos\theta_j$ term disappears from the LHS and the RHS is zero by (3.37), so that (3.32) reduces to (3.24).

3.5 Invariance Properties of Equilibrium Laws

Conformal invariance is a remarkable property of the models of equilibrated foams. Of course, the exact symmetry group depends on the dimension and on the model, that is, on the set of equations fulfilled at equilibrium. The equations may be divided into two sets: *i*) the film, or cell boundaries, Young–Laplace equation ($\Delta P = 2\gamma H$); *ii*) Plateau's laws (3.21, 3.22), or their 2D counterparts (3.23, 3.24), for the Plateau borders, which are the co–dimension 2 skeleton of the cellular complex.

In standard foams, without any externally applied field, the films are constant mean curvature surfaces (CMCS). In general, this property is not preserved by conformal mappings of the embedding space or region.

When external fields, such as gravity or electromagnetic forces, act on the foam, the films may not be CMCS anymore. This is also the case when the embedding space is not flat, as for foams on a curved wall [AL92, PGL93]. Indeed, the pressure difference is the sum of two curvatures: the geodesic (longitudinal) one and the normal one, which may both vary along the curve even if the sum H is constant. This is the more general situation considered here. If only the second set of equations is kept (Plateau), then the symmetry group is the group of conformal transformations. Let us treat the higher dimensional case first.

Conformal invariance of the Plateau borders

In Euclidean spaces of dimension larger than 2, any conformal transformation is the composition of similarities (translations, rotations, dilatation) and inversions (Liouville Thorin theorem [DFN92]).

In a dry 3 or D-dimensional foam, consider a triple made of a Plateau border ψ and three films $\mathcal{F}_j$, $j = 1, 2, 3$. Then *the line equilibrium equations (3.21) and (3.22) are preserved by conformal transformations of space.*

Our proof is similar to that of [Wea99]. By definition of conformality, equation (3.21), stating that the dihedral angles between the films $\mathcal{F}_j$ at ψ are constant, is invariant by conformal transformations.

Next, let us treat (3.22). In Liouville Thorin's decomposition, the similarities obviously preserve (3.21) and (3.22), so we only need to check invariance for inversions. Let $\mathbf{r}_j \in \mathbb{R}^3$ be the position of a point in $\mathcal{F}_j$ and H_j the mean curvature at that point. Under the inversion $\tilde{\mathbf{x}} = \frac{\mathbf{x}}{x^2}$, the mean curvature transforms to $\tilde{H}_j$ given by [Wil96]:

$$\tilde{H}_j = -H_j r_j^2 - 2\,\mathbf{r}_j \cdot \mathbf{n}_j. \tag{3.39}$$

Then for any point $\mathbf{r}$ of $\tilde{\psi}$, the image of ψ, thus common to all the $\tilde{\mathcal{F}}_j$, the linear

combination with coefficients γ_j yields

$$\sum_{j=1}^{3} \gamma_j \tilde{H}_j = -r^2 \sum_{j=1}^{3} \gamma_j H_j - 2\,\mathbf{r} \cdot \sum_{j=1}^{3} \gamma_j \mathbf{n}_j. \tag{3.40}$$

The terms on the right hand side of (3.40) vanish by (3.22) and (3.26) respectively, proving the claim. □

Obviously, the tetrahedral figures around equilibrated vertices in 3D space are conserved by angle preserving transformations.

In 3 and higher D-dimensional foams, the conformal group of similarities and inversions is a symmetry of the entire foam, including the films satisfying Laplace's equation, only if the films are spherical caps; this is a very restricted subclass. In chapter 7 we will use the conformal invariance of this subclass of foams to prove a remarkable property of tetrahedral spherical bubble.

In the 2D Euclidean plane, however, any CMCS is a line of constant curvature, that is, a circle. Then, indeed, the symmetry group of 2D foams is $\mathrm{SL}(2,\mathbb{C})/\{1,-1\}$, the group of linear fractional, or Moebius, transformations [Mou97, Wea99, MO03], as we have seen in section 2.4 pag.22. The two sets of equations, including Laplace, are preserved in this case. Foams in standard flat Hele–Shaw chambers fulfil all these conditions [WH99, Wea99].

Conformal invariance of 2D foams

Specific to 2D is the existence of a much larger set of conformal transformations. This larger set is a symmetry of foams as characterised by the Plateau set of equations only. The geodesic curvatures k_j are not necessarily constant, the graph edges are of any smooth shape, but nodal equilibrium (Plateau conditions) is still assumed.

A further extension is that the degree (or coordination) d of the vertices is arbitrary (but finite), whereas standard 2D foams have degree $d = 3$.

The embedding plane may be identified to the complex plane: $\mathbb{R}^2 \simeq \mathbb{C}$. In the plane, a foam is a planar graph.

Equilibrium in 2D

The 2D equilibrium conditions (3.23, 3.24) at the vertices may be rewritten:

$$\sum \gamma_j \boldsymbol{\tau}_j = 0, \tag{3.41}$$

$$\sum \gamma_j k_j = 0, \tag{3.42}$$

where k_j are the film geodesic curvatures and $\boldsymbol{\tau}_j$ the unit vectors tangent to the films. The sums are over the d edges incident to the considered vertex.

Conformal maps

Two dimensional conformal maps are given by complex holomorphic functions f of the variable $z = x^1 + ix^2$ in $\mathbb{C} \simeq \mathbb{R}^2$. Indeed, Cauchy–Riemann's equation,

$$\partial_{z^*} f = \frac{1}{2}(\partial_1 + i\partial_2)(f^1 + if^2) = 0, \tag{3.43}$$

is equivalent to the conformality condition on the Jacobian matrix. The complex derivative is written $f' = \partial_z f$.

The scalar product in the plane is $x \cdot y = \mathrm{Re}(x^* y) = \mathrm{Re}(x\, y^*)$ for any complex x, y.

Paths under conformal maps

The edges of the graphs are described by parameterized C^2 curves $\boldsymbol{\phi} : [t_1, t_2] \to \mathbb{C}$, $t \mapsto \boldsymbol{\phi}(t)$.

If the arc length is $\mathrm{d}s = |\,\mathrm{d}\boldsymbol{\phi}| = |\dot{\boldsymbol{\phi}}|\,\mathrm{d}t$, the local Frenet basis $(\boldsymbol{\tau}, \mathbf{n})$ is composed of $\boldsymbol{\tau} = \frac{\dot{\boldsymbol{\phi}}}{|\dot{\boldsymbol{\phi}}|}$ and $\mathbf{n} = i\boldsymbol{\tau}$; i is the imaginary unit. The scalar curvature is

$$k = \frac{\mathbf{n} \cdot \ddot{\boldsymbol{\phi}}}{|\dot{\boldsymbol{\phi}}|^2}\,, \tag{3.44}$$

and the curvature vector is

$$\boldsymbol{\kappa} = k\,\mathbf{n} = \frac{\mathrm{d}\boldsymbol{\tau}}{\mathrm{d}s} = \frac{\ddot{\boldsymbol{\phi}} - (\boldsymbol{\tau} \cdot \ddot{\boldsymbol{\phi}})\,\boldsymbol{\tau}}{|\dot{\boldsymbol{\phi}}|^2}\,. \tag{3.45}$$

By a conformal f, a path $\boldsymbol{\phi}$ is mapped to an image $\tilde{\boldsymbol{\phi}} : [t_1, t_2] \ni t \mapsto \boldsymbol{\phi}(t) \overset{f}{\mapsto} \tilde{\boldsymbol{\phi}}(t) = f(\boldsymbol{\phi}(t)) \in \mathbb{C}$. The transformation rules are

$$\dot{\tilde{\boldsymbol{\phi}}} = f'\,\dot{\boldsymbol{\phi}}\,, \tag{3.46}$$

$$\ddot{\tilde{\boldsymbol{\phi}}} = f'\,\ddot{\boldsymbol{\phi}} + f''(\dot{\boldsymbol{\phi}})^2\,, \tag{3.47}$$

$$\tilde{\boldsymbol{\tau}} = \frac{f'}{|f'|}\,\boldsymbol{\tau}\;; \quad \tilde{\mathbf{n}} = \frac{f'}{|f'|}\,\mathbf{n}\,, \tag{3.48}$$

$$\tilde{k} = \frac{\tilde{\mathbf{n}} \cdot \ddot{\tilde{\boldsymbol{\phi}}}}{\dot{\tilde{\boldsymbol{\phi}}}^2} = \frac{1}{|f'|}\left(k + \mathrm{Re}\left[-i\frac{f''}{f'}\boldsymbol{\tau}\right]\right), \tag{3.49}$$

where $f' \equiv f'(\boldsymbol{\phi}(t))$, etc.

Conformal invariance of nodal equilibrium

Let $X = (V, E, \gamma)$ be a planar graph with vertex set V, edges E (given as twice differentiable curves) and line tensions $\gamma : E \to \mathbb{R}$.

Let f be a conformal map of the plane. Then the equilibrium conditions (3.41, 3.42) are satisfied at all vertices of $\tilde{X} = f(X)$ if and only if they are satisfied by X. Indeed, any vertex x of the graph is a point common to all its incident edges $j = 1, \ldots, d$. The equivalence for (3.41) is an immediate consequence of conformality as, by (3.48),

$$\sum \gamma_j \tilde{\boldsymbol{\tau}}_j = \frac{f'(x)}{|f'(x)|} \sum \gamma_j \boldsymbol{\tau}_j \,. \tag{3.50}$$

For (3.42), we may use (3.49):

$$\sum_{j=1}^{d} \gamma_j \tilde{k}_j = \frac{1}{|f'|} \left(\sum \gamma_j k_j + \mathrm{Re}\left[-i \frac{f''}{f'} \sum \gamma_j \boldsymbol{\tau}_j \right] \right), \tag{3.51}$$

where everything is evaluated at x. By (3.41), the real part on the right vanishes so that the two sums, around $\tilde{x}$ and x, are proportional. □

Drenckhan et al. [DWC04] gave an alternative argument, based on the known invariance of Plateau's laws under homographies and Taylor expansion to second order.

The embedding plane $\mathbb{C}$ may be replaced by analytic (Riemann) surfaces. Invariance and the first proof still hold true in these more general cases where X is a foam in a first surface M, $\tilde{X} = f(X)$ is the image of X by a conformal map to a second surface: $f : M \to \tilde{M}$.

3.6 Example: Hele–Shaw Cell

One of the most common settings, for both experimental and theoretical investigations, is the Hele–Shaw cell consisting of two flat and parallel plates separated by a small distance. The foam confined in the interstice may often be considered as quasi bi–dimensional; the equilibrium equations are 2D versions of Plateau's equations [WR84, WH99]. The gravity effects are negligible. The plane of the plates is normally mounted horizontally and, since h is small, the hydrostatic pressure variation is not appreciable. Moreover, since the foam is dry, the effects of the gravity on the drainage of liquid are negligible (capillary effects dominate).

This set–up allows to verify many theoretical prediction about 2D foams like von Neumann's law (section 5.2-5.3) and Aboav–Weaire's law [WH99, SG89]. Even in this simple setting, the predictions of straightforward dimensional reduction may fail when the thickness of the bubbles are not much smaller than their

diameter in the plane of the plates. If the condition of small h is not verified some instabilities can occur (Rayleigh–Plateau instability) [dGBWQ02, ÁLOC04]. The 3D foam loses its cylindrical symmetry: bubbles could assume a "wine–bottle" shape and a bubble could detach away from one of the plates. These instabilities were the object of some papers in the study of the "flower" problem [CWV02, WCG02, BM02, SMD03, Boh93, FRVT04] where by considering the third dimension it was possible to understand some discrepancies between numerical and experimental 2D foams. For example, for a single bubble of volume V in a Hele–Shaw cell, the limit of stability is given by $h < \sqrt[3]{\pi V}$ [BM02].

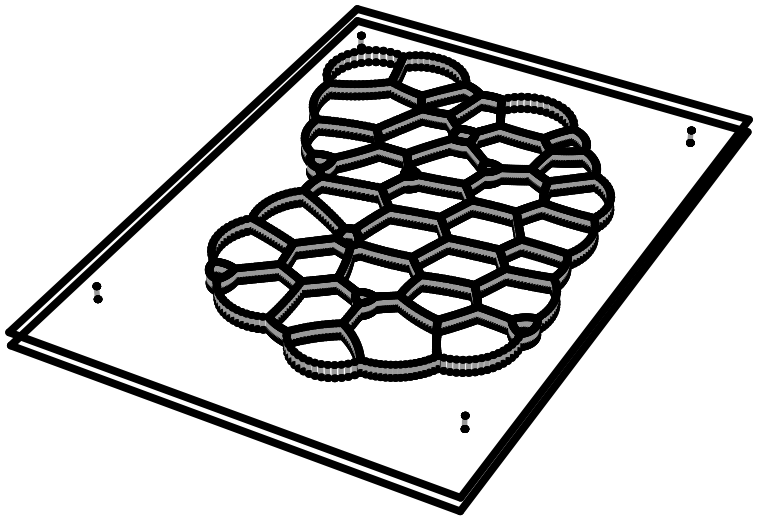

Figure 3.4: Scheme of a Hele–Shaw cell to realize experimental 2D foams.

Let us consider a 3D dry foam trapped in a standard Hele–Shaw experimental set–up and assume that the glass plates separation h is smaller than any typical length (curvature radius or cell diameter) of the 2D foam (figure 3.4). Since the gas in the foam is the same for any bubble, by the normal incidence property, if the foam is equilibrated then equations (3.27) and (3.28) are verified at both glass plates of the cell.

In particular since the films have to be orthogonal to both plates, which are very close to each other, then the curvature k_n of the films in the direction normal to the plates (equation (3.18)) is approximately zero in the limit where h goes to zero.

Therefore, using Laplace's equation (1.1), the pressure drop on a film is:

$$\Delta P = 2\gamma H = \gamma(k_n + k_g)\,, \tag{3.52}$$

and, in the limit of small h, it is:

$$\lim_{h\to 0} \Delta P = \gamma k_g\,. \tag{3.53}$$

Therefore 2D foams obtained by a Hele–Shaw cell satisfy approximately the equilibrium equations (3.21) and (3.22) with the involved quantities redefined for the 2D situation: line tension γ_j, edge tangent vector $\mathbf{b}_j$ and curvature $H_j = (2r_j)^{-1}$, r_j being the signed curvature radius of film i. On the other hand these are the equations theoretically defined in chapter 2. In 2D foams, the films and vertices are respectively the orthogonal sections of three–dimensional films and Plateau borders. Moreover, since at equilibrium the pressure inside the bubble is constant and the curvature in the direction normal to the plate is zero, Young's law implies that in equilibrated 2D flat foams the edges are circular arcs.

Conclusions

At equilibrium when a triple (a three–dimensional Plateau Border) is in contact with a solid, smooth and clean surface, then the pattern formed by the traces of the film on the surface verifies two geometric relations at the contact point $\mathbf{p}$ between the triple and the surface (2D vertex). These relations are implied by 3D equilibrium equations.

In the most common case, where the films are in normal incidence with the surface, these equilibrium properties are very similar to the 2D foams equilibrium equations. On the surface, at any $\mathbf{p}$:

- The sum of the tangent vector to the film traces which meet at $\mathbf{p}$, weighted by the surface tensions of the films, is zero.
- The sum of the geodesic curvature of the traces of the films meeting at $\mathbf{p}$, weighted by the surface tensions of the films, is zero.

Unlike equilibrated 2D foams, the second set of equations are generally valid only at the 2D vertex $\mathbf{p}$ because far from this point geodesic and normal curvatures can both vary along the curve even if the sum, $2H$, is constant. The equilibrium equations at the surface are invariant for analytical transformations.

In the next chapter we analyse the case where the setting of the Hele–Shaw cell is slightly deformed and one of the two plates is no longer flat.

Chapter 4

Deformed Hele–Shaw Cell: Conformal Foams

Several experiments showed that certain two–dimensional patterns that occur naturally are identifiable as conformal transformations (CT) of simpler ones. In particular some patterns resemble to the image of a perfect hexagonal lattice transformed by some CTs.

For example in many systems governed by cellular growth, the pattern found and called *phylotaxis* (florets of a sunflower or the scales of a pineapple) is the image of a hexagonal honeycomb structure by a conformal map [Jea84, AGH].

Pieranski [Pie89] observed experimentally that the structure formed by magnetized steel balls, constrained to stay in a plane and in presence of an external force field (with translational symmetry), was the image of hexagonal lattice by a CT. The link between this structure, called *gravity rainbow*, and the conformal transformations was proved theoretically, using symmetry arguments, by Rothen *et al* in two beautiful papers [RPRJ93, RP96].

Elias *et al* showed experimentally that the deformed structure obtained by two–dimensional ferrofluid foams submitted to an external force field was also the image of a hexagonal lattice by CTs [EBdMS99, RRED99]. A 2D ferrofluid foam is a system which consists of cells separated by magnetic fluid boundaries, confined between two horizontal plates and subjected to a perpendicular homogeneous magnetic field [EFB$^+$97, EDC$^+$98]. The patterns exhibit the topological characteristics of standard 2D soap foams (edges meet three by three making Plateau angles and the average number of edges for a cell is equal to six). Moreover, the equilibrated structure is stable in time because of the competition between a long–range magnetic dipolar repulsive interaction and a short–range attractive interaction. When an external force field is added in the plane of the layer the structure is deformed. The structure remains locally hexagonal but the directions of the hexagonal lattice are bent and new morphologies are formed

on a long range. When the external field is the gravity, obtained by tilting the cell with respect to the horizontal plane, it was observed that the formed pattern looked like the image of the hexagonal lattice by a logarithmic map. When the cell is subjected to a magnetic field gradient, radial in the plane of the cell, the observed patterns resemble the images of a honeycomb lattice by the CT $f(z) = z_0 z^\beta$, where β depends on the intensity of the applied field.

For soap foams, in recent experiments, Drenckhan, Weaire and Cox studied the pattern formed by a monodispersive foam in a Hele–Shaw cell where the simple parallelepiped geometry was modified [DWC04]. Changing the upper plate's slope the authors tried some special non–parallel chambers and noticed that each resulting 2D foam could be related to the reference regular honeycomb pattern (in a conventional Hele–Shaw cell) by a conformal map. The conformal transformation was attributed by imposing the volume conservation. Tilting or curving the upper plate, as the volume of the bubbles is conserved, the 2D area (on the plate) of the quasi cylindrical bubbles varies in inverse proportion to the thickness h. A question addressed in this chapter is whether the shape of the films, that is, the local geometry of the foam, can also be related to the conformal map and how it does it [MO05a, MO05b]. Conformality means that the transformation locally reduces to a simple isotropic dilatation, preserving angles. However, in the plane general conformal transformations are not compatible with Laplace's law. The only compatible conformal transformations which map circular arcs to circular arcs are the Moebius transformations (homographies) [Mou97, Wea99, MO03]. In the case of algebraic functions (with exponents other than ± 1), or the logarithm, or any other holomorphic function, is conformality only a long wavelength approximation or is there a correction to the 2D equilibrium?

On one hand, as we proved in the last chapter, the equilibrium conditions at the Plateau borders —of dimension 2 less than the embedding space, the edges in 3D, the vertices in 2D— are invariant by conformal mappings and this result is exact within the standard models of dry foams in any dimension. On the other hand, regarding the films —bubbles interfaces, of co-dimension 1— in thin cells, we will show that incorporating the curvature in the third direction (orthogonal to the plates) restores compatibility with Laplace's law, implying a relation between the profile and the map. In fact, when the foam is sandwiched between plates that are not parallel, the films must bend in the direction normal to the plates. This modifies slightly the pressure balance and while the geodesic curvature can be related to the conformal map, the curvature in the normal direction can be linked to the separation between the plates.

The first section (4.1) contains the calculation to the first order, in the limit of small thickness h, of the curvature in the normal direction to the plates. Section 4.1.1 considers the deviation with respect to Laplace's law when this first order approximation is done. In section 4.2 the link between the conformal map and

the thickness slope is made and the case of constant pressure will be solved explicitly. Finally, in section 4.3, comparisons with constant volume settings, including experimental ones, are also done.

4.1 Normal Contribution to the Mean Curvature

Among all the planar conformal maps, only the homographies, or Moebius transforms, map circles to circles. As we said in section 3.6, in the traditional setting of the Hele–Shaw cell, the edges are circular arcs. Under mappings such as the logarithm or any other one not equal to a homography, the image of a circle arc is not a circle arc. So the resemblance of the experimental pictures with the complex map may be questioned.

When the foam is sandwiched between two plates that are not parallel, by normal incidence condition, the films must bend in the direction normal to the plates. We now examine the pressure balance: using that at equilibrium the pressure inside any bubble is constant a relation between CTs and the thickness h is determined.

The upper plate —more precisely its face wet by the foam— can be described by a height function $h(x^1, x^2)$ defined in the plane at the bottom of the cell. Both h and its slope $|\nabla h|$ are supposed to be small to avoid instability [Fom90, CWV02, SMD03, BM02, Boh93, FRVT04]. As a two dimensional vector, ∇h locally indicates the direction of maximal slope. Because the film meets both top

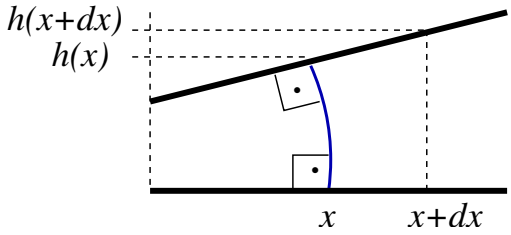

Figure 4.1: A film joining two non parallel plates.

and bottom faces orthogonally, it must be curved: to lowest order, its sectional, or normal, curvature in the vertical direction is (see figure 4.1):

$$k_v \simeq -\frac{\nabla h \cdot n_{\mathcal{F}}}{h} \sqrt{\frac{1}{1 + (\nabla h \cdot n_{\mathcal{F}})^2}} \simeq -n_{\mathcal{F}} \cdot \nabla h / h \,. \tag{4.1}$$

We used that the angle θ spanned by the film, in the direction $n_{\mathcal{F}}$ normal to the film, is given by $\theta \simeq \tan\theta \simeq \nabla h \cdot n_{\mathcal{F}}$. Within the same degree of approximation,

we get the mean curvature H by adding the horizontal sectional curvature, which nearly is the geodesic curvature $k \equiv k_g(\phi, \mathcal{S})$ of the curve $\phi = \mathcal{F} \cap \mathcal{S}$ in the upper or lower boundary $\mathcal{S}$. Then, Laplace's law says

$$P_1 - P_2 = 2\gamma H_{\mathcal{F}} = \gamma\,(k + k_v) \simeq \gamma \left(k - \frac{n_{\mathcal{F}} \cdot \nabla h}{h} \right). \tag{4.2}$$

Thus, in equilibrium, with a pressure difference constant along the film, the geodesic curvature differs from a constant by the last term in (4.2), representing contributions from curvatures in the third direction.

Next, let us explicit the deformation from circularity. Suppose the foam X is conformally related to a reference one by $\tilde{X} = f(X)$. Any edge ϕ has an image $\tilde{\phi} = f \circ \phi$ in the reference $\tilde{X}$. Using $n = i\tau$, let us solve formula (3.49) of for the curvature vector k:

$$k = |f'|\tilde{k} + \mathrm{Re}\,[n\,(\ln f')']\,. \tag{4.3}$$

In our approximations, $n_{\mathcal{F}} \simeq n$. Using (4.2), translated into complex notations, and (4.3) gives

$$(P_1 - P_2)/\gamma \simeq |f'|\tilde{k} + \mathrm{Re}\,[n\,\partial_z(\ln f' - 2\ln h)]\,. \tag{4.4}$$

This equation, valid on any edge of the foam, is a constraint relating the conformal map f and the cell profile h; it involves the edge through the pressure drop, the curvature of the reference edge and the unit normal.

For an equilibrated foam containing gas, the pressure drop on the left hand side of equation (4.4) should be constant along any edge. Now, except for special cases, making the right hand side constant seems to imply an intricate relation between the geometry of the edges, the mapping f and the profile h.

Interesting cases are when the mapping f leaves some freedom to the choice of the foam. For example, global motion by translation and rotation, eventually with appropriate deformation. These criteria are met when $P_1 - P_2$ and $\tilde{k}$ are both identically zero. Let us treat some of these cases in section 4.2.

4.1.1 Circle–Film Approximation

The approximation that we have made assuming that the film curvature in the direction orthogonal to the plates is constant, generally, could appear very strange. In fact our approximation corresponds to assume that, considering the line $\phi = \mathcal{F} \cap \mathcal{S}_B$ formed by a film $\mathcal{F}$ and a bottom plate $\mathcal{S}_B$, each line formed by the intersection of $\mathcal{F}$ and a plane, orthogonal to ϕ, is a circular arc of curvature k_v. We refer to this approximation as *circle–film approximation*.

To verify the validity of the circle–film approximation, we calculate the difference between the pressure drop ΔP across the film at the bottom plate, which,

by Laplace's law, must to be constant along the film, and the pressure drop measured as function of the height function h. It results that this difference is only of second order in h.

We evaluate the mean curvature of the film in the circle–film approximation as function of h and, using Laplace's law (1.1), we calculate the pressure drop.

Let $\boldsymbol{\phi}(s) = (\phi_1(s), \phi_2(s), 0)$ be the coordinates of the intersection of a film with the bottom plate ($z = 0$) where s is arc length. $\boldsymbol{\tau}(s)$ and $\partial_s \boldsymbol{\tau}(s) = k\,\mathbf{n}(s)$ are respectively the unit tangent vector and the curvature vector of $\boldsymbol{\phi}$. k is the signed scalar curvature of the two–dimensional film on S_B in equation (4.2). Calling $s \equiv u_1$, the coordinates of the film $\mathcal{F}$ in the circle–film approximation are given by (see figure 4.2):

$$\mathbf{x}(u_1, u_2) = \boldsymbol{\phi}(u_1) + r(u_1)\,\mathbf{n}(u_1)(\cos u_2 - 1) + r(u_1)\,\mathbf{z}\sin u_2\,, \tag{4.5}$$

where $\mathbf{z}$ is the unit vector orthogonal to $\mathcal{S}_B$ and $r(u_1) = -1/k_v$ is the signed curvature radius of the film in the vertical direction given by equation (4.1). The angle u_2 varies between zero and the angle $\theta \simeq -|\mathbf{n} \cdot \nabla h|$.

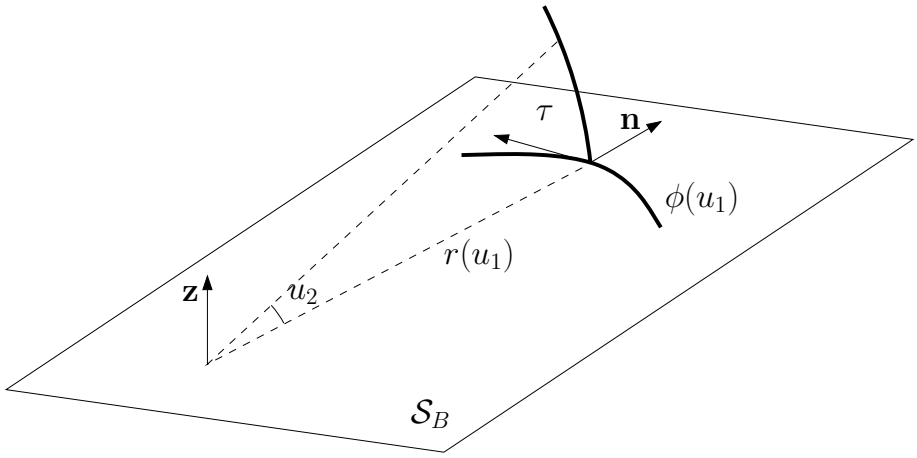

Figure 4.2: Set of coordinates for a film in the circle–film approximation.

A basis for the tangent plane $T\mathcal{F}$ to the film is given by $\mathbf{x}_i \equiv \partial\mathbf{x}/\partial u_i$ for $i = 1, 2$ (see section 3.1):

$$\mathbf{x}_1 = (1 + r(u_1)\,k\,(1 - \cos u_2))\,\boldsymbol{\phi} - r'(u_1)(1 - \cos u_2)\,\mathbf{n} + \sin u_2\, r'(u_1)\,\mathbf{z}, \tag{4.6}$$

$$\mathbf{x}_2 = -r(u_1)\sin u_2\,\mathbf{n} + \cos u_2\, r(u_1)\,\mathbf{z}\,. \tag{4.7}$$

As k_v, $\mathbf{n}$, $\boldsymbol{\phi}$ are all functions only of the variable u_1, we note by prime the derivation with respect to this variable.

Calculating the operator $\mathbf{x}_{ij} \equiv \partial_{u_i}\partial_{u_j}\mathbf{x}$, for $i, j = 1, 2$ and using equation (3.16) we can calculate the mean curvature H of the film. Calling the pressure

drop at $u_2 = 0$ (or $z = 0$) $\Delta P_0 = \gamma H(u_1, 0)$ we find that the pressure drop at $u_2 \neq 0$ is of second order in $u_2 \ll 1$:

$$\Delta P(u_1, u_2) - \Delta P_0 = \frac{1}{2(k_v)^2} \left(k\, k_v(k - k_v) + k_v''\right) (u_2)^2 + O(u_2)^4 \,. \tag{4.8}$$

As the maximum of u_2 is achieved when the film touches the upper plate: $u_2 = \theta$, then, by equation (4.1), $u_2 \simeq |k_v|h$. Taking the absolute value of both sides of (4.8) and replacing the maximum of u_2, we have that:

$$|\Delta P(u_1, u_2) - \Delta P_0| \leq \frac{1}{2} |k\, k_v(k - k_v) + k_v''| (h)^2 + O(h)^4 \,. \tag{4.9}$$

Equation (4.9) shows that the circle–film approximation gives a deviation from Laplace's law, which predicts a constant pressure drop across equilibrated films, of second order in the height of the chamber. As we assume h much smaller than the radius of the 2D bubbles to avoid instabilities, our approximation is sufficiently good.

4.2 Conformal Maps and Laplace's Law: Implications

For specificity, we assume that the reference foam $\tilde{X}$ is in a standard parallel Hele–Shaw cell. Then the curvature $\tilde{k}$, on the right, is proportional to the pressure difference in the reference: $\tilde{P}_1 - \tilde{P}_2 = \tilde{\gamma}\tilde{k}$. Moreover, when the pressure is constant in both the curved and reference foams, equation (4.4) reduces to

$$\mathrm{Re}\,[n\, \partial_z (\ln f' - 2 \ln h)] \simeq 0. \tag{4.10}$$

If the bubbles are small compared to the length scale over which f and h vary, then the 2D vector $\partial_z(\ln f' - 2 \ln h)$ must vanish. As $\ln f'$ is analytic and $\ln h$ real, the solution of this equation is $\ln h/h_0 = \mathrm{Re}\,[\ln f']$, or

$$h/h_0 \simeq |f'|, \tag{4.11}$$

where h_0 is positive a constant.

Following Drenckhan *et al* [DWC04], we take the hexagonal foam as reference (fig. 4.3) and now we consider two examples.

Log map

The logarithmic map

$$F(\tilde{z}) = \frac{1}{a^*} \ln(a^* \tilde{z}), \tag{4.12}$$

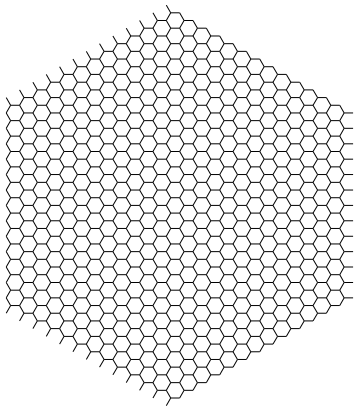

Figure 4.3: The reference regular hexagonal foam.

where a is a complex number or 2D vector, maps the outside of the unit disc to the upper half plane when a is purely imaginary. This is one of the examples experimentally demonstrated in [DWC04]. This mapping is also involved in gravity arches observed in ferro–fluid suspensions under gravity [RPRJ93, RP96] and in ferro–fluid bi–dimensional foams [EBdMS99]. It was observed that logarithm is the only conformal map translationally invariant [RPRJ93, RP96, RRED99].

Applying (4.11) to the inverse mapping $f(z) = F^{-1}(z) = \frac{1}{a^*}\exp(a^* z)$, the solution for the profile is

$$h(z) \propto |f'| = \exp(\mathrm{Re}[a^* z]) = \exp(a \cdot z). \tag{4.13}$$

This exponential profile matches the experimental one, at least within the observable precision.

With formula (4.3), we can explicit the edge curvature:

$$k \simeq |a\tilde{\phi}|\tilde{k} + a \cdot n. \tag{4.14}$$

In (4.14), the first term on the right is the effect of the local scale change by $|f'|$ ($\tilde{k} = 0$ in a constant pressure reference, as assumed here); according to the second term, the edges nearly parallel to a are almost not deformed, up to similarities, whereas those perpendicular to a are bent. See fig. 4.4 where $a \propto i$ is vertical.

Power laws

Upper plates with circular symmetry are described by height functions depending on distance only: $h = h(|z|)$. For the conformal map, the candidate functions are of the form $f(z) \propto z^\alpha/\alpha$. An exponent $\alpha = m/6$, m integer, will induce a disinclination of the hexagonal crystal. The isobar condition (4.11) then implies

$$h(|z|) \propto |f'(z)| = |z|^{\alpha-1}. \tag{4.15}$$

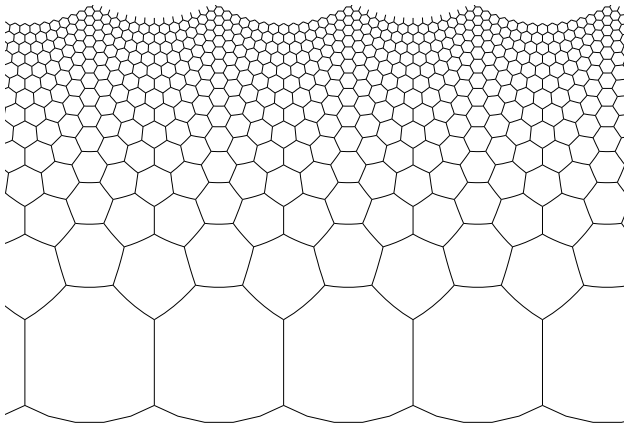

Figure 4.4: Image of the regular hexagonal foam by the log map.

For example, a spherical profile corresponds to $\alpha - 1 = 2$, that is, to a figure with 18-fold symmetry if the reference foam is the regular honeycomb (fig. 4.5). This result, derived from constant pressure, differs from the prediction of constant volume (4.16), which is $2(\alpha - 1) = 2$, implying 12-fold symmetry.

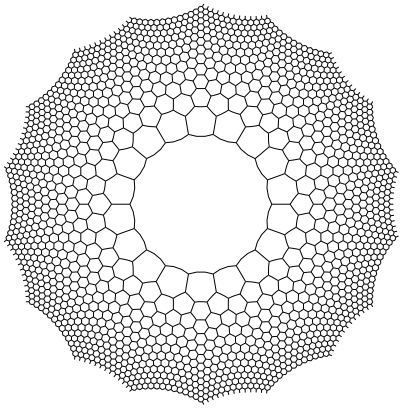

Figure 4.5: This 18-fold symmetric pattern maps to the hexagonal foam of fig. 4.3 by $f(z) \propto z^3$.

Equation (4.4) insures compatibility with Laplace's law for films in a thin curved interstice. In the next section we compare this result with the constant volume condition used by Drenckhan *et al* in [DWC04].

4.3 Comparing with the Experimental Results

Recently, Drenckhan *et al.* [DWC04] furnished experimentally the demonstration of conformal maps with two–dimensional foams. The set–up was similar to the conventional Hele–Shaw cell, except that the upper plate was not parallel to the bottom one. It was either tilted or moderately curved. Bubbles of equal volume were generated by blowing nitrogen at constant pressure through a nozzle into a surfactant solution. Glycerol was added to the solution to prolong the lifetime of the foam. The bubbles then were trapped between two glass surfaces and a variation of the apparent 2D bubble area with position within the pattern could be imposed by using a curved upper surface.

The major constraint, on the mapping, was *volume* conservation in each bubble. In the long wavelength approximation, equal volume of the reference and the transformed bubbles amounts to the following condition: $h|F'|^2 = h|f'|^{-2} =$ const., or

$$h/h_0 = |f'|^2 \tag{4.16}$$

for some constant h_0. In fact, defined the CT which maps the hexagonal foam in its conformal image as $z = F(\tilde{z})$, and its inverse $\tilde{z} = f(z) = F^{-1}(z)$, the area of the 2D bubbles in the transformed foam varies as $\mathrm{d}A(z) \sim |f'(z)|^{-2}\,\mathrm{d}A(\tilde{z})$. On the other hand, if the image of F is the observed pattern, then volume conservation implies that the distance between the plates $h(z)$ must vary as $h(z) \sim |f'(z)|^2 h_0$.

A tilted upper plate was used to approximate an exponential profile and generate a conformal map with translational symmetry. In order to generate a conformal 2D foam with rotational symmetries with decreasing 2D bubble area with the distance from the centre, a large spherical vessel was used as upper plate. Finally, an elastic membrane was used as upper plate. The membrane was stretched across the end of a short cylinder and its centre attached to a piece of string, which was pulled to produce a funnel shape. In this way a 2D foam, with bubble area growing with the distance from the centre, was obtained.

In [DWC04], the constant volume predictions do not always match the experiments. The clearest evidence is with a spherical upper plate, where constant volume predicts 12-fold symmetry ($\alpha = 2$) whereas the sample has 9-fold symmetry. Possible explanations of this discrepancy may rely in boundary effects, both near the origin where the liquid occupies a significant region and at the outer boundary where the absence of the outer part may induce relaxations, and departure from the ideally infinite model. The experimental protocol followed from the reference to the curved foam may be of importance too.

Compared to (4.16), equation (4.11) appears as a constant perimeter condition: at constant film thickness, the amount of liquid per bubble would be the same in the reference and in the transformed froth. This is just an interpretation

because (4.11) was derived from a constant *pressure* hypothesis and equilibrium.

As already noticed, the predictions deduced from equations (4.16) and (4.11) are different, except for the trivial case where $|f'| \equiv 0$, corresponding to changing the chamber thickness while keeping the two plates parallel, and where (4.16) and (4.11) are compatible.

Let us see the consequences of assuming both constant volume and local film equilibrium. Inserting (4.16) into the expression (4.2) for the vertical curvature gives

$$\begin{aligned} \tfrac{1}{2}k_v &\simeq -\frac{(n\cdot\nabla h)}{2h} = -\mathrm{Re}\left[n\,\partial_z \ln h\right] = \\ &= -\mathrm{Re}\left[n\,\partial_z \ln |f'|^2\right] = -\mathrm{Re}\left[n\,\partial_z \ln f'\right] = -k\,, \end{aligned} \tag{4.17}$$

where in the last equality we used equation (4.3). Therefore Laplace's equation for the pressure difference (4.2) becomes

$$(P_1 - P_2)/\gamma = k + k_v \simeq -k\,, \tag{4.18}$$

a result opposite to what a direct readout from the 2D foam and equations would predict. For example in figure 4.4 equation 4.18 predicts that the pressure *decreases* as one moves up.

In many cases, a single bubble or liquid bridge between non parallel plates is unstable [CF98]. So, for foams, stability is a collective effect; the inner bubbles repel the outer ones.

In the long wavelength limit, we can clarify the respective status of the previous equations. On one hand, with global symmetries such as rotation or unidirectional translation, bubble volume preservation, equation (4.16), essentially forces the positional ordering of the cells with respect to each other, implying a long range order. On the other hand, equation (4.4), or its constant pressure version (4.11), represents the equilibrium condition for the films; this is a shorter range constraint because the films are small, of the order of the bubble size, and bounded by the Plateau borders. How this effect propagates across film junctions is not clear yet. Neither is it obvious, a priori, that the two conformal maps, in (4.16) and (4.4), should be the same, despite the fact they were both called f.

Analogy with foams in gravity

When the film is subjected to a force field $\mu\,\mathbf{g}$ per unit surface (length in 2D), the force balance in the normal direction is [dGBWQ02]

$$(P_1 - P_2) - 2\gamma H + \mu\,\mathbf{g}\cdot\mathbf{n} = 0. \tag{4.19}$$

The force balance in the tangent direction implies that the surface tension slightly varies with position on the film: $\gamma = \gamma(\mathbf{r})$. When, moreover, the fluids on both

sides of the film are liquids of mass density ρ_1, ρ_2, the local hydrostatic pressure difference is $(P_1 - P_2) = (\rho_1 - \rho_2)\,\mathbf{g}\cdot\mathbf{r}+$ const. . In particular, if the liquids are the same, as in ferro–fluid foams [EBdMS99], or if the cells contain gas of negligible weight, then $(P_1 - P_2)$ is constant along the film, with a good accuracy.

Comparing (4.4) and (4.19) shows that a non parallel profile affects the foam as an effective force field $\nabla_z(\ln f' - 2\ln h)$.

Let us consider now the case where the flat Hele–Shaw cell which contains the 2D *ferro–fluid* foam is subjected to an external force field per unit of length ρg, where $h = const$ is the distance between the plates of the chamber, ρ is the linear density of the fluid and the complex number g is an acceleration. The pressure drop on a film in an observed pattern X is given by the two–dimensional version of equation (4.19):

$$(P_1 - P_2) = \gamma k - \rho\,\mathrm{Re}(n\,g^*)\,, \tag{4.20}$$

where the complex number n is the normal to the film. Supposing that X is conformally related by f to the reference hexagonal foam $\tilde{X}$ ($\tilde{X} = f(X)$) then:

$$\frac{P_1 - P_2}{\gamma} = \mathrm{Re}\left[n\,\left(\partial_z(\ln f') - \frac{\rho\,g^*}{\gamma}\right)\right]\,, \tag{4.21}$$

where we used that in the hexagonal foam $\tilde{k} = 0$. We solve this equations in the case where the bubbles in the formed pattern have the same pressure, that implies $P_1 - P_2 = 0$.

Let us suppose that X and $\tilde{X}$ are related by a logarithmic map as in (4.12). The solution of equation (4.21), for $\Delta P = 0$, is:

$$\frac{\rho g^*}{\gamma} = a^*\,. \tag{4.22}$$

Therefore g is constant. It corresponds to the experiment set–up realized by Elias *et al.* [EBdMS99] (first part) where the ferro–fluid foam was subjected to an external force field by tilting the chambers from an angle β with respect to the horizontal position. So, in the plane of the foam, the force field is $-i\rho\,|g|\sin\beta$, the planar component of the gravitational force in the direction of the y-axis.

Imposing that the conformal map $f(X) = \tilde{X}$ has rotational symmetry: $f(z) = z^\alpha/\alpha$ and solving equation (4.21) we obtain:

$$\frac{\rho g}{\gamma} = \frac{\alpha - 1}{z^*}\,. \tag{4.23}$$

In this case the force g has to be radial and proportional to $1/z$. Moreover, the exponent of the mapping α depends on the intensity of the force. This property coincides with the measurements made be Elias *et al.* [EBdMS99] (second part) where a horizontal cell was subjected to a magnetic–field gradient, which was

radial in the plane of the cell. It was observed that different mappings (or disclinations of different values) were obtained varying the value of the magnetic–field gradient.

Conclusions

In this chapter we have considered an application of the equations at the boundary found in the previous chapter (3). We have analysed the films equilibrium conditions for foams enclosed between two non–parallel plates. We were inspired by the experiments made by Drenckhan *et al* [DWC04], where the link between some special non–conventional Hele–Shaw and conformal maps was demonstrated. Following [DWC04], we have supposed that the 2D pattern, formed on the curved plates, is the image of a flat 2D foam. As in the experiments the top plate was kept flat while the bottom one had a particular profile. Using that equilibrium equations at the boundary are invariant by conformal transformations, we have found an equation which associates the observed curvature with the curvature in the flat foam and the conformal transformation.

In the limit where the thickness, slope and typical wave vectors of the profile are small, imposing Laplace's law for any three–dimensional film of the foam we deduced an approximate map–profile equation (eq. 4.4). This equation links the profile of the top plate to the map which transforms a reference flat 2D foam in the observed pattern. The equation was then solved in the case of constant pressure and illustrated in conditions comparable to available experiments.

In the experimental demonstrations of conformality, the length scale of the mapping is large compared to cell diameter. As a small scale condition, our equation completes longer range ones such as the constant volume condition. Moreover, the effect of slightly non parallel plates can be interpreted as an effective force field on the 2D foam.

Examining the projected foam only can be misleading. For example, on the bottom figure 4.4, which is the model for a foam confined in an (approximately) exponential cell as on figure 3(b) of [DWC04], the pressure seems to increase as one moves up (the pressure is higher on the convex side of a curved edge). But this is wrong. In these conditions, solving the equilibrium problem in 3D, taking into account the vertical curvature implied by normal incidence between non parallel plates, leads to the same image (fig. 4.4) even at constant pressure; then, at each edge, the curvature in the vertical direction is exactly opposite to the horizontal one seen in projection, so that $\Delta P/\gamma = H \simeq 0$. The same computation at constant volume even predicts that the pressure decreases as one moves up in figure 4.4. Our derivation of the map–profile relation relies on an approximation where the vertical curvature is retained only to the lowest order, constant (circle–film approximation in section 4.1.1).

Chapter 5

Standard 2D Foams: ⅄− △ Equivalence

In the previous chapter we have never considered the gas diffusion between the bubbles. This was a good ansatz to define equilibrium of soap foams by minimizing the films surface (or perimeter, in 2D), under the constraint of constant bubbles volume (or area). In reality the gas always flows across the films and, driven by pressure differences, it flows from a bubble to another with smaller pressure. As the equilibration time of the foam is short compared to the rate at which the bubbles grow or shrink by diffusion, the foam is essentially relaxed, or equilibrated, at any time during the evolution. Experimentally, the diffusion time scale can be controlled by choosing the gas (see Koehler *et al.* [KHS00]). While in three dimensions the evolution of the foam by gas evolution is not yet completely understood (see [Sir94, MVA98], and more recently [HKKS01, HKKS01, vDH03, HKRS04, CG04]), in two dimensions an elegant theory, though valid only in the ideal case, exists. This theory, due to von Neumann [vN52], was originally applicable only to 2D ideal dry foams in the plane and it states that the change in area of a bubble depends only on the number of its sides. Correction to this theory must be considered when some liquid is added to the vertices, in other words when the foam is "simply" dry [FW92a], or when the friction of the films on the surface is considered [GW92, KWM$^+$04]. By geometrical properties of 2D foams and since, in average, big bubbles have more sides then small bubbles, von Neumann's law implies that small bubbles shrink and big bubbles grow. As bubbles typically change their number of sides many times during the evolution (topological changes), von Neumann's law is applicable only within small time intervals between two topological changes. In fact at any topological process there is a change in the "structural parameters" (the topological charge of the bubbles) which enters in the von Neumann evolution. Moreover, when a film shrinks to a point or when a bubble disappears,

in general the foam will fall into a non–equilibrated state. Then the foam will jump, changing its topology, to a new minimum of the energy in a time of the order of the equilibration time. For example, if we look at the total perimeter of the films during the evolution, as long as no topological change occurs, it varies continuously. When a T1 or T2 occurs, in general a sudden change in the energy is expected and so the evolution is not continuous.

The aim of this chapter is to show that the topological process T2(3), where a bubble with three edges (triangle) disappears, is continuous: the system does not jump from an equilibrium state to another and any quantity varies continuously. As we will see, discontinuities occur in the first time derivative of the energy. The other processes T2(4), T2(5), where a four or five–sided bubble disappears, are clearly discontinuous. For example, when a T2(4) occurs, four edges meet in the point where the bubble has disappeared, and this configuration is not of equilibrium; then a T1 has to occur.

To prove the T2 continuity we have to prove the main result of this chapter: the star–triangle equivalence (⅄−△). This theorem states that for any 2D equilibrated ideal dry foam, each triangular bubble or triangle (having three edges) contains a virtual equilibrated vertex inside it. This virtual vertex is obtained by prolonging, in the bubble, the films separating two by two the three external neighbors. Then it turns out that the foam, obtained by taking an equilibrated foam and substituting in it a triangular bubble by its virtual vertex and the prolongation of the films meeting on it, is still equilibrated.

Since during gas diffusion the foam can be considered equilibrated at any time between two topologial processes, star–triangle equivalence is applicable during the slow evolution. As a corollary, the ⅄−△ theorem implies that the T2 process is continuous: in the disappearance of a triangular bubble any physical quantity varies continuously (area, perimeter). During a T2 process the discontinuities will emerge only in the first time derivative of the physical quantities.

Another application of this equivalence could be to use it to reduce the number of coordinates, thereby improving the efficiency of numerical minimization. For example, taking in non–equilibrated foams, they could be relaxed to the equilibrium by eliminating small bubbles. Afterwards, small bubbles could be added to the equilibrated structure.

Star–triangle equivalence can not be used to eliminate three–sided bubbles during diffusion, in fact, as we will see in the last section, the application of the equivalence prejudices the time evolution of the foam.

In the next chapter we will prove the ⅄−△ equivalence in more general context.

5.1 Von Neumann's Law in Curved Surfaces

Let us consider an equilibrated 2D foam, very dry (ideal) and embedded in a regular two–dimensional Riemannian manifold $\mathcal{S}$ of $\mathbb{R}^3$. As example of experimental set–up of this foam we can take the standard Hele–Shaw cell ($\mathcal{S}$ is a plane) or the hemispherical cell of [MS05] ($\mathcal{S}$ is a spherical cap) in the limit of very small thickness between the plates to prenvent (Rayleigh–Plateau) instabilities.

At equilibrium, by Laplace's equation, the films of a 2D foam are lines of constant geodesic curvature k_g on $\mathcal{S}$ given by the bubbles pressure difference ΔP divided by the line tension γ (chapter 3). We assume that the line tension is constant on every film of the foam (standard foams). At any vertex, equilibrium laws (eqs. 3.21-3.22) are given:

$$\sum_{i=1}^{3} \boldsymbol{\tau}_i = 0 \tag{5.1}$$

$$\sum_{i=1}^{3} k_g^i = 0 \tag{5.2}$$

To derive the von Neumann evolution, the following assumptions are made:

- The foam is ideal.
- The gas diffuses very slowly compared to the equilibration.
- The approximation of incompressibility of the gas inside the bubbles is valid (sec. 1).
- There are no dissipative forces opposing the motion of the films.
- The flow is proportional to the films length and the pressure difference between neighbouring cells (Fick's law).

The ideality of the foams permits to neglect the effect of the liquid at the vertex. Weaire calculated the corrections to this model in the case where some liquid is present at the vertices ([FW92b, FW92a]), we will see these later (section 5.3). As the gas is assumed incompressible, the flow of gas corresponds to the area flow (in 3D, it corresponds to the volume flow). Regarding the evolution, the equilibration time of the boundaries is short compared to the rate at which the bubbles grows or shrink by diffusion, so the foam is relaxed, or equilibrated, at any time. Moreover, as the films slide freely (without dissipation) on $\mathcal{S}$, the edges are curves of constant geodesic curvature, proportional to the pressure differences.

Classically, the proof of von Neumann's law is given by supposing the foam in a plane (as in the definition of 2D foams given above) but it can be proved for

2D foams embedded on a general two–dimensional surface. Here, we derive von Neumann's law in this more general case and we will see the flat case in the next chapter. The original derivation was found by Avron and Levine [AL92].

Let $A_n(t)$ be the area of a n-sided bubble of a 2D foam on $\mathcal{S}$. The flow of the gas through the films is equal to the bubble area's first derivative. Fick's law is:

$$\frac{dA_n}{dt} = -\sigma \sum_{i=1}^{n} l_i \Delta P_i \tag{5.3}$$

where l_i and ΔP_i are respectively the length and the pressure drop of the i-th film and σ is the constant of permeability of the gas through the films.
Using Laplace's equation:

$$\Delta P = \gamma k_g \,, \tag{5.4}$$

the pressure drop in (5.3) can be replaced by the geodesic curvature. In soap foams the pressure difference along a film is constant at equilibrium, then each film i has constant geodesic curvature k_g^i. Denoting the bubble's boundary by ∂A_n, we have

$$\frac{\mathrm{d}A_n}{\mathrm{d}t} = -\sigma\gamma \sum_{i=1}^{n} l_i k_g^i = -\sigma\gamma \sum_{i=1}^{n} \int_i k_g^i \,\mathrm{d}l_i = -\sigma\gamma \int_{\partial A_n} k_g \,\mathrm{d}l \,. \tag{5.5}$$

The right–hand side of (5.5) is one of the terms in the Gauss–Bonnet theorem [Mor98]. The Gauss–Bonnet theorem is a classical theorem of differential geometry which links the geodesic curvature of a closed curve with the Gaussian curvature, definition (3.4), of the surface where the curve is embedded:

Theorem 5.1. *Let A be a smooth disc in a smooth two–dimensional Riemannian manifold $\mathcal{S}$ with Gauss curvature G. Let ∂A be the boundary composed by a set of lines ϕ_i, for $i = 1, \ldots, n$, with geodesic curvature k_g^i, which meet at external angles α_i. Then*

$$\int_{\partial A} k_g \,\mathrm{d}l + \int_A G \,\mathrm{d}A = 2\pi - \sum_{i=1}^{n} \alpha_i \,. \tag{5.6}$$

The first term of (5.6) is proportional to the right–hand side of (5.5). The foam is equilibrated, so the outer angles between the edges are constant: $\alpha_i = \pi - \frac{2\pi}{3} = \frac{\pi}{3}$ (see fig. 5.1). Replacing the integral of k_g in (5.5) by (5.6) we obtain:

$$\frac{\mathrm{d}A_n}{\mathrm{d}t} = -\sigma\gamma \left(2\pi - \sum_{i=1}^{n} \alpha_i - \int_{A_n} G \,\mathrm{d}A \right) = \frac{\sigma\gamma\pi}{3}(n-6) + \sigma\gamma \int_{A_n} G \,\mathrm{d}A \,. \tag{5.7}$$

Equation (5.7) is von Neumann's law describing the evolution of the bubbles. For a bubble with n sides the time derivative of the area depends on n, A and on

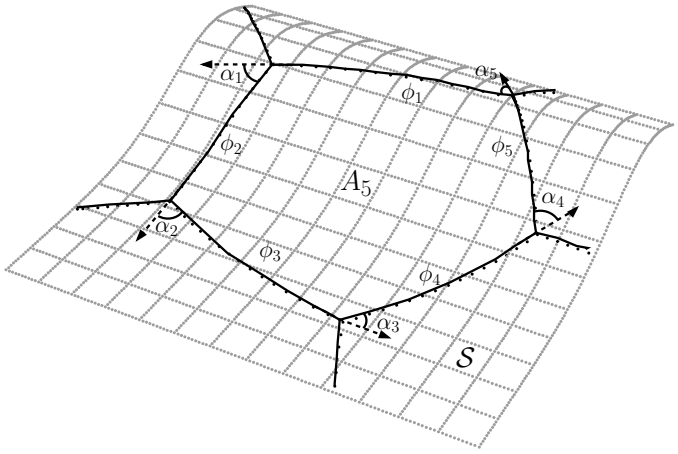

Figure 5.1: Five–sided bubble of area A_5 in a 2D foam embedded on a surface $\mathcal{S}$. On the tangent plane, at the vetices, the angles formed by the edges are $\frac{2\pi}{3}$.

intrinsic characteristics of the surface $\mathcal{S}$. It is worth noting that in the second equality of (5.3) the assumption of constant line tension has been used to take out γ from the summation. This assumption makes von Neumann's law valid only for standard 2D foams.

If $G > 0$ and $n < 6$, or $G < 0$ and $n > 6$, stationary bubbles exist for certain areas. For example if G is constant everywhere on $\mathcal{S}$ then the bubbles with area $A = \frac{\pi}{3}\frac{(6-n)}{G}$ are stationary. When $G = 0$ six–sided bubbles are stationary irrespective of size.

Equation (5.7) implies also that no bubble is stable on a positively curved surface, while all stationary bubbles are stable in a surface with $G < 0$. In fact, if ϵ_0 is a small perturbation of a stationary solution A_{stat}: $A(t) = A_{stat} + \epsilon_0$, solving (5.7) with G constant one obtains

$$\epsilon(t) = \epsilon_0 \exp(\frac{\alpha 3G}{\pi}) \,. \tag{5.8}$$

From (5.8) it is clear that when $G < 0$, a perturbation of a stationary bubble on a $G < 0$ surface will die out; the bubble will return to its original size at an exponential rate. In contrast, when $G > 0$, enlarging or shrinking the bubble's area will cause further enlargement or shrinkage of it.

It would be interesting to study, in the experimental set–up used by Di Meglio and Senden [MS05], to what approximation (5.7) is verified. Numerical simulations, using the Potts model, have been carried out to study the effect of surface curvature on grain growth [PGL93] and 2D foams. In fact, equation (5.7) applies, choosing adequate multiplicative factors, to a wider class of problem including grain growth (Mullin's law [Mul56]). In this case, the pressure differences become

negligible, the boundary velocities of the grains are simply proportional to the local curvature and the porosity constant should be replaced by the grain–boundary mobility [KWM+04].

5.2 VN'Laws in Flat Surfaces

As we saw in sections 2.1 and 3.6, when the surface $\mathcal{S}$ where the foam is embedded is the plane, the geodesic curvature of the edges corresponds to the "usual" curvature of the films. So, films are circular arcs which verify (5.1-5.2) (assuming straight lines as circles of infinite radius). Moreover, the term in (5.7) which depends on the Gaussian curvature vanishes and the classical version of von Neumann's law is obtained:

$$\frac{\mathrm{d}A_n}{\mathrm{d}t} = \kappa(n-6)\,, \qquad \text{with} \quad \kappa = \frac{\sigma\gamma\pi}{3}\,. \tag{5.9}$$

Bubbles with more then six edges grow and those with less than six shrink. Bubbles with exactly six edges are stationary and their size is constant if topological changes don't occur. So in a 2D flat foam, big bubbles, which have in average many neighbours, grow and smaller bubbles shrink.

The factor $q_n = (6-n)$ in (5.9) is often called the *topological charge* of the n-sided bubble [GJJF01]. q_n quantifies the deviation from a hexagonal lattice. Equivalently, we can say that a n-sided bubble is a disclination bearing the geometrical charge [GJJF01]:

$$q_g(n) = \frac{\pi}{3}(6-n) = 2\pi - \frac{n\pi}{3}\,. \tag{5.10}$$

When a topological change occurs the topological charge q changes. During a T1 (sec. 2.1.1), the charge of two of the four bubbles implied in the phenomenon changes as $q \to q+1$ and in the other two as $q \to q-1$. In a T2, the neighbours of the disappeared bubble change as $q \to q-1$. This implies that at a topological change occurrence the equation describing the slow evolution changes.

Von Neumann's law predicts that the final state of each finite flat soap foam is constituted by only a big bubble (all the plane or the exterior of the initial cluster). Equation (5.9) predicts also that the mean radius of bubbles grows as a power one–half of the time:

$$\langle r\rangle \propto \sqrt{\langle A\rangle} \propto t^{\beta}\,, \qquad \text{where} \quad \beta = \frac{1}{2}\,. \tag{5.11}$$

We will see in section 5.3 the experimental results on the validity of von Neumann's law.

As a purely 2D model, Von Neumann's law is valid also when there is a local dissipative force opposing the motion of the interfaces (see Kern *et al.* in

[KWM+04] and references therein). In this model, called *viscous froth model*, the equation of equilibrium in the direction normal to each film is given by:

$$\Delta P_{ij}(s) - \gamma k_{ij}(s) = \lambda v(s)\,, \tag{5.12}$$

where s is the position along the film shared by bubbles i and j. ΔP_{ij} and k_{ij} are respectively the pressure drop between the bubbles and the curvature of the interface. The right–hand side is the friction of the film opposing the motion, with drag coefficient λ. v is the velocity of the film in the direction normal to the film. Only normal velocities are considered in agreement with the experiments (Cantat and Delannay [CDK04][1]). After some manipulation, including the application of theorem 5.1 with $G = 0$, a modified version of (5.9) is found. This modified version differs from the original only for the diffusion constant:

$$\kappa \to \kappa' = \frac{\pi}{3}\frac{\sigma\gamma}{1+\sigma\lambda}\,. \tag{5.13}$$

We have to note that the viscous froth model is not an accurate representation of any experimental realization of a 2D froth. The hypothesis that films are planar curves is essential. Considering a foam in a Hele–Shaw cell in presence of a dissipative force, this force is applied at the contact of the films with the plates. So the normal incidence is no more verified and then the foam loses its cylindrical symmetry. This implied that the Fick's law, and so von Neumann's law, are not valid in this case.

In three dimensions there is no simple equivalent of von Neumann's law: in 2D the topological constraints are sufficient to fix the dynamics, this is not the case in 3D. In 2D the average number of sides per bubble is six (see (2.20)). In 3D there is an extra degree of freedom, so the equations for the number of faces per bubble are under–determined [GW92]. If $\langle f\rangle$ is the average number of faces per bubble and $\langle n_f\rangle$ is the average number of edges per face, then for an infinite foam the two quantities are related by: $\langle n_f\rangle = 6 - 12/\langle f\rangle$. By analogy with von Neumann's law, River [GW92], using a maximal entropy argument, proposed that a possible law for the 3D dynamics could be:

$$\frac{\mathrm{d}V_f}{\mathrm{d}t} = \kappa(\langle f\rangle - f) \tag{5.14}$$

where V_f is the volume of a bubble with f faces and κ is a diffusion coefficient. The value of $\langle f\rangle = 13.7$ has been found experimentally by Matzke [Mat46]. Later, using the results of a Potts model simulation, Glazier *et al.* [Gla93, GPG+95] proposed an empirical "normalized" version of (5.14):

$$V_f^{-1/3}\frac{\mathrm{d}V_f}{\mathrm{d}t} = \kappa(f - f_0) \tag{5.15}$$

[1] Actually, in agreement with the theory of Bretherton which deduced the dissipation of a bubble in a cavity [Bre61], the authors of [CDK04], have measured a dissipative force proportional to $v^{2/3}$.

where f_0 was not fount equal to $\langle f \rangle$. Weaire and Glazier [WG93] deduced empirically that

$$f_0 = \langle f \rangle \left(1 + \frac{\mu_2}{\langle f \rangle^2} \right) ,$$

where $\mu_2 = \langle f^2 \rangle - \langle f \rangle^2$ is a measure of the foam disorder. Equation (5.15) was also derived by Sire [Sir94] using geometrical and maximal entropy arguments and it was verified experimentally, in average, by Monnereau and Vignes–Adler [MVA98]. Equation (5.15) remains a law true for ensembles, unlike von Neumann's law, which should hold for individual bubbles. In section 5.5 the simple case where only two bubbles form a cluster is studied and an analytical solution for the coarsening is found.

5.3 VN's Law Experiments

In the last decade a lot of experimental studies have been made to verify von Neumann's law's prediction (eq. 5.9). An exhaustive review on the experimental validation of von Neumann's law is furnished in [GW92]. In typical experiments in a Hele–Shaw cell, with flat and parallel glass plates, Glazier *et al* [GGS87] and Fu [Fu88] found that, within the accuracy of the experiment, (5.9) is verified on average for ensembles of bubbles with up to nine sides, but failed for individual bubbles. They also found that the diffusion constant κ in (5.9) remained constant. This was in contrast with the theory because von Neumann's law is local and it should be obeyed by each bubble individually. Successive measurements (Glazier and Stavans [SG89, GS89]) explained partly the discrepancy with the theory showing that the average internal angle of bubbles were not exactly $\frac{2\pi}{3}$ as predicted by equilibrium. They proposed also a *modified* version of von Neumann's law assuming an n-dependent typical internal angle $\theta(n)$, where n is the number of sides:

$$\frac{\mathrm{d}A_n}{\mathrm{d}t} = \kappa \left[3n \left(1 - \frac{\theta(n)}{\pi} \right) - 6 \right] . \tag{5.16}$$

It was observed that the slower rate of shrinkage of few–sided and many–sided bubbles and the faster than linear increase, for bubbles with n between 9 and 14, slightly support (5.16) rather than (5.9).

Another discrepancy between theory and experiments was highlighted by Glazier and Stavans: in the scaling state, the exponent of the average bubble area $\langle a \rangle$ was found smaller than the one predicted by the theory. The *scaling state* is a state in which the distributions of normalized bubble area and number of sides remain constant in time. In a scaling state, von Neumann predicts that $\langle a \rangle \propto t^1$. A simple theoretical argument for this property can be found in [Gla89, GS89]. In [GS89] the authors argued that during the coarsening, since

the fluid volume is very small, the excess fluid tends to accumulate in Plateau borders, carrying the foam out of the von Neumann hypothesis. The theoretical works of Weaire and Boltom ([FW92b, WB90, FW92a]), and the experimental ones of Glazier *et al* [GAG90] and Stavans, in a drained experimental cell [Sta90], verified that, taking in account the effects of the Plateau borders, the exponent of the scaling state agrees with von Neumann's prediction. Calling p the pressure in the bubble with area A_n, surrounded by n bubbles of pressure p_i, with $i = 1, \ldots, n$, and defining p_b as the pressure of the Plateau borders (assumed constant throughout the foam) the modified version of (5.9), including the effects of Plateau borders found by Weaire and Boltom [FW92b], is given by:

$$\frac{\mathrm{d}A_n}{\mathrm{d}t} = \frac{3\kappa}{\pi}\sum_{i=1}^{n}\cos^{-1}\left\{1 - \frac{1}{2\left[\frac{p-p_i}{2(p-p_b)} - 1\right]\left[\frac{p-p_{i+1}}{2(p-p_b)} - 1\right]}\right\} - 6\kappa\,. \tag{5.17}$$

5.4 A Simple Example: Two–Bubble Cluster

In this subsection, as an application of von Neumann's law, we calculate analytically the solutions of the diffusion law for a cluster made of only two bubbles. The perimeter and the radius of the films as function of time are found showing that the scaleing law (5.11) is verified. Let us consider an equilibrated cluster

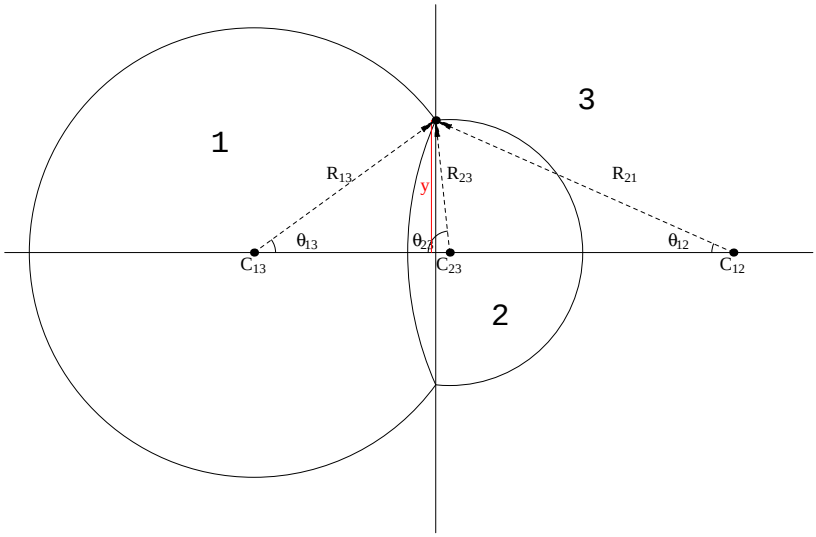

Figure 5.2: Parameters involved in the geometry of 2 bubbles.

in the plane with only two bubbles a_i, with $i = 1, 2$. In the notation of section 2.3, $F = 3$: the total number of bubbles counting the exterior of the cluster and $\mathbf{a} = (a_1, a_2)$. Integrating von Neumann's equation eq. (5.9), for F=3, we have

that

$$\mathbf{a}(t - t_0) = \mathbf{a}(t_0) - \kappa t(4, 4) = (a_1 - 4\kappa t, a_2 - 4\kappa t)\,. \tag{5.18}$$

Choosing $t_0 = 0$, rescaling the areas $a \to a/(4\kappa)$ and then defining $t_i = a_i(0)$, for $i = 1, 2$, we can write the last equation as:

$$\mathbf{a}(t) = (t_1 - t, t_2 - t) \tag{5.19}$$

Eq. (5.19) is valid until a topological change occurs. As, in the F=3 case, there is a single Γ matrix (only a possible topology), only T2 phenomena are possible. The linearity of $\mathbf{a}(t)$ implies that the first bubble to disappear is that one with smallest initial area. As we suppose $a1 \geq a2$, the time interval where eq.(5.19) is valid is $(0, t_2)$. The shape of the cluster is described by the scale invariant quantity

$$k(t) \equiv \frac{a_2(t)}{a_1(t)} = \frac{t_2 - t}{t_1 - t} = \frac{g(\theta_{12})}{g(-\theta_{12})} \tag{5.20}$$

where $g(\theta)$ is defined in (2.9) and θ_{12} is shown in figure 5.2.
$k(t)$ is scale invariant because it doesn't depend on y, the only dimensional variable. In fact θ_{12} can be written as a ratio of two radii.

The last equation shows that the area ratio k is, at any time, on the graph of the function $g(\theta_{12})/g(-\theta_{12})$. In figure 5.3 the flux diagram of the evolution is shown. The ratio $k(0) \leq 1$ fixes an initial point on the curve $g(\theta_{12})/g(-\theta_{12})$; as time goes, the 2-bubble system moves on the curve toward greater values of θ_{12}. When $\theta_{12} = \pi/3$ bubble 2 disappears: this is the most simple T2 process. The time at which $\theta_{12} = \pi/3$ is $t = t_2$, the life time of bubble C_2. $k(0) = 1$ is

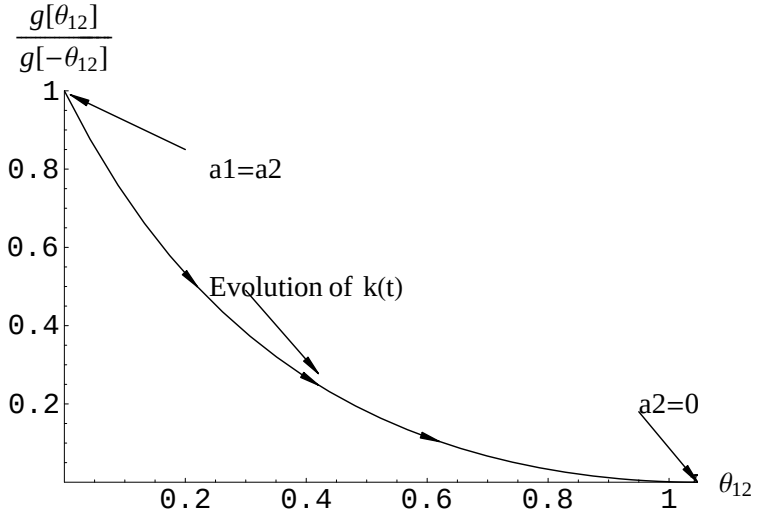

Figure 5.3: Flux diagram.

an unstable fixed point of the flux ($k(t) = k(0)\ \forall t \geq 0$): the cluster stays at

$\theta_{12} = 0$ up to $t = t_1 = t_2$ when both bubbles disappear. $\theta_{12} = 0$, corresponding to $R_{21} = \infty$, is the case when the bubbles have the same area.

In figure 5.4 and 5.5 typical evolutions of $\theta_{12}(t)$ and of the perimeter are plotted respectively. We used equation (2.11) for the perimeter ($L = \frac{2}{\gamma}(\boldsymbol{\lambda} \cdot \mathbf{a})$). Let us note the anomalous behavior of θ_{12} for $t \to t_2^+$ where the time derivative of the perimeter goes to infinity.

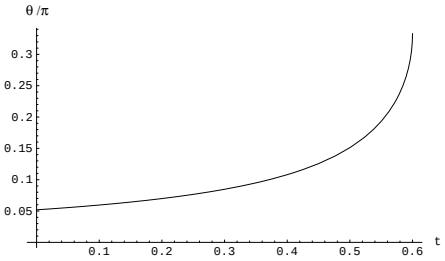

Figure 5.4: $\frac{\theta_{12}(t)}{\pi}$ for $k(0) = 0.6$.

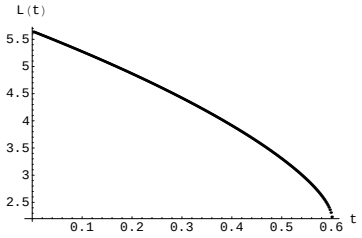

Figure 5.5: $L(t)$, case $k(0) = 0.6$.

Figure 5.6 shows the behavior of θ_{12} different for some values of $k(0)$ following the flux diagram while, in figure 5.7, successive configurations of the cluster are overlapped.

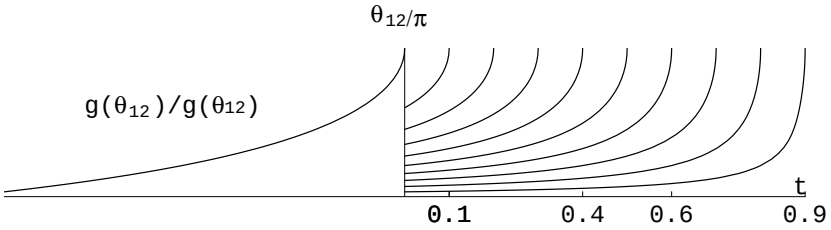

Figure 5.6: $k(0) = 0.1, 0.2 \ldots, 0.9$.

The special symmetric configuration

When the two bubbles have equal area, $a_1 = a_2$, the equilibrium state has two mirror symmetries (reflexion with respect the x and y axes). This case, $k(t) = k(0) = 1$, is an unstable fixed point of the flux. The shape remains constant in time; the evolution reduces to a pure change in length scale. Beside the simple equalities $x = 0$, $R_{21} = \infty$ and $t_1 = t_2$, there is an explicit solution for the radius $R = R_{13} = R_{23}$ and the perimeter:

$$R(t) = \tfrac{1}{\varkappa}\sqrt{a(t)}\,, \qquad L(t) = 4\varkappa\sqrt{a(t)}\,,$$

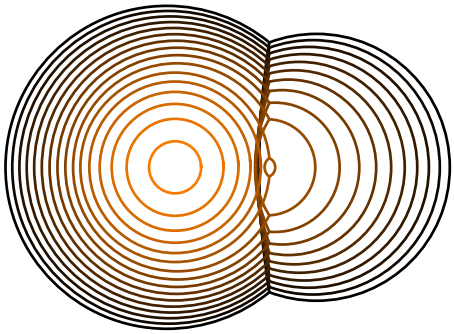

Figure 5.7: The two–bubble cluster at different time.

where $\varkappa = \sqrt{(\frac{2\pi}{3} + \frac{\sqrt{3}}{4}}$. Both quantities behave like $(t_1 - t)^{1/2}$ as predicted by dimensional arguments.

The limit $a_1 \gg a_2$

Ultimately, any non symmetric 2–bubble cluster converges to this limit.

For $a_1 \gg a_2$ and $t \leq t_2$, we find by Taylor expantion,

$$L(t) = 2\sqrt{\pi \Delta a} + \sqrt{3 g_0}\,\sqrt{t_2 - t} + 3\sqrt{\tfrac{\pi}{2\Delta a}}\,(t_2 - t) + o(t_2 - t)^{3/2}\,,$$
$$y(t) = \tfrac{1}{\sqrt{g_0}}\,\sqrt{t_2 - t}\,(1 + o(t_2 - t)) \quad \text{and}$$
$$\theta_{12}(t) = \tfrac{\pi}{3} - \sqrt{\tfrac{\pi}{g_0 \Delta a}}\,\sqrt{t_2 - t}\,(1 + o(t_2 - t))\,,$$

where $g_0 = \frac{8\pi}{9} - \frac{2}{\sqrt{3}}$ and $\Delta a = a_1 - a_2 = cst.$

5.5 Two Bubble–Cluster in 3D: Equilibrium and Evolution

As we remarked in section 2.2, to find the equilibrium configuration for a two–dimensional foam is very hard. In this section, making some assumptions, we find the equilibrium shape of a two–bubble cluster in 3D. The cluster at equilibrium has rotation symmetry around an axis, and we suppose that this symmetry is maintained also out of equilibrium and that the films are spherical caps. The rigorous mathematical proof of the existence and stability of this solution was furnished in full generality by Hutchings *et al.* [HMRR00]. We have also analyzed the behavior of the two–bubble cluster during the diffusion of the gas. The cluster is supposed ideally dry: the films are thin and the liquid at the borders is negligible. Making the additional assumptions that the diffusion verifies Fick's

law and that gas inside the bubble is incompressible, we find that the surface area of the cluster, as in the two–dimensional case, changes with a constant rate.

Noting that this 3D case is the same that the 2D case modulo the symmetry (in 2D we had symmetry under reflexion on the x-axis, here we have symmetry by rotation around the x-axis [FAB$^+$93, Hut97]), we can fix the conventions as in the two–dimensional case (section 2.3 and 5.4).

The cluster is composed by two three–dimensional regionss with volume V_i, for $i = 1, 2$. In the cluster there are three spherical cap films: a film between the two bubbles and one between any bubble and the outside.

A non–equilibrated 3D cluster has volumes:

$$\begin{cases} V_1(y, \theta_{13}, \theta_{23}, \theta_{12}) = \frac{4\pi}{3} y^3 \left[\frac{2-\cos(\theta_{13})}{\sin^3(\theta_{13})} \cos^4(\theta_{13}/2) - \frac{2+\cos(\theta_{12})}{\sin^3(\theta_{12})} \cos^4(\theta_{12}) \right] , \\ V_2(y, \theta_{13}, \theta_{23}, \theta_{12}) = \frac{4\pi}{3} y^3 \left[\frac{2-\cos(\theta_{23})}{\sin^3(\theta_{23})} \cos^4(\theta_{23}/2) + \frac{2+\cos(\theta_{12})}{\sin^3(\theta_{12})} \cos^4(\theta_{12}) \right] . \end{cases} \tag{5.21}$$

The total area of the films surface is given by the following expression:

$$S(y, \theta_{13}, \theta_{23}, \theta_{12}) = 2\pi y^2 \left[\frac{1+\cos(\theta_{13})}{\sin^2(\theta_{13})} + \frac{1+\cos(\theta_{23})}{\sin^2(\theta_{23})} + \frac{1-\cos(\theta_{12})}{\sin^2(\theta_{12})} \right] . \tag{5.22}$$

Minimizing

$$G(y, \theta_{13}, \theta_{23}, \theta_{12}, \boldsymbol{\lambda}; \mathbf{V}_0) = \gamma S + \boldsymbol{\lambda} \cdot (\mathbf{V}_0 - \mathbf{V}) ,$$

where $\boldsymbol{\lambda} = (\lambda_1, \lambda_2)$ are the Lagrange multipliers and $\mathbf{V}_0 = (V_{01}, V_{02})$ are the constant volumes of the bubbles, we obtain

$$\begin{cases} \boldsymbol{\lambda} = 2\gamma(\frac{1}{R_{13}}, \frac{1}{R_{23}}), \\ \frac{1}{R_{21}} = \frac{1}{R_{23}} - \frac{1}{R_{13}}, \\ \theta_{13} = \frac{\pi}{3} - \theta_{12}, \qquad \theta_{23} = \frac{\pi}{3} + \theta_{12}; \end{cases}$$

where we have supposed that $V_{01} > V_{02}$.

For the time evolution, Fick's law says:

$$\frac{\mathrm{d}V_i}{\mathrm{d}t} = -\sigma \int_{S_{ij}} \Delta P \mathrm{d}S = -2\gamma\sigma \int_{S_{ij}} \frac{\mathrm{d}S}{R_{ij}} = -4\pi\gamma\sigma R_{ij} \Delta(\cos\theta_{ij}) \tag{5.23}$$

where S_{ij} is the surface of the film between bubbles i and j. Setting $\kappa = 4\pi\gamma\sigma$ we obtain by eq.(5.23)

$$\begin{cases} \dot{V}_1 = -\kappa \left[R_{13}(1+\cos(\theta_{13})) - R_{21}(1-\cos(\theta_{12})) \right] , \\ \dot{V}_2 = -\kappa \left[R_{23}(1+\cos(\theta_{23})) + R_{21}(1-\cos(\theta_{12})) \right] . \end{cases} \tag{5.24}$$

To find the equations of the motion we derive eqs.(5.21) with respect to the time and impose the equality to eq.(5.24). We obtain:

$$\begin{cases} \dot{\theta}_{12} = \kappa \frac{\sin(3\theta_{12})}{5\pi y^2}, \\ \dot{y} = \kappa \frac{2\cos(3\theta_{12})-7}{15\pi y} . \end{cases} \tag{5.25}$$

We also obtain that, at the equilibrium, the energy of the cluster:

$$E = \gamma S = \frac{3}{2}\boldsymbol{\lambda}\cdot\mathbf{V} = \gamma\frac{18\pi\ y^2}{1+\cos(3\theta_{12})}\,; \tag{5.26}$$

deriving it with respect to time, we get that the variation of the energy is constant:

$$\dot{E} = \boldsymbol{\lambda}\cdot\dot{\mathbf{V}} = -6\gamma\kappa\,. \tag{5.27}$$

Equations (5.26) and (5.27) are already found in (2.14) and (2.15), respectively.

5.6 Continuity of T2, limit case

We saw before in section 5.2 that topological changes (T1, T2(3), T2(4) ....) determine the time intervals where von Neumann's law is applicable. During such processes the topological charge of some bubbles changes, so the time evolution area of these bubbles changes its slope (5.9). Moreover, if the resulting configuration is not equilibrated, the system will relax quickly to a new quasi–equilibrium configuration. So, topological processes could cause a discontinuity of the energy function (then in the total length of the film). In this section we prove that, in the limit where the area of a triangular bubble goes to zero, the point where the bubble collapses is an equilibrated vertex for the foam (equations (5.1) and (5.2) are verified). So, there is no abrupt variation of the physical parameters; the foam is, at any time, equilibrated. This implies that the foam, in a T2(3) process, doesn't need to do any new equilibration adjustment and that the perimeter changes continuously. We will prove the T2(3) continuity in much more generality in the next sections. For the proof we use the set of coordinates defined in section 2.5.

Let's consider a bubble which is contained in an equilibrated foam. We suppose that this bubble has three neighbouring bubbles and that its area is very small compared with those of the neighbours. Figure 5.8 shows a typical 3-edge bubble in an equilibrated foam. Let t_2 be the collapse time of the three–sided bubble. We will prove that properties (5.1) and (5.2) are verified at any time before and after the T2 ($t = t_2$). Taking fig.5.8 as reference, we assume for this proof a particular notation: the vertex and line associated with the vertex are indicated with the letters. The curvatures are defined as $k_{ij} = \frac{1}{R_{ij}}$; they are always positive and the equations where they appear must be considered already with the good signs. The Laplace relations for the vertices $A = \{1,2,4\}$, $B = \{1,2,3\}$, $C = \{1,3,4\}$ are:

$$\begin{cases} k_{24} = k_{23} + k_{34} \\ k_{12} = k_{13} + k_{23} \\ k_{14} = k_{13} - k_{34}\,. \end{cases} \tag{5.28}$$

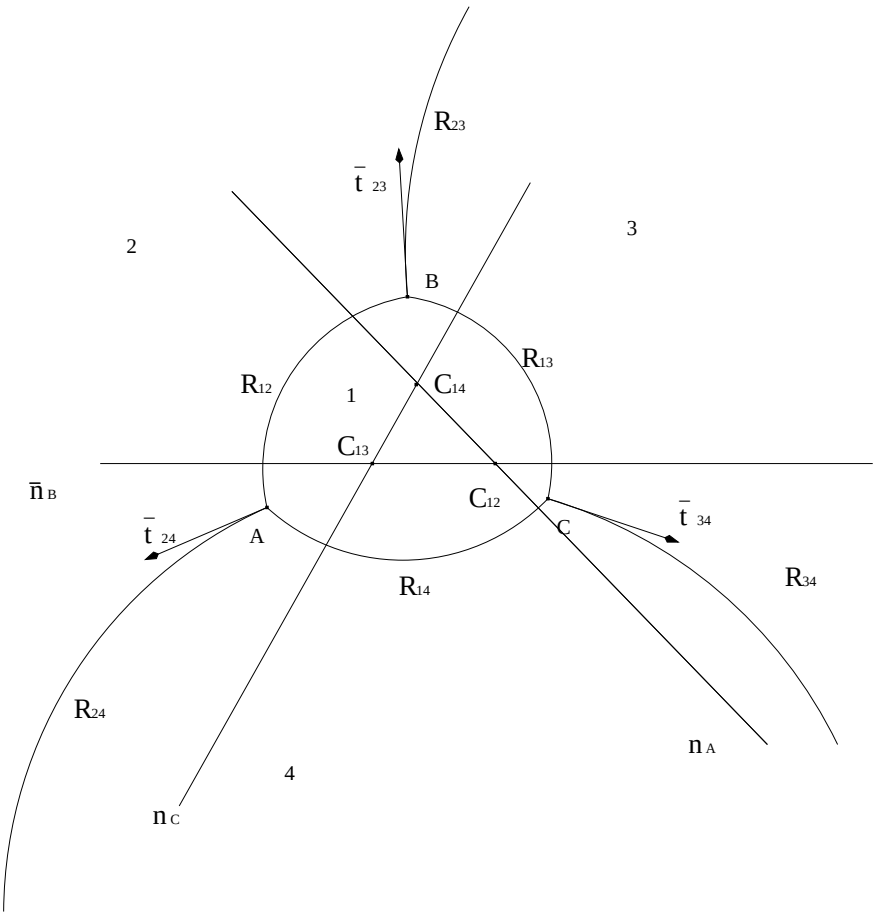

Figure 5.8: Typical three sided–bubble.

In the limit $t \to t_2$, we suppose that $k_{13} = 1/\epsilon$, where ϵ is small compared with k_{23}, k_{24} and k_{34}. This means that a radius of bubble 1 goes to zero. The exact dependence of ϵ on time is not important. What matter is that $\epsilon \to 0$ while $t \to t_2$. This is sufficient to see that the bubble disappears into a point and that P-L equilibrium is preserved. Clearly, taking the limit $\epsilon \to 0$, (5.28) is verified and it gives the relation for the vertex formed by the collapse of the bubble:

$$k_{24} = k_{23} + k_{34} \tag{5.29}$$

so it remains to verify the validity of (5.1).

First, using that ϵ is small, we find the inequality relation out of all the curvatures:

$$\begin{cases} k_{12} = \frac{1+\epsilon k_{23}}{\epsilon} > \frac{1}{\epsilon} = k_{13} \\ k_{14} = \frac{1-\epsilon k_{34}}{\epsilon} < \frac{1}{\epsilon} = k_{13}\,. \end{cases} \tag{5.30}$$

Let us determine the angles at each vertex to second order in ϵ:

$$\begin{cases} \theta_A = \arctan(\sqrt{3}\frac{k_{14}}{k_{12}+k_{24}}) = \frac{\pi}{3} - \frac{\sqrt{3}}{2}k_{24}\epsilon + O(\epsilon)^2 \\ \theta_B = \arctan(\sqrt{3}\frac{k_{13}}{k_{12}+k_{23}}) = \frac{\pi}{3} - \frac{\sqrt{3}}{2}k_{23}\epsilon + O(\epsilon)^2 \\ \theta_C = \arctan(\sqrt{3}\frac{k_{14}}{k_{13}+k_{34}}) = \frac{\pi}{3} - \frac{\sqrt{3}}{2}k_{34}\epsilon + O(\epsilon)^2 \end{cases} \tag{5.31}$$

By θ_i, with $i = A, B, C$, we can calculate the relative coordinates of the curvature centres (equation 2.25). At A, $k_{12} > k_{14} > k_{24}$, so that:

$$\begin{cases} C'_{14}(A) = -\frac{1}{k_{14}}\cos(\theta_A) = -\frac{\epsilon}{2} - \frac{1}{4}(3k_{23} + 5k_{34})\epsilon^2 + O(\epsilon)^3 \\ C'_{24}(A) = \frac{1}{k_{24}}\cos(\frac{\pi}{3} - \theta_A) = \frac{1}{k_{24}} - \frac{3}{8}k_{24}\epsilon^2 + O(\epsilon)^3 \\ C'_{12}(A) = -\frac{1}{k_{12}}\cos(\frac{\pi}{3} + \theta_A) = \frac{\epsilon}{2} - \frac{1}{4}(5k_{23} + 3k_{34})\epsilon^2 + O(\epsilon)^3\,. \end{cases} \tag{5.32}$$

At B, $k_{12} > k_{13} > k_{23}$, so that:

$$\begin{cases} C'_{12}(B) = -\frac{1}{k_{12}}\cos(\frac{\pi}{3} + \theta_B) = \frac{\epsilon}{2} - \frac{5}{4}k_{23}\epsilon^2 + O(\epsilon)^3 \\ C'_{23}(B) = \frac{1}{k_{23}}\cos(\frac{\pi}{3} - \theta_B) = \frac{1}{k_{23}} - \frac{3}{8}k_{23}\epsilon^2 + O(\epsilon)^3 \\ C'_{13}(B) = -\frac{1}{k_{13}}\cos(\theta_B) = -\frac{\epsilon}{2} + \frac{3}{4}k_{23}\epsilon^2 + O(\epsilon)^3\,. \end{cases} \tag{5.33}$$

Similary, at C, $k_{13} > k_{14} > k_{34}$:

$$\begin{cases} C'_{13}(C) = -\frac{1}{k_{13}}\cos(\frac{\pi}{3} + \theta_C) = \frac{\epsilon}{2} - \frac{3}{4}k_{34}\epsilon^2 + O(\epsilon)^3 \\ C'_{34}(C) = \frac{1}{k_{34}}\cos(\frac{\pi}{3} - \theta_C) = \frac{1}{k_{34}} - \frac{3}{8}k_{34}\epsilon^2 + O(\epsilon)^3 \\ C'_{14}(C) = -\frac{1}{k_{14}}\cos(\theta_C) = -\frac{\epsilon}{2} - \frac{5}{4}k_{34}\epsilon^2 + O(\epsilon)^3\,. \end{cases} \tag{5.34}$$

At first order in ϵ, for each $i = A, B, C$, the distance between each relative origin $\vec{O}_i$ and any centre of curvature of the sides of bubble 1 placed on the same line is $\frac{\epsilon}{2}$ (for example: for B, the distance between $\vec{C}_{12}$ or $\vec{C}_{13}$ and $\vec{O}_B$). So, in the limit $\epsilon \to 0$, the centres $\vec{C}_{12}$, $\vec{C}_{13}$ and $\vec{C}_{14}$ form an equilateral triangle and the length of its edges is ϵ.

Moreover, if we calculate the value of y_i for $i = A, B, C$, the distance between the origin $\vec{O}_i$ and the vertex i, we obtain (to second order in ϵ):

$$\begin{cases} y_A = \frac{\sqrt{3}}{2}\epsilon - \frac{\sqrt{3}}{4}(k_{23} - k_{34})\epsilon^2 + O(\epsilon)^3 \\ y_B = \frac{\sqrt{3}}{2}\epsilon - \frac{\sqrt{3}}{4}k_{23}\epsilon^2 + O(\epsilon)^3 \\ y_C = \frac{\sqrt{3}}{2}\epsilon + \frac{\sqrt{3}}{4}k_{34}\epsilon^2 + O(\epsilon)^3\,. \end{cases} \tag{5.35}$$

When ϵ goes to zero, the triangle formed by the vertices coincides with that one formed by the centres of curvature of the smallest bubble's films. Then, when $t \to t_2$ ($\epsilon \to 0$) bubble 1 collapses to a point; the centres and the vertices related to bubble 1 coincide.

Now we prove that Plateau's law is valid when bubble 1 collapses, so that the equilibrium conditions hold in a T2 process. To prove (5.1) is equivalent to verify

that the angle between the tangents to the films at the three vertices is always $\frac{2\pi}{3}$. For example, let us consider the angle between the tangents to the films 23 and 24:

$$\angle(\vec{t}_{23}, \vec{t}_{24}) = \angle(\vec{t}_{23}, \widehat{n}_A) + \angle(\widehat{n}_A, \widehat{n}_B) + \angle(\widehat{n}_B, \vec{t}_{24}) \,, \tag{5.36}$$

where $\widehat{n}_i$, with $i = A, B, C$, is the direction of the line where the centres of curvature of the films meeting in vertex i stay. Using (5.31), for small ϵ

$$\begin{cases} \angle(\vec{t}_{23}, \widehat{n}_A) = \frac{\pi}{6} - \theta_B \\ \angle(\widehat{n}_A, \widehat{n}_B) = \frac{\pi}{3} \\ \angle(\widehat{n}_B, \vec{t}_{24}) = \frac{\pi}{6} - \theta_A \end{cases} \tag{5.37}$$

then

$$\angle(\vec{t}_{23}, \vec{t}_{24}) = \frac{2\pi}{3} - \frac{\sqrt{3}}{2}(k_{24} + k_{23})\epsilon + O(\epsilon)^2$$

and

$$\lim_{\epsilon \to 0} \angle(\vec{t}_{23}, \vec{t}_{24}) = \frac{2\pi}{3}$$

Plateau and Laplace laws are preserved in the limit where the area of bubble 1 tends to zero, this implies that T2(3) processes are continuous. Moreover, we can say that in the limit of small area, the three–sided bubble forms an equilateral curved triangle where the vertices are also the centres of curvature of the opposite edges.

5.7 Star–Triangle Equivalence

In the last section we have proved that in the limit where the area of a three–sided bubble or triangle goes to zero, the equilibrium of the foam is preserved: Plateau and Laplace conditions, (5.1) and (5.2), are verified at any time and the point where the bubble collapses is a new equilibrated vertex of the foam. On the other hand, if t_2 is the instant when a three–sided bubble disappears, vertex equilibration implies that at $t = t_2$ the centres of curvature of the outgoing films are aligned and that their mutual distances are determined by the values of these curvatures.
Are these properties verified only at the bubble's disappearance or are they verified also before the bubble collape? To answer this question corresponds to prove the star–triangle equivalence ($\curlywedge - \triangle$) for standard equilibrated foams:

Equivalence[MO03] 5.1. *For any three–sided bubble (triangle) within a standard flat equilibrated two–dimensional foam,*

1. *When prolonged into the triangle, the three external edges meet at a common point, star point or vertex.*

2. *The angles of the prolonged edges at the star point satisfy the Plateau–Laplace conditions (5.1-5.2).*

Remark. The hypothesis of standard foam, for which the line tension is constant and, so, all the angles are equal to $\frac{2\pi}{3}$ can be removed. In this case, for the proof of the equivalence, Moukarzel's duality has to be introduced [Mou97] and we will see that in the next chapter. Since for soap foams, generally, the tension line is assumed constant, here we furnish the proof of ⅄−△ equivalence in the standard case.

The proof of the equivalence (5.1) is based on the invariance of flat foams equilibrium laws by Moebius transformations or homographies (which we saw in sec. 2.4 pag.22) and the *local reflection principle*. We enunciate these before giving the proof of the ⅄−△ equivalence.

Inversion

The symmetry group G of equilibrated flat 2D foams is the group of conformal transformation of the compactified plane $\overline{\mathbb{C}} = \mathbb{C} \cup \{\infty\}$, conformally equivalent to the sphere S^2. This is an extension of the two–dimensional Euclidean group by inversions (sec. 2.4 pag.22). In $\overline{\mathbb{C}}$, a pure inversion is $z \mapsto \alpha/(z - z_0)$, where z_0 is the *inversion point* and α is a constant.

Besides preserving angles (conformality), these transformations map circles to circles; in particular, any circle passing through the inversion point is sent to a straight line (and *vice versa*). Moreover the equilibrium conditions (5.1-5.2) are conserved by these transformation [Mou97, Wea99].

Local reflection principle

A straight edge (curvature equal to zero) is a symmetry axis for the figure formed by any of its end vertices and the two circles incident to that vertex. Indeed, the circles are defined by the vertex v, the tangent at that point and curvature. The tangents are symmetric by the Plateau condition (5.1); equality of curvatures (up to the sign) follows from the Laplace condition (5.2). In particular the line defined by the centres of the two circles through v is orthogonal to the straight edge (see figure 5.9). This reflection principle is only valid for standard foam where the line tensions have the same value.

Proof of 5.1. If the star point exists, the Laplace relation (5.2) is trivially verified for the external legs meeting on it. It is assured by the fact that the bubbles touching the triangle form a closed path, see eq. (2.5).

We saw in section 2.5 that in 2D flat equilibrated foams the curvature centres of the three edges (arcs of circle) meeting at any vertex v are aligned. As two intersecting circles meet at two points (the degenerate case is not interesting

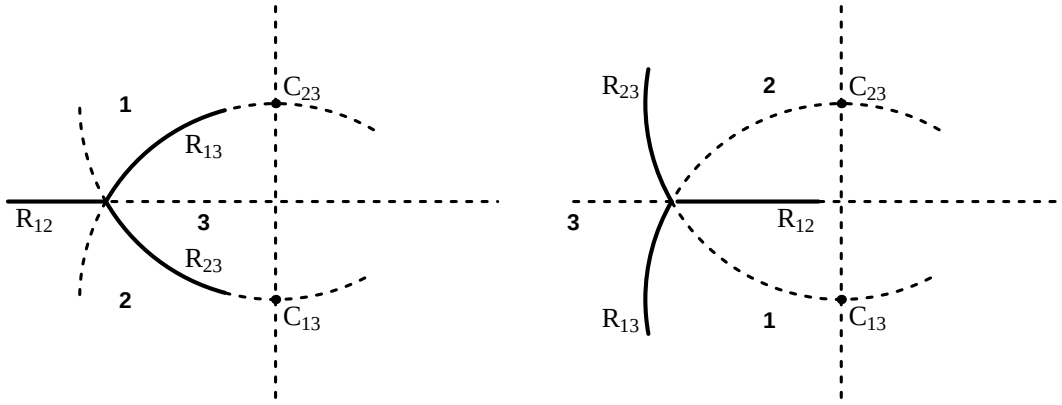

Figure 5.9: Two cases of straight edge where the reflection symmetry applies. $i, j = 1, 2, 3$ is the bubbles numeration while R_{ij} and C_{ij} are the radius and the centre of curvature of the film $\{i\,j\}$.

for foams), the alignment property is equivalent to the existence of a point v^*, conjugate to v, where the three circles also meet. v^* is symmetric to v with respect to the line of the centres. When one of the edges is straight, alignment reduces to orthogonality, as implied by local reflection symmetry.

Let us consider a generic three sided bubble or triangle in the setting of figure 5.10 and let us apply an inversion transformation with respect to the point v^*_{123}, conjugate of v_{123}.

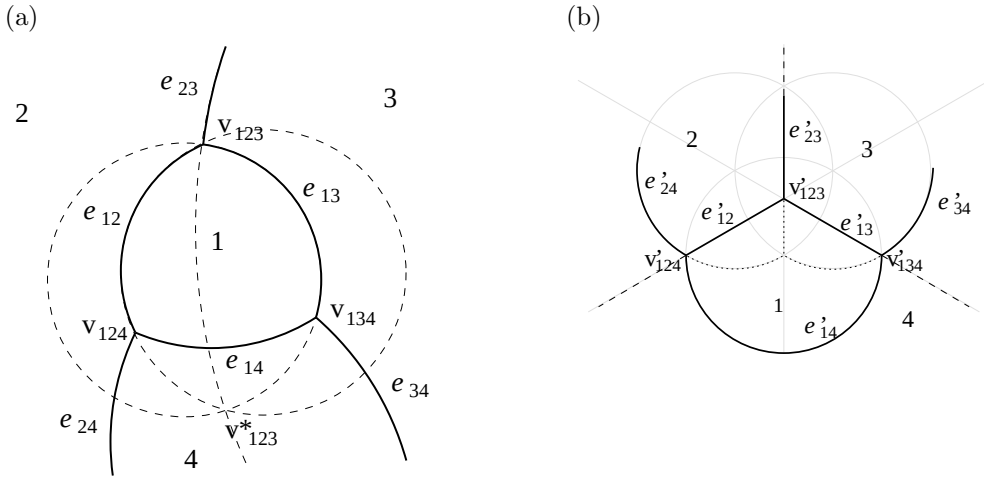

Figure 5.10: a) A generic three–edge bubble contained in an equilibrated foam. b) The same bubble transformed by a suitable inversion.

The circles of the edges e_{23}, e_{13} and e_{12}, passing through v^*_{123}, are mapped on to lines, e'_{23}, e'_{13} and e'_{12} meeting at v'_{123} with angles of $\frac{2\pi}{3}$ by inversion conformality

(figure 5.10(b)). We can assume that v'_{123} is at the origin 0.

Let us consider the vertex v'_{124} on the line e'_{12}. As the angle of $2\pi/3$ is preserved, the tangent to e'_{14} at v'_{124} must be vertical (parallel to e'_{23}). So the centre c'_{14} of e'_{14} is on the same horizontal line as v'_{124}. By the same argument at v'_{134}, we find that v'_{134}, v'_{124} and c'_{14} are on the same horizontal line. Therefore e'_{14} is a half–circle centred on the axis e'_{23} which, thus, become a symmetry axis for the triangle. The reflection principle can now be applied to the two straight edges e'_{12} and e'_{13} to extend the symmetry to the figure made of the triangle and the circles supporting its legs. This figure becomes completely symmetric under the group D_3 (generated by mirrors at $\pi/3$).

In particular, the two circles supporting e'_{24} and e'_{34} intersect a point, v'_{234}, on the axis e'_{23}, proving convergence, and they meet with angle $2\pi/3$, proving the Plateau condition (5.1). Applying the inverse transformation ensures the required properties for the original three–bubble.

□

The star–triangle equivalence could be considered as a *Bubble decoration theorem*, in reference to the "vertex" decoration theorem of Weaire [FW92b] (theorem 6.1): triangular bubbles can be considered as a "decoration" of the foam.

As corollary of 5.1, equilibrated triangles are rigid modulo homographies. For example, by $SL(2,\mathbb{C})$, any equilibrated three–sided bubble can be mapped on to the regular equilateral curved triangle with angles $2\pi/3$ and straight external legs (figure 5.11). The inversion point to obtain this symmetrical configuration is the conjugate point of the star point ($z_0 = v^*_{234}$).

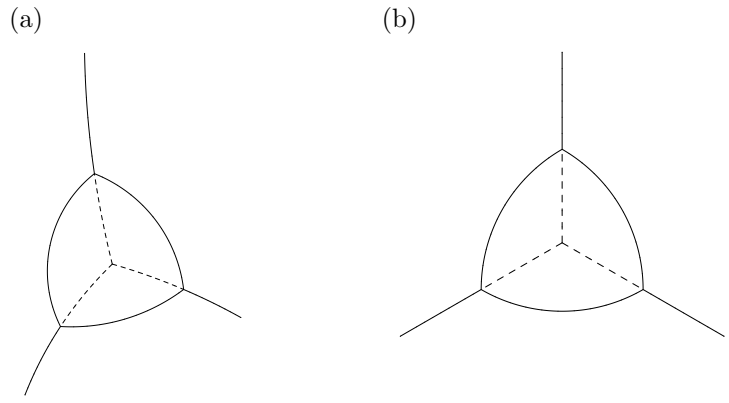

Figure 5.11: A generic three–sided bubble (a) can be mapped into a regular equilateral curved triangle (b) by a suitable Moebius transformation.

5.8 T2 Continuity and ⅄− △ Equivalence

The main corollary of ⅄−△ equivalence is continuity at T2(3) processes. During the evolution of the foam by gas diffusion, when a three–sided bubble shrinks, the outside edges extend to a virtual equilibrated star figure at any time. So, precisely when the triangle degenerates to a point, the star vertex becomes real and the figure is in equilibrium (as proved in sec. 5.6). No fast evolution, or discontinuity on small scale, is needed.

To see that more explicitly, let us consider an equilibrated cluster, constituted by F bubbles, during the diffusion ruled by von Neumann's equation (5.9). Besides, let us consider a time interval $(0, t_1)$ where only one bubble disappears, by a T2(3), (for example, bubble m at $t = t_2 < t_1$). No more topological changes occur. The quasi equilibrium expressions of the energy and its derivative, respectively equations (2.11) and (2.14), are for any $0 < t < t_2$:

$$E(t) = \gamma L = \gamma \sum_{\{Edges\}} l_j = 2 \sum_{i=1}^{F} P_i(t) A_i(t) = 2 \sum_{i=1}^{F} P_i(t)(A_i(0) + \kappa\, q_i\, t)\,, \quad (5.38)$$

$$\frac{\mathrm{d}E(t)}{\mathrm{d}t} = \sum_{i=1}^{F} P_i(t) \dot{A}_i(t) = \kappa \sum_{i=1}^{F} P_i(t) q_i\,; \quad (5.39)$$

where we have used von Neumann's law (5.9) in the last equalities of (5.38) and (5.39). Here q_i represents the topological charge of bubble i and P_i is the pressure of bubble i with respect to the pressure outside the cluster. At $t = t_2$, $q_i \to q'_i$, where $q_i = q'_i$ except for bubble m ($q'_m = q_m - 3 = -6$), which has to be removed from the energy expression, and its neighbours ($q' = q - 1$). For $t_1 > t \geq t_2$, we can write (5.38) as

$$E(t) = 2 \sum_{i=1,\, i\neq m}^{F} P_i(t) \left[A_i(0) + \kappa\, q_i\, t_2 + \kappa\, q'_i (t - t_2)\right]\,. \quad (5.40)$$

$\mathrm{d}E(t)/\mathrm{d}t$, for $t_1 > t \geq t_2$, is obtained by replacing q_i with q'_i in (5.39) and removing the term corresponding to m. Clearly $E(t)$ is continuous. Pressures, linked to the curvatures by Laplace's equation (5.4), vary continuously during T2 by ⅄−△ equivalence. Therefore equations (5.38) and (5.40) coincide at $t = t_2$.

When bubble m shrinks, the curvature of its films and its pressure could diverge. So, the term in (5.38) corresponding to bubble m could not be regular. We will prove its regularity. To see that, we use the fact, proved in section 5.6, that in the limit where it vanishes, bubble m assumes the form of a regular equilateral curved triangle, where the vertices are also the centres of curvature of the opposite edges. Let us calculate the perimeter and radius of a curved triangle of area A_m as in figure 5.12:

The area of the internal equilateral triangle is $A_T = \frac{\sqrt{3}}{4}R^2$ while the area of the circular section formed by a film and an edge is $A_S = \frac{\pi}{6}R^2 - A_T$. Then $A_m = (\frac{\pi}{2} - \frac{\sqrt{3}}{2})R^2$. As the perimeter of the curved triangle is $l_m = \pi R$, we obtain that for $t \to t_2$

$$l_m = \frac{\pi}{\sqrt{\frac{\pi}{2} - \frac{\sqrt{3}}{2}}} A_m^{1/2} \propto A_m^{1/2} \propto \sqrt{t_2 - t}\,. \qquad (5.41)$$

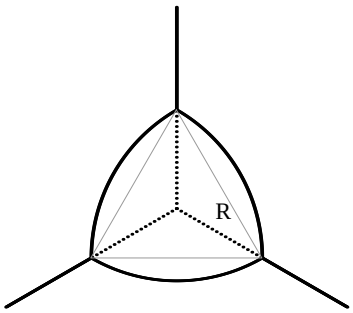

Figure 5.12: Curved equilateral triangular bubble in the limit where the $A \to 0$.

Therefore, when the area A_m tends to zero it is evident from (5.41) that, the term l_m in (5.38) tends to zero too.

The discontinuities, in T2(3) processes, affect the first time derivative of the energy (5.39). At $t = t_2$, a sudden change in the topology makes the limits of $\mathrm{d}E(t)/\mathrm{d}t$, for $t \to t_2^{\pm}$, different. By (5.41), the perimeter of bubble m scales with $l_m \propto \sqrt{t_2 - t}$. As the area is proportional to the time, it results that $P_m(t) \propto 1/(t_2 - t)$; then the pressure of the shrinking bubble diverges. This implies that, while the limit from the right of $\mathrm{d}E(t)/\mathrm{d}t$ ($t \to t^+$) exists, that one from the left is $-\infty$. The negative sign of the limit derives from the facts that the topological charge q_m in (5.39) is negative ($q_m = -3$) and the pressure field can be translated, giving any bubble a positive pressure.

Therefore the energy, or equivalently the perimeter, of a 2D foam during the von Neumann evolution, has a downwards vertical slope at a T2(3) process. We have already observed, in the simple two bubble evolution, the vertical slope of the perimeter just before of the smaller bubbles disappearing (figure 5.5).

Finally we have to observe that ⅄−△ equivalence is a pure equilibrium property that cannot be extrapolated to either mechanical response or time evolution. To demonstrate this point, let us compare two samples slowly evolving by gas diffusion under the von Neumann hypothesis. The two foams are identical at time $t = 0$ except for a star–triangle transformation. Let us also assume that no other topological changes occur during the lifetime t_0 of the triangular bubble (of area B). Initially, if a bubble with n sides ($q_n = n - 6$) and area A has the star participating to its boundary, its replica neighbouring the triangle has $n + 1$ and area $A - A_0$ (figure 5.13). At any later time $t \le t_0$, the bubble area obeys to (5.9). So, at the time $t_0 = B/(3\kappa)$ when the triangle vanishes, and the topology of the two samples converges, the area of the neighbour is $A + \kappa\, q_n t_0$ in one case, and $A - A_0 + \kappa\,(q_n + 1)t_0$ in the order. So there is a metric difference of $\kappa t_0 - A_0 = B/3 - A_0$ between the two situations; in general, replacing a triangle by a vertex changes the way the foam coarsens.

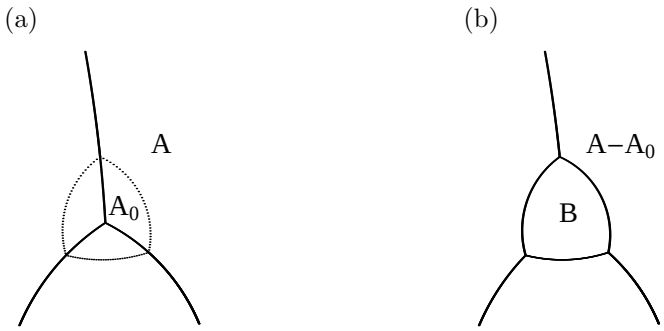

Figure 5.13: A bubble of area A gains one side and loses a portion of area A_0 in a neighbouring triangle. The area B of the triangle is composed of three such portions.

⅄−△ Reduction

Star–triangle equivalence could be useful to reduce the number of coordinates, thereby improving the efficiency of numerical minimization. For example, taking in non–equilibrated foams, they could be relaxed to equilibrium by eliminating small bubbles. Afterwards, small bubbles could be added to the equilibrated structure (see fig. 5.14).

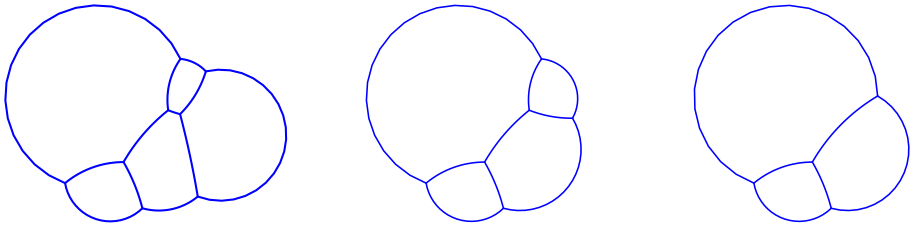

Figure 5.14: Reduction of a cluster by ⅄−△. A five–bubble cluster is reduced by successively steps to three–bubble cluster.

Conclusions

In the case of ideal 2D foams, in the theoretical limit where the liquid fraction goes to zero, the evolution of the foam due to the gas diffusion through the films is very slow compared to the equilibration process. Therefore the foam can be considered at equilibrium during the coarsening if topological processes, which break suddenly equilibrium, don't occur.

Von Neumann's equation links the topology of the bubble with the variation of the bubble's area. It has been solved in the simple case of two bubbles in the plane. The continuity of the perimeter and the discontinuity of its time derivative have been established when the smaller bubbles' area goes to zero (the simplest

T2 process). Moreover, we have explicitly shown that the linear length quantities vary proportionally to the square root of the time as predicted by dimensional arguments.

Analyzing the same problem of two bubbles in three dimensions we have found that the first derivative of the bubbles' area is again constant as in two dimensions.

Starting from the observation made for a two–bubble cluster we have found that the process T2(3), where a three–sided bubble disappears, is continuous: the perimeter, that is the energy, varies continuously during the process. This property is due to the fact that when the triangular bubble disappears the foam is equilibrated. In the limit where the bubble area is small, the point where the bubble collapses becomes, after the T2(3), an equilibrated vertex of the foam. Successively we have proved, using the symmetry properties of the equilibrated foams, that any three–sided bubble has an internal equilibrated virtual vertex formed by the prolongations of the external edges incident to the triangle (star–triangle equivalence). When the bubble collapses, this virtual vertex becomes a real vertex of the foam and so the foam does not go out of equilibrium.

The continuity of the energy or perimeter at T2(3) is assured by ⅄−△ equivalence. We saw this continuity by using an expression for the perimeter which depends only on the bubbles' area and the pressure. Therefore, we have shown that the time derivative of the perimeter is discontinuous from the left.

⅄−△ equivalence can not be used to study coarsening: replacing a triangle by a vertex changes the way the foam coarsens.

Successivelyn the future we would like extend the ⅄−△ equivalence, proved only on the plane, to the case where the foam is embedded on a generic curved surface.

Chapter 6

Non–Standard 2D Flat Foams

In real three or two–dimensinal dry soap foams the surface tension (line tension) γ is generally assumed to be constant on any film through the foam; yet, as we saw in section 1.1, equilibrium laws can be written also in the case where the surface tension varies from a film to another (1.9-1.10) (*non–standard* foams). In this case the surface tensions are the "weights" by which any film appears in the Plateau and Laplace equations. A non–standard foam can modelize a soap foam where the films have different thicknesses and then different surface tensions (thick films, common black films and Newton black films) [HDPF$^+$00].

We introduced non–standard foams not only for "a need of generality" but because, in this more general case, a 2D–equilibrated flat foam has some important properties which turn out to be very useful to prove the generalization of the $\curlywedge\!\!-\,\triangle$ equivalence and its corollaries. While for standard 2D flat foams, the star–triangle equivalence implies the continuity of the processes T2(3), in this case, the equivalence permits to prove the "decoration" theorem of Weaire [Wea99, WH99]:

Theorem 6.1. *Any 2D dry foam, with uniform and isotropic line tension, can be decorated by the superposition of a Plateau border at each threefold vertex, to give an equilibrated wet foam structure, provided these Plateau borders do not overlap.*

The decoration theorem, very important in the theory of two–dimensional flat foams, allows to relate the equilibrium of a 2D ideal foam, where the liquid fraction is assumed to be zero, to the equilibrium of a 2D dry foam where a little liquid is concentrated in a small region at the vertices (see sec. 2.1). In fact, in a 3D dry foam the liquid is assumed to be only in the Plateau borders. In two dimensions, Plateau borders correspond to the vertices of the foam. So, the presence of a small quantity of liquid could be considered as a small triangular bubble at the vertex with a lower pressure than that of the gas in the cells and a different line tension at the interfaces.

To prove $\curlywedge - \triangle$ equivalence in the general case, we have to introduce Moukarzel's *duality* [Mou97]. Moukarzel proved an equivalence between equilibrated non–standard ideal 2D foams and a generalization of the Voronoï partition (VP): sectional multiplicative Voronoï partition (SMVP). This powerful result is based on the fact that SMVP and non–standard 2D foams are both partitions of the plane in cells separated by circular arcs. Finding the conditions that a circular partition has to verify to be a SVMP and proving that these conditions are the necessary ones to have equilibrium in the foam, Moukarzel establishes the correspondence between SMVP and equilibrated foams. The condition that a circular partition must verify to be a foam (and a SMVP) is the existence of a *dual*, or *orientated reciprocal figure*.

In the first two sections of this chapter we give a small introduction to Moukarzel's duality. For the seek of simplicity, we don't give any proof, which can be found in the original paper [Mou97]. In the third section we prove the $\curlywedge - \triangle$ equivalence for non–standard foams and in the last two sections we re–derive the decoration theorem as a corollary of $\curlywedge - \triangle$.

6.1 SMVP and Moukarzel's Duality

Let us consider an n–dimensional space where F points $\{f_i\}_{i=1}^{F}$ are given (*sources*). The Voronoï partition of the space (VP) with respect to $\{f_i\}$ is a partition of the space into cells Ω_i defined by $x \in \Omega_i$ if f_i is the closest source to x [OBS92]:

$$\Omega_i = \{x \in \mathbb{R}^n | \, d(x, f_i) < d(x, f_j) \quad \forall \, j \neq i\}, \tag{6.1}$$

where $d(\cdot, \cdot)$ denotes the euclidean distance. Two neighboring cells Ω_i and Ω_j are delimited by an interface Γ_{ij} of points equidistant from f_i and f_j:

$$\Gamma_i = \{x \in \mathbb{R}^n | \, d(x, f_i) = d(x, f_j) < d(x, f_k), \quad \forall \, k \neq i, j\}. \tag{6.2}$$

The interfaces are $(n-1)$–dimensional hyperplanes normal to the line joining f_i and f_j. In two dimensions, the VP separates the plane in convex polygonal cells. The interfaces are straight lines and the vertices v_{ijk} are defined as the points where three interfaces (Γ_{ij}, Γ_{ik} and Γ_{jk}) meet. Any vertex is the centre of a circle through the sources of the three neighbouring cells. The possibility of higher multiplicity vertices exists but only for particular locations of the sources (on the same circle, for example); and in the generic case, they can be ignored. As the concept defining VPs is the equidistance between the sources, generalizations of them can be obtained by changing the way the distance to the sources is measured.

The sectional Voronoï partition (SVP), in the plane, is defined as a two–dimensional cut of a three–dimensional VP. The sources are defined as the projections of the original sources f_i in the plane. The cells are the intersections of

the 3D–cells with the plane. If the sources of the VP are $f_i = (x_i, y_i, z_i)$, the projection of these on the plane $\Pi_z \equiv \{z = 0\}$ defines the SVP's sources $P_i = (x_i, y_i)$, which have associated *heights* z_i. The cells are then defined as:

$$\Omega_i = \{x \in \Pi_z |\, d(x, P_i)^2 + z_i^2 < d(x, P_j)^2 + z_j^2, \quad \forall\, j \neq i\}, \tag{6.3}$$

where $d(\cdot, \cdot)$ is the eucliden distance in the plane. In SVP, interfaces are still straight lines which meet at triple vertices (generally). Moreover, though an interface Γ_{ij} is still normal to the line joining P_i and P_j, in general, it is not equidistant from them. Another property, which differs form VP, is that in this case there may be sources to which no cell is associated (the 3D–cell is not cut by Π_z). These structures, equivalent to Laguerre partitions [IIM85], are frequently used as approximate models for cellular structures and, in particular, for 2D grain growth, where the pressure difference between the grains is negligible [OBS92].

In the case of 2D foams, to take in to account the circularity of the films, Moukarzel examines a further generalization of the Voronoï partitions: the sectional multiplicative Voronoï partition (SMVP) [Mou97]. As in SVP, sectional multiplicative Voronoï partitions are two–dimensonal cuts of a partition in the three–space, but here another parameter, the *intensity* a_i, is associeted to any source P_i; the distance, used to define the cells depends also on this parameter[1]. The cells and films are defined respectively by:

$$\Omega_i = \left\{ x \in \Pi_z |\, \frac{d(x, P_i)^2 + z_i^2}{a_i} < \frac{d(x, P_j)^2 + z_j^2}{a_j}, \quad \forall\, j \neq i \right\}, \tag{6.4}$$

$$\Gamma_{ij} = \left\{ x \in \Pi_z |\, \frac{d(x, P_i)^2 + z_i^2}{a_i} = \frac{d(x, P_j)^2 + z_j^2}{a_j} < \frac{d(x, P_k)^2 + z_k^2}{a_k},\ \forall\, k \neq i, j \right\}. \tag{6.5}$$

The interfaces are circular arcs which meet (generally) in three–fold vertices. The first property of SMVP is that if a vertex v_{ijk} exists, then the continuation of the films Γ_{ij}, Γ_{ik} and Γ_{jk} also meet at a conjugate point v^*_{ijk}. This property implies that the centres of curvature of the three interfaces are aligned. To see that let us suppose that v_{ijk} is a vertex. Then v_{ijk} is the solution of the system of equations which define the interfaces in (6.5):

$$\frac{d(x, P_i)^2 + z_i^2}{a_i} = \frac{d(x, P_j)^2 + z_j^2}{a_j} = \frac{d(x, P_k)^2 + z_k^2}{a_k}\,. \tag{6.6}$$

[1] In a previous paper Moukarzel studied the multiplicative Voronoï partition, where the only parameter associed to the sources is the intensity. This partition reproduces the property of the foams as the alignment of the curvature centres but it can not describe all possible equilibrated foams [Mou93]

If the circles Γ_{ij} and Γ_{jk} meet in v_{ijk}, then they have to meet also at another point v^*_{ijk} where they verify the first and second equality of (6.6). Then, by transitivity, the first and the third terms of (6.6) are also equal at v^*_{ijk}, so that Γ_{ik} also passes through the conjugate point v^*_{ijk}. As in sectional partitions, there may be sources with no associated cell where the corresponding 3D cell is not cut by Π_z. Another property of SMVP is that, considering an interface Γ_{ij}, the centre of curvature of the film, C_{ij}, is on the straight line containing the sources and always outside the segment which joins them.

A *circular partition of the plane* is defined as a partition of the plane into domains, or cells, delimited by arbitrary circular arcs that meet at triple points (vertices). The circular partition is called *aligned* if the vertices are aligned (the curvature centres relative to a vertex are aligned)[Mou97].

Given a circular partition, its reciprocal figure, or dual graph, is defined by assigning a point P_i to any cell Ω_i of the circular partition and joining these points by straight edges orthogonal to the interfaces. The dual is called *oriented* if: a) the curvature centre C_{ij} of the interface between Ω_i and Ω_j is not between P_i and P_j, and b) on the line $\overline{C_{ij}P_iP_j}$, starting from C_{ij}, the points P_i and P_j are found in the same order as Ω_i and Ω_j.

From the properties of the sectional multiplicative Voronoï partition, if a circular partition is a SMVP, then it is aligned and it admits an oriented reciprocal figure. These last two conditions are the necessary conditions for a circular partition to be a SMVP. Moukarzel proves that these conditions are also sufficient [Mou97], which implies that a circular partition is a SMVP.

6.2 SMVP and Non–Standard 2D Foams

Let us now consider a non–standard equilibrated 2D foam $\mathcal{F}$. The films verify:

$$\sum_{i=1}^{3} \gamma_i \boldsymbol{\tau}_i = 0 \quad \text{at any vertex } v\,, \tag{6.7}$$

$$\sum_{i=1}^{3} \gamma_i k_i = 0 \tag{6.8}$$

where k_i and $\boldsymbol{\tau}_i$, for $i = 1, 2, 3$, are the curvature of the film i and the unit vector tangent to the film at v. γ_i is the line tension of the film. The angle formed by films at the vertices are not, in general, the Plateau angle ($2\pi/3$) as in standard foams, but the films are still circular: at equilibrium, constant pressure of the bubbles implies, by Laplace's law $\Delta P_i = \gamma_i k_i$, that curvatures are constant (see previous chapters). So an equilibrated 2D foam is a circular partition of the plane. In [Mou97], it is proved that equations (6.7) and (6.8) imply that, for any vertex of $\mathcal{F}$, the centres of the three interfaces meeting at it are aligned. Moreover it is proved that the equilibrium equations impliy also that a reciprocal figure exists and that is always possible to find, among all possible reciprocal figures, al least

one which verifies the orientation condition. Therefore, the theorem proved by Moukarzel states:

Theorem 6.2. *A cellular pattern bounded by circular arcs meeting at threefold vertices represents an equilibrated foam $\mathcal{F}$ if and only if there is an oriented dual figure $\mathcal{F}^*$.*

So, 2D non–standard equilibrated foams are equivalent to SMVP's of the plane and then, to establish if a circular partition is an equilibrated foam or not it is sufficent to know it wheter admits an oriented reciprocal figure.

6.3 ⅄− △ Equivalence for Non–Standard 2D foams

By theorem 6.2, the star–triangle equivalence 5.1 can be extended to the case where the line tension doesn't assume the same value for each film of the foam.

Let us consider a three–sided bubble Ω_1 and its three neighbours Ω_2, Ω_3, Ω_4. These neighbouring cells correspond, respectively, to the sources P_2, P_3, P_4 which form a triangle in $\mathcal{F}^*$. The central bubble Ω_1 is represented by a point P_1 connected to the neighbouring point by three bonds (figure 6.1-a). Removing or inserting the three–bubble in $\mathcal{F}$ is the same as removing or inserting the source P_1 in $\mathcal{F}^*$ (figure 6.1-b).

Now the outer edges each satisfy an equality $d_i(x) = d_j(x)$ for a pair $i < j$ taken in $\{2, 3, 4\}$. Here, $d_j(x)$ denotes the distance between the source P_i and the point of the plane x used for SMVP's (definition 6.4): $d_j(x) = (d(x, P_j)^2 + z_j^2)/a_j$. When two edges meet at some x_0, say $d_2(x_0) = d_3(x_0)$ and $d_3(x_0) = d_4(x_0)$, then the third equality is also satisfied by transitivity. The condition on the angles follows from the fact that the vertices built in such a way are automatically equilibrated (see [Mou97]).

6.4 Decoration Theorem as Corollary of ⅄− △ Equivalence

Let us consider now a standard dry 2D foam (section 2.1). In the model of dry foam [FW92b], a little amount of liquid, present in the foam, is concentrated in a small region at the vertices (Plateau border) and the films are still thin. This liquid region is maintained at some pressure $P_{_L}$ lower than that of the gas in the cell. Experimentally, in a Hele–Shaw cell, Plateau borders occur at the intersection between soap films and also where the films meet the top and bottom surfaces. The latter sort of Plateau border does not concern us here except to note that this system of channels at the surfaces allows the equalization of pressure between vertical Plateau borders. So, we can assume that all the

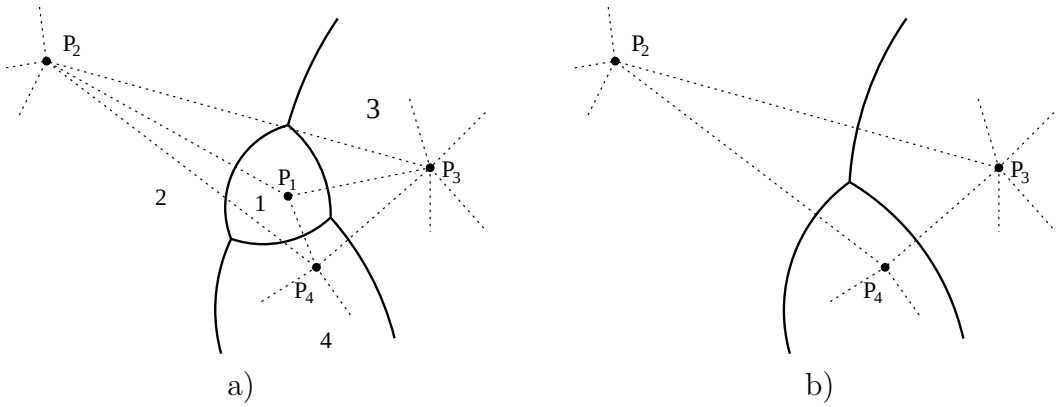

Figure 6.1: a) A three–edge bubble with its neighbours and the dual figure (dotted lines). b) Same part without the three–edge bubble.

Plateau borders at the vertices are maintained at the same pressure. For the case of zero disjunction pressure (sec. 1.1), at any vertex the liquid–gas interfaces are in mechanical equilibrium with the films. A horizontal section of a Plateau border at a vertex is shown in fig. 6.2.

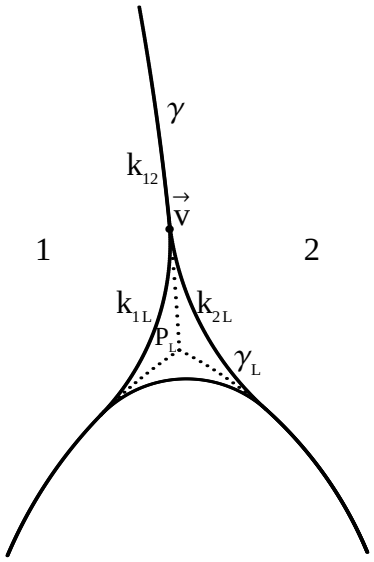

Figure 6.2: A generic Plateau border inside an equilibrated 2D dry foam. The Plateau border can be considered as a bubble with smaller pressure than its neighbours and where the interfaces have line tension γ_L.

Two different line tensions are present in the foam: γ, of the films, and γ_L, of the liquid–gas interfaces. At the point $\vec{v}$ of figure 6.2, the following equilibrium

equations are verified:

$$\gamma\vec{\tau}_{12} + \gamma_{L}\vec{\tau}_{2L} + \gamma_{L}\vec{\tau}_{L1} = 0\,, \qquad \text{at } \vec{v}, \tag{6.9}$$

$$\gamma k_{12} + \gamma_{L} k_{2L} + \gamma_{L} k_{L1} = 0\,, \tag{6.10}$$

where, considering the liquid–gas interface between bubble i, for $i = 1, 2$, and the Plateau border: $k_{iL} = -k_{Li}$ is the curvature of the interface and $\vec{\tau}_{iL} = \vec{\tau}_{Li}$ is the unit tangent vector of the interface at $\vec{v}$ (directed away from the vertex). The pressure difference across the liquid–gas interface is related to the curvature by Laplace's equation $P_L - P_i = \gamma_{L} k_{Li}$. k_{12} and $\vec{\tau}_{12}$ are the film curvature and unit tangent vector respectively. Therefore a Plateau border is a three–cell which has smaller pressure than its neighbours and where the interfaces have line tension γ_{L}. Applying the decoration theorem, or $\curlywedge - \triangle$ equivalence in the non–standard case, we find that the prolongations of the films joining the same Plateau border converge at an equilibrated vertex. Therefore it is possible consider the equilibrium of a slightly wet 2D foam as if the liquid fraction was zero.

Resolving equation (6.9), in the case of zero disjoining pressure, that is in the case where all tangent vectors at a node are parallel, we find that $\gamma_{L} = \gamma_{12}/2$, as expected by considering that any liquid–gas interface contributes to tension line by $\gamma/2$. When the disjoining pressure is different from zero and the film has a thickness h (see section 1.1), the tangent vectors $\vec{\tau}_{iL}$, at $\vec{v}$, form an angle θ_i with $\vec{\tau}$. The projections of equation (6.9) on the directions $\vec{\tau}$ and $\vec{\tau}^{\perp}$ imply respectively:

$$\gamma = 2\gamma_{L}\cos\theta_1\,, \tag{6.11}$$

$$\theta_1 = \theta_2\,. \tag{6.12}$$

Using equation (1.8), with $\gamma = 2\gamma_L$, and supposing the film's thickness h constant, we have that:

$$\gamma = 2\gamma_L + \int_0^{\Pi(h)} h\,\mathrm{d}\Pi = 2\gamma_L + \Pi h \tag{6.13}$$

and then

$$\Pi = \frac{2\gamma_L}{h}(\cos\theta - 1)\,. \tag{6.14}$$

6.5 Decoration Theorem for 2D foams in contact with a rigid wall

In this section we extend theorems 5.1 and 6.1, the star–triangle equivalence and the decoration theorem respectively, to the case where the standard 2D foam is in contact with a rigid straight line, reppresenting a boundary of the foam container.

As the powerful theory of Moukarzel is not adapted to include external wall to the model (SMVP, and so foams are partitions of all the plane), we have to prove the two theorems separately. We do not know at present any other proof of these properties. We will furnish the proof of this equivalence for a standard 2D foam in contact with a rigid wall so that all the films of the foam have constant line tension γ. The rigid wall is a fixed straight line l, in the plane of the foam. It is assumed clean, as in chapter 3, so that the films can freely slide along l.

6.5.1 $\curlywedge - \triangle$ Equivalence at the Boundary

Assuming that the 2D foam is ideal (the liquid fraction is zero), let us consider a film in contact with l in non–wetting condition. As said in section 3.2, the bubbles separated by this film have the same gas, then at equilibrium the contact angle is $\pi/2$. So, films are in normal incidence with the wall l at equilibrium. Now let us consider a bubble in contact with l and two other bubbles. In the setting of figure 6.3, the films e_{12} and e_{13} are orthogonal to l. We will prove that

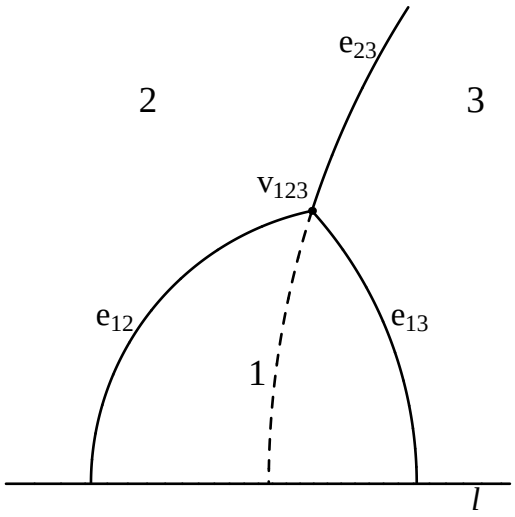

Figure 6.3: Bubble at contact with a rigid wall l. Normal incidence and equilibrium imply that the prolongation of the film e_{23} is orthogonal to l

the prolongation of the film e_{23} touches the wall orthogonally too, so the foam obtained by replacing bubble 1 by the prolongation of e_{23} is still in equilibrium (and reciprocally). The proof is very simple. e_{12}, e_{13} are orthogonal to l, so their centres are on l. As the vertex v_{123} is equilibrated, the centres of curvature of e_{12}, e_{13} and e_{23} are aligned. This implies that the centre of e_{23} stays on l, then e_{23} is orthogonal to l.

6.5.2 Decoration Theorem at the Boundary

Now, let us consider a slightly wet foam where l is the straight line representing the solid wall which the foam touches. We assume zero disjoining pressure and total wetting of the boundary: a thin film of liquid (negligibly thin) wets the wall [dGBWQ02]. A little liquid is concentrated in a region around the vertices and at the point where the film touches l. The decoration theorem for the vertices was already discussed in the previous section. For the region of contact, equilibrium implies that:

- As the disjoining pressure is zero, the liquid–gas interface has to be tangent to the film (sec.6.4, [FW92b]).
- By the total wetting condition, the interfaces have to be tangent to l at the point where the thickness of the wetting film reaches zero [dGBWQ02].

Taking as reference figure 6.4, let $R = \frac{1}{k_{12}}$, $R_A = \frac{1}{k_{1L}}$ and $R_B = \frac{1}{k_{2L}}$ be the radii (positive) of the film e_{12} and of the two liquid–gas interfaces (e_{1A} and e_{2B}) respectively. Let us also define the centres C_{12}, C_{1A} and C_{2B} of e_{12}, e_{1A} and e_{1B} resp.

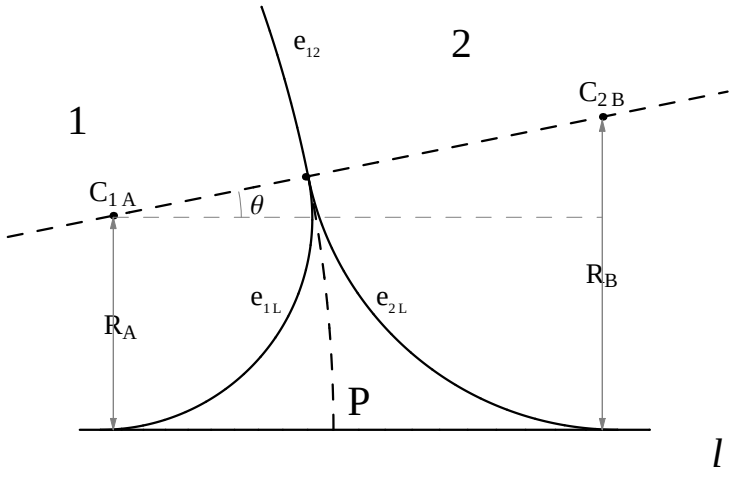

Figure 6.4: Film in contact with a rigid wall l in a slightly wet foam. The equilibrium conditions imply that the prolongation of the film e_{12} is orthogonal to l

The first property and equation (6.7) imply that the liquid–gas intefaces have tension line $\gamma_{_L} = \gamma/2$ (sec.6.4 and [WH99]) where γ is the line tension of the films. Equation (6.8) imply:

$$\frac{2}{R} = \frac{1}{R_A} - \frac{1}{R_B}. \tag{6.15}$$

The first property implies also that the three centres are on the same line, while the second property implies that the distances between $d(C_{1A}, l)$ and $d(C_{2B}, l)$ are R_A and R_B respectively (see fig. 6.4).

As in the $\curlywedge - \triangle$ equivalence, to prove that the prolongation of e_{12} is normal to the wall, it is sufficent to verify that C_{12} stays on l. To make that, we calculate de distance between C_{12} and l. It is given by:

$$d(C_{12}, l) = R_B - (R + R_B)\sin\theta, \tag{6.16}$$

where θ is the angle between the line containing the centres and l:

$$\sin\theta = \frac{R_B - R_A}{R_A + R_B}. \tag{6.17}$$

Using eq. (6.15) in (6.17) we obtain immediately that the distance is zero. Then the prolongation of the film e_{12} meets orthogonally the wall l.

In the case where the wetting is not total and the dijoining pressure is different from zero, the angles which the gas–liquid interfaces form with the boundary line and the angle formed by the films and the Plateau borders are respectively θ_{LG} and θ_{P}. The equilibrium at point $\mathbf{v}$, where the gas–liquid interfaces meet the film, implies that the three centres of curvature are on the same line and that there exists a conjugate vertex where the prolongations of the arcs also meet. Using an inversion transformation with respect to the conjugate vertex , the three arcs are mapped onto lines while the boundary line l is mapped into the circle l'. A symmetrical figure is obtained: a triangle with a curved edge. By angle preservation of inversions the angles at the curved edge are θ_{LG} and the angle at $\mathbf{v}'$ is θ_{P}. The line e'_{12} is an axis of symmetry for the curved triangle, so that it intersects the cicle l' orthogonally. Applying the inverse transformation ensures the required property for the original Plateau border.

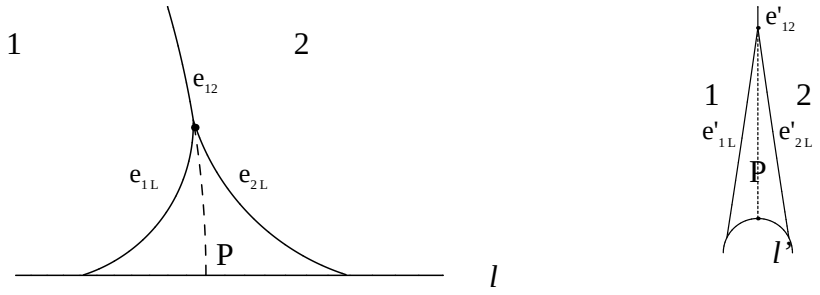

Figure 6.5: Inversion transformation sends the Plateau border at the contact with the boundary into a symmetric triangle

Remark. The hypotesis of straight line, for the wall, is necessary in both proofs. Figure 6.6 shows an example where the wall line is not straight. In this case the shape of the line could change in the region inside the bubble, then the prolongation of the external edge would not be normal to the wall l.

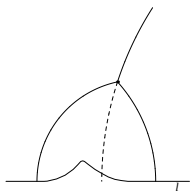

Figure 6.6: Example of not straight border.

6.6 What About Multipods?

Can the same argument be applied to cells —gas or liquid— with more than 3 legs? Consider, for example, a four–sided cell. In the reciprocal figure, it is represented by a source point connected to four neighbours. Removing this source without changing anything else will replace the 4-cell in the foam by a pattern made of two vertices joined by a curved edge, each of these vertices being connected to two of the former legs, suitably prolonged (figure 6.7). In the class of generalised model foams, which is the natural context of the theory, the new pattern is perfectly equilibrated. The trouble is that the value of the line tension, inherited by the new edge from the parameters of the dual sources, has nothing to do with any physically plausible value. Looking at figure 6.7, the angles of the new edge with the legs are far form $2\pi/3$, apparently violating Plateau's law. More precisely, generalised Plateau (P) is still satisfied, but the theoretical value γ_e required to make the new configuration a true equilibrium does not match the physical one, supposing one would realize the transformation physically. This mismatch renders the substitution of a 4–bubble by an H incompatible with equilibrium. When one of these bubbles shrinks, this mismatch persists down to zero area where it breaks equilibrium, triggers dynamical processes (fast or slow) and the foam needs to adjust its configuration in order to equilibrate the *physical* tensions.

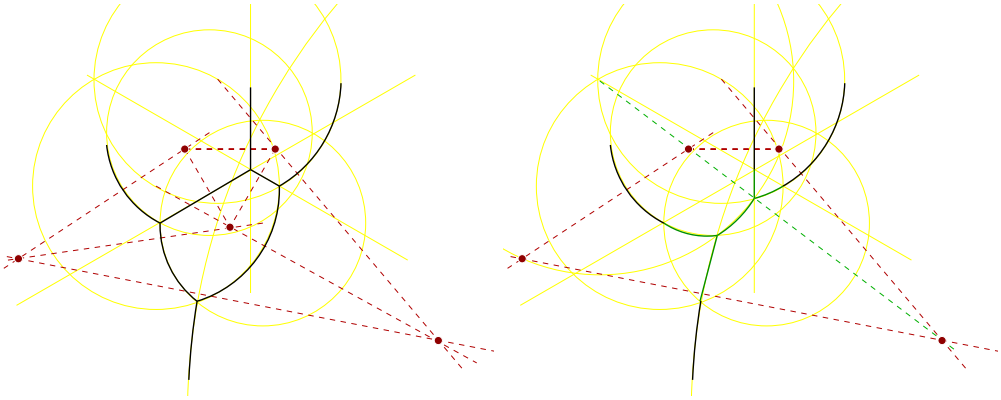

Figure 6.7: A 4–bubble (left) transformed into a linked pair of vertices (right).

Conclusions

The Star–Triangle theorem is also valid in the more general case of 2D foams where the line tensions are not all equal in the foam but they change from a film to another (non–standard 2D foams). In this case a geometrical proof, as in the standard case given in the previous chapter, is not simple. Using Moukarzel dualization [Mou97], we have proved that, at equilibrium, also for non–standard foams, to any three–sided bubble corresponds an equilibrated virtual vertex given by prolonging its external edges into the bubble.

As Von Neumann's equation doesn't work for general foams (see section 5.1, after theorem 5.1) we do not know how the foam evolves but, if a three–sided bubble disappears, then it is continuous.

As a corollary, $\curlywedge - \triangle$ equivalence implies the decoration theorem of Weaire [FW92b, FW92a, Wea99]: the equilibrium of a slightly wet foam can be obtained from that of a dry foam by "decorating" the vertices with the liquid.

$\curlywedge - \triangle$ equivalence and the decoration theorem are valid also in the presence of a straight rigid wall. In the first case, replacing a bubble, which touches the wall and two other bubbles, with the prolongation of the external film incident to it, the foam obtained is still equilibrated. In the second case, the prolongation of the film within a Plateau border touching the wall, is normal to the wall too. So, also when the foam is in contact with some wall, is possible to decorate it, preserving equilibrium, to obtain a slightly wet foam.

Chapter 7

Star–Triangle Equivalence for Spherical Foams

In two dimensions the star–triangle equivalence allows to prove that during a T2(3) process, where a three–sided bubble disappears because of gas diffusion, the energy of the foam varies continuously or, equivalently, the foam does not leave its local equilibrium configuration. For three–dimensional foams one could ask if the equivalence $\curlywedge - \triangle$ and the continuity at the bubble disappearamce are true. In this chapter we treat this question in the special case where the films of the foams are spherical; we prove the star–triangle equivalence.

We prove that in a dry ideal spherical three–dimensional foam, the tetrahedral bubbles (figure 7.1) have an internal virtual point where the prolongation of the external films incident on the bubble meet. It results that this virtual point is

(a) (b)

Figure 7.1: Two views of a generic four–sided bubble contained in an equilibrated 3D spherical foam obtained by Surface Evolver software [Bra92]. In a) the external zero curvature films are shown while in b) only the borders are drawn.

an equilibrated node and then the foam obtained by replacing the tetrahedral

bubble by the prolongated external films is still equilibrated.

The proof of $\curlywedge - \triangle$ in 3D is simpler than in 2D and we use, again, the fact that spherical foams are invariant by inversion transformations as shown in section 3.5.

As in two–dimensions, this equivalence implies, as a corollary, that in spherical foams, during coarsening, when a four–edged bubble disappears, the foam remains in a local minimum energy configuration, no sudden changes occur and the phenomenon is continuous.

Although sphericity could appear as a very strong constraint which restricts the usefulness of the $\curlywedge - \triangle$ equivalence in 3D, its corollary is useful, also in the general case where the films are not spherical, to prove the continuity of the T2 process. During the coarsening, the bubbles that shrink lose faces, eventually ending up as tetrahedra of typically very small volume. In fact, it was found experimentally by Doornum and Hilgenfeldt [vDH03] that $L_4/\langle L\rangle \lesssim 0.1$ where L_4 is the average length of a tetrahedral bubble, and $\langle L\rangle$ is the average edge length in the foam. Because of their small size, tetrahedral bubbles have a much larger mean curvature and larger internal pressure p_0 than typical bubbles. The shape of tetrahedra depends on the much lower pressure p_i, with $i = 1, \ldots, 4$, in the four neighbouring bubbles. If all p_i are equal, the four tetrahedral spherical faces are identical and the nodes are on the vertices of a regular tetrahedron of edge length L_4 (*Reuleaux tetrahedron* or *isotropic tetrahedron*). If a pressure drop between the neighbouring cells exists then there is a small anisotropy. In [vDH03], the authors demonstrated that the Reuleaux tetrahedron was a good approximation for disappearing bubbles in a 3D foam by measuring the anisotropy of tetrahedral bubbles and showing that it was small. So, at the shrinkage, tetrahedral bubbles are, with good approximation, isotropic, therefore spherical, and the $\curlywedge - \triangle$ equivalence can be used to prove the continuity of the T2 process.

Spherical foams are also important for the study of the coarsening. In recent works [HKKS01, vDH03, HKRS04, KRvS04], *isotropic Plateau polyhedra*, which are idealized bubbles with F identical, spherical–cap faces which satisfy Plateau's laws, are used to study the geometry and diffusive growth rate of soap bubbles in 3D dry foams.

However, the implications of the $\curlywedge - \triangle$ equivalence for spherical foams are important also for experimentalists. For example, star–triangle equivalence could be used to reduce the number of bubbles, thereby improving the efficiency of numerical minimisation or reducing the time of reconstruction in tomographic techniques.

For the $\curlywedge - \triangle$ equivalence, we first prove that, given an equilibrated vertex where four borders meet, there is another equilibrated conjugate vertex where the prolongations of the borders meet too. Therefore, using inversion invariance for spherical foams proved in section 3.5, we transform a generic tetrahedral bubble into a very symmetrical case for which we prove the equivalence. After

that, applying the inverse transformation ensures the required properties for the original tetrahedral bubble.

7.1 Existence of a Conjugate Vertex

Let us consider a three–dimensional ideal dry foam (the liquid fraction tends to zero) where the films are spherical caps. The pressure drop across a film is $\Delta P = \gamma/r$, where r is the radius of the film. The surface tension γ is supposed constant in the foam.

Plateau's laws (chapter 1) state that three films meet on a line, the Plateau border, at an angle of $2\pi/3$ and six films (or four borders) meet at a point forming a perfectly symmetric tetrahedral figure. The angles between edges all have the value $\phi = \cos^{-1}(-1/3)$ (Maraldi angle).

Let V be a node where four borders b_i, for $i = 1, \ldots, 4$, meet. At any border b_i three spherical caps (films) meet. Assuming that the border b_i has length greater than zero (it is not a point), which excludes degenerate cases, by an elementary geometrical property (for example see [mat]) the centres of the spherical caps intersecting on b_i are aligned on a straight line r_i. Each line r_i contains three centres. Moreover, the border b_i is a circular arc the centre of which is a point of r_i; b_i is in a plane orthogonal to r_i and passing through its centre. Let n_i be the unit vector orthogonal to this plane; of course, it is the direction of r_i.

Near the vertex V, each film is common to two Plateau borders meeting on V; then any line r_i meets the others at the centre of the common film. Given two lines, for example r_1 and r_2, these span a plane p containing five centres. As the total number of centres related to V is six, imposing that another line, for example r_3, intersects r_1 and r_2 implies that r_3 is on the same plane p. So all the centres linked to V are in the plane p.

The planes n_i, for $i = 1, \ldots, 4$, passing respectively through the centre of b_i, are orthogonal to r_i and then they meet on a straight line normal to p. The existence of this line is assured by the fact that these planes, containing the borders, are orthogonal to p and they must meet in the point V. By symmetry, the borders which meet in V have to meet also in the point V^*, the conjugate of V, symmetric of V with respect to the plane p.

7.2 ⅄− △ Equivalence

Let us consider now a four–faced bubble, called 0, in an equilibrated spherical foam (figure 7.2). This bubble has four faces, four vertices and six Plateau borders. Bubble 0 is surrounded by four bubbles i, for $i = 1, \ldots, 4$. Let us use the following notation:

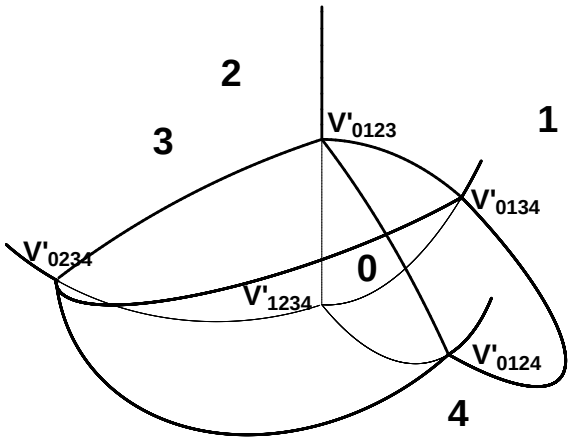

Figure 7.2: Typical tetrahedral bubble. The $\curlywedge - \triangle$ equivalence states the existence of the vertex V_{1234}.

- If bubbles i and j are neighbours, for $i, j = 0, \ldots, 4$, $\mathcal{F}'_{ij}$, with $i < j$, is the spherical–cap film between them, with $H'_{ij} = -H'_{ji}$ and C_{ij} its mean curvature and its centre, respectively.
- If the films $\mathcal{F}'_{ij}$, $\mathcal{F}'_{jk}$ and $\mathcal{F}'_{ik}$, for $i, j, k = 0, \ldots, 4$, meet then b'_{ijk}, with $i < j < k$, is the circular Plateau border.
- V'_{ijks}, for $i, j, k, s = 0, \ldots, 4$ and with $i < j < k < s$, is the vertex.

Let us consider, for example, the vertex V'_{0123}. As, by the previous section, it admits a conjugate vertex V'^*_{0123} let us apply an inversion transformation with respect to this point ($\mathbf{r} \to \alpha \frac{\mathbf{r} - V'^*_{0123}}{|\mathbf{r} - V'^*_{0123}|^2}$) as showed in figures 7.3. We proved, in section 3.5, that the mapped spherical foam preserves equilibrium (Plateau's laws are preserved).

All the spheres passing through V'^*_{0123} ($\mathcal{F}'_{01}$, $\mathcal{F}'_{02}$, $\mathcal{F}'_{03}$, $\mathcal{F}'_{12}$, $\mathcal{F}'_{23}$, $\mathcal{F}'_{13}$) are mapped on to planes (zero curvature films) through V_{0123} ($\mathcal{F}_{01}$, $\mathcal{F}_{02}$, $\mathcal{F}_{03}$, $\mathcal{F}_{12}$, $\mathcal{F}_{23}$, $\mathcal{F}_{13}$). The intersection of these planes are straight Plateau borders b_{012}, b_{013}, b_{023} and b_{123}. By conformality of the inversion transformation the angles are preserved, then the vertex V_{0123} is the vertex of a regular tetrahedron. Let us fix the vertical axis parallel to the straight border b_{123}. The reference scheme is shown in figure 7.4.

Let us prove now that the transformed tetrahedral bubble is a regular tetrahedron except for the face $\mathcal{F}_{04}$ which is a spherical cap. As the planar films have curvature zero, equation (1.3) around the straight borders implies that the curvature of the films $\mathcal{F}_{04}$, $\mathcal{F}_{14}$, $\mathcal{F}_{24}$, $\mathcal{F}_{34}$ are equal. For example, considering the border b_{034}, Laplace's law around this border implies:

$$H_{04} + H_{43} + H_{30} = 0. \tag{7.1}$$

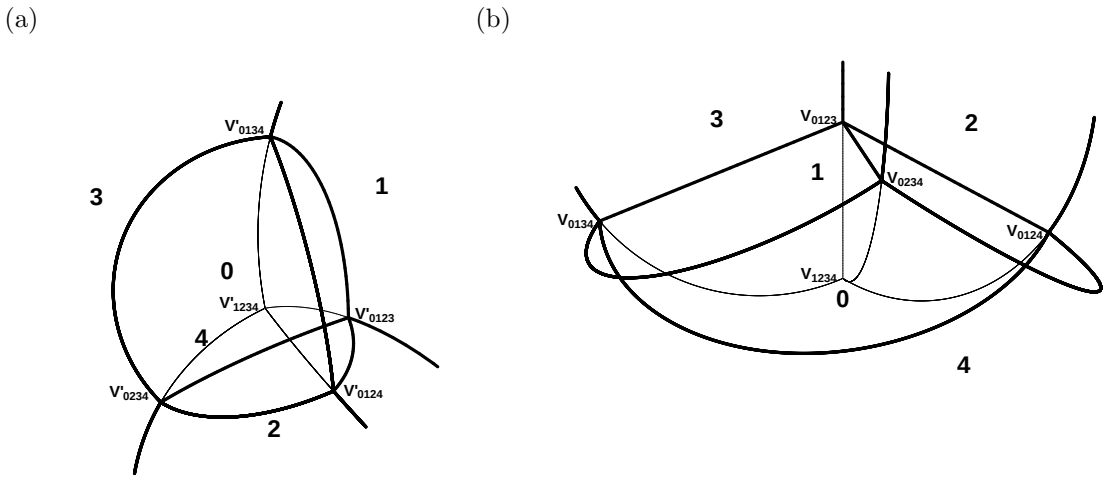

Figure 7.3: a) A generic four–sided bubble contained in an equilibrated 3D spherical foam. b) The same bubble transformed by a suitable inversion.

As $H_{30} = 0$, then $H_{04} = H_{34}$. Applying Laplace at all the circular borders we have proved the assertion.

C_{14}, C_{24}, and C_{34} are on a plane orthogonal to b_{123}. Considering for example the border b_{124}. F_{12} is a plane through b_{123} and it contains the circular arc $b_{124} = F_{14} \cap F_{24}$. So, the line containing C_{14} and C_{24} must be orthogonal to F_{12} and then orthogonal to b_{123}. Iterating this argument for b_{134} and b_{234} we prove the stated property.

Moreover, as the films $\mathcal{F}_{14}$, $\mathcal{F}_{24}$ and $\mathcal{F}_{34}$ have the same radius, their centres are on the vertices of an equilateral triangle (see figure 7.5) at the centre of which, the point a, the vertical axis passes (and then the b_{123} prolongation). The centre of a curved border is placed in the middle of any edge of this triangle (for example the centre of the border b_{124} is at the middle of the edge formed by C_{14} and C_{24}).

The borders b_{124}, b_{134} and b_{234} have the same curvature. In fact they are the intersections of equal radius spheres placed at the vertices of an equilateral triangle. So, if they meet, they have to do it on the vertical axis. To prove that circular borders meet, let us consider the planar cut of the tetrahedral bubble by the plane of the equilateral triangle formed by C_{14}, C_{24}, C_{34}.

Assuming figure 7.5 as reference, we have to prove that the distance d between the centre C_{124} of b_{124} and the centre of the triangle a is smaller than, or equal to, the radius of the border. In this way the three borders b_{124}, b_{134} and b_{234} meet in some place on the vertical axis inside the bubble 0, the vertex V_{1234} that we searched.

Looking at the figure, and using the properties of equilibrium, we see easily that if $R = 1/|H_{14}|$ is the radius of curvature of the film $\mathcal{F}_{14}$, then the radius of

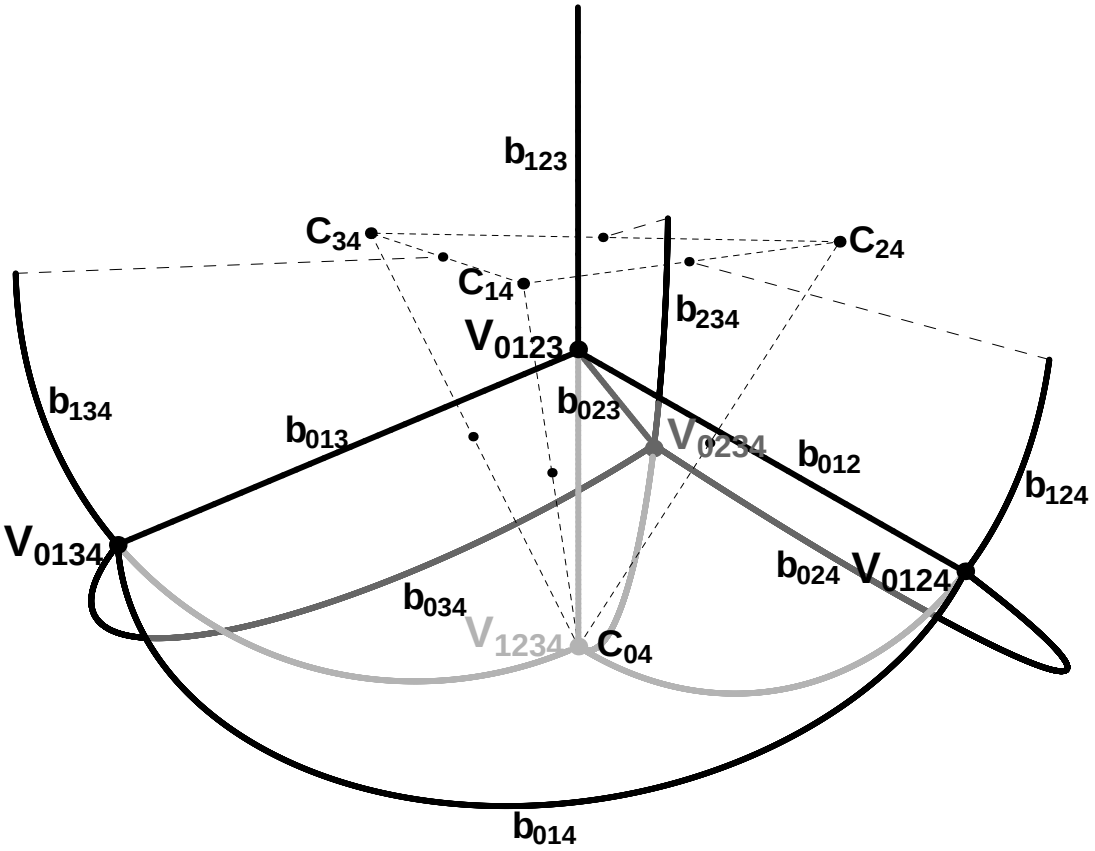

Figure 7.4: Transformed four–sided bubble. The films passing through V_{0123} are flat, zero curvature, while the others all have spherical cap of the same radius. The centres of the spherical films are at the vertices of a regular tetrahedron.

the border is $r_{123} \equiv r = R\sin(\pi/3) = R\sqrt{3}/2$ while the distance d is

$$d = \frac{R}{2}\tan(\pi/6) = \frac{R}{2\sqrt{3}} < r = R\frac{\sqrt{3}}{2}\,. \tag{7.2}$$

So, the prolongation of the borders b_{124}, b_{134} and b_{234} meet with the prolongation of b_{123} in the point V_{1234}.

Let us prove now that V_{0123} is equilibrated. Consider two border prolongations b_{124} and b_{134} meeting at V_{1234}, we prove that the angle formed by them is the Maraldi angle $\angle(b_{124}, b_{134}) = \cos^{-1}(-1/3)$. The coordinates of the borders b_{124} and b_{134} are respectively:

$$\mathbf{b}_{124}(\theta_1) = (0, -d, 0) - r(0, \sin\theta_1, \cos\theta_1)\,, \tag{7.3}$$

$$\mathbf{b}_{134}(\theta_2) = (\frac{\sqrt{3}d}{2}, \frac{d}{2}, 0) + r(\frac{\sqrt{3}}{2}\sin\theta_2, \frac{1}{2}\sin\theta_2, -\cos\theta_2)\,. \tag{7.4}$$

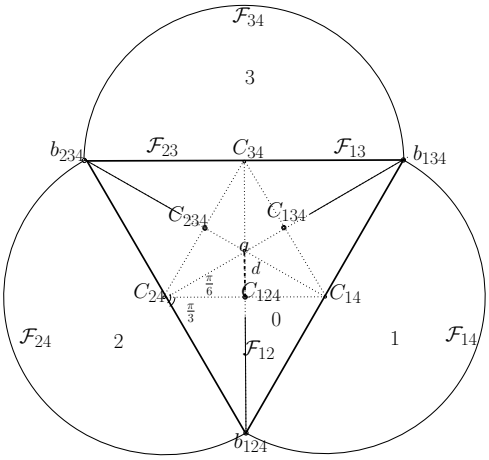

Figure 7.5: Intersection of the tetrahedral bubble cluster with the plane containing the centres of the curved films.

We proved that $\mathbf{b}_{124}$ and $\mathbf{b}_{134}$ meet at V_{1234} which is on the z axis ($\mathbf{b}_{123}$ prolongation). At V_{1234}, the x and y components of $\mathbf{b}_{124}$ and $\mathbf{b}_{134}$ are zero; then the values of the parameters of the borders at V_{1234} are $\tilde{\theta}_1 = \tilde{\theta}_2 = \sin^{-1}(-d/r)$. The unit vectors tangent to the two borders are:

$$\boldsymbol{\tau}_{124}(\theta_1) \equiv \frac{\mathbf{b}_{124}}{|\mathbf{b}_{124}|} = (0, -\cos\theta_1, \sin\theta_1)\,, \tag{7.5}$$

$$\boldsymbol{\tau}_{134}(\theta_2) \equiv \frac{\mathbf{b}_{134}}{|\mathbf{b}_{134}|} = \left(\frac{\sqrt{3}}{2}\cos\theta_2, \frac{1}{2}\cos\theta_2, \sin\theta_2\right)\,. \tag{7.6}$$

Taking the scalar product between the unit tangent vectors calculated at V_{1234} we obtain:

$$\cos(\angle(b_{124}, b_{134})) = pmb\tau_{124}(\tilde{\theta}_1)\cdot\boldsymbol{\tau}_{134}(\tilde{\theta}_2) = -\frac{d}{r} = -\frac{1}{3}\,, \tag{7.7}$$

which proves that V_{1234} is equilibrated.

Next, applying the inverse transformation ensures the ⅄− △ equivalence for spherical foams.

We don't furnish the proof of the ⅄− △ equivalence for the case of non–standard foams where the surface tensions differ. In this more general case a proof should be obtained by generalizing Moukarzel's duality (sec. 6.1).

Conclusion

In the first part of the manuscript we found the equilibrium equation of the two–dimensional foam formed by the contact of a liquid foam with a rigid surface, generalising the case of a standard Hele–Shaw cell. The first law, concerning 2D films, states that at any vertex the sum of the vectors tangent to the films meeting on it, of norms equal to the line tensions, is zero ($\sum \gamma_i \boldsymbol{\tau}_i = 0$). The second law imposes that the sum of the geodesic curvatures of the films at a vertex, multiplied by their line tension, is zero ($\sum \gamma k_i^g = 0$). We proved also that these equilibrium equations are invariant under conformal transformations.

Considering a foam between two non–parallel glass plates in a set–up similar to the standard Hele–Shaw cell, we analyzed the results obtained by recent experiments which show that the 2D foam formed on the plates is the image of a monodispersive flat foam by a conformal transformation which depends on the thickness slope. We found, by a first order calculation in the limit of small thickness, the curvature in the normal direction to the plates. Restoring the 3D Laplace law we found an approximate equation which links the pressure of the bubbles, the conformal transformation f and the thickness h. In the case of constant pressure, we solved this equation for logarithm and power law maps ($h \propto |f|$). In the case of constant volume ($h \propto |f|^2$), we compared our theoretical result with the experimental data. We found that the contribution to the pressure arising from the normal curvature is twice that one coming from the observed curvature, making the pressure smaller on the convex side of a curved edge, a result opposite to what a direct readout from the 2D foam equations would predict. Further investigations are still needed to control this approximation or to get exact results on foams between non parallel plates.

In the second part of the thesis, we considered 2d flat foams. Using the geometry of the equilibrated foams, we found the property of the three–sided cell called star–triangle equivalence ($\curlywedge\!\!-\triangle$). $\curlywedge\!\!-\triangle$ states that the prolongations of the external edges of a three–sided bubble meet in a virtual equilibrated vertex inside the bubble. Then the foam made by replacing the three–sided bubbles by their virtual vertices and edge prolongations is also equilibrated. We saw that $\curlywedge\!\!-\triangle$ implies that the topological process T2(3), where a three–sided bubble disappears, is continuous: the system does not jump from an equilibrium state to

another and any quantity varies continuously. Using the variational expression of the perimeter, we show also that discontinuities occur in the first time derivative of the energy. We studied the example of the two–bubble cluster, in two and three dimensions, where the continuity of the T2, is explicitly showed by solving the diffusion equation.

We proved also $\curlywedge - \triangle$ in the more general class of foam where the edges have non–equal tension line. The proof was given by using Moukarzel's duality. As a consequence, $\curlywedge - \triangle$ implies the decoration theorem. The Decoration theorem was also extended to the wet vertices touching a flat boundary.

In the last chapter of this thesis, we proved $\curlywedge - \triangle$ for 3D spherical foam, proving the continuity of the T2 for 3D bubbles in the limit where the disappearing tetrahedral bubbles can be considered as spherical.

Future Improvements

We would like to extend, if it is possible, the star–triangle equivalence to the most general case of 2D foams defined on a non–flat surface and to 3D foams where the films are not constrained to be spherical.

We would like to extend, to use the set of coordinates of the centres of the films defined in the second chapter to study systematically some problems in the 2d foams equilibration. For example the problem of the flower cluster where, in the purely theoretical 2D foam model, some symmetry breaking occurs.

Remerciements

Je voulais tout d'abord remercier les rapporteurs et tous les membres du jury qui ont accepté de venir à Cergy pour participer à ma soutenance en ce triste jour du 13 juillet. Le deuxième merci va à tous les membres du Laboratoire de Physique théorique et modélisation de l'Université de Cergy–Pontoise pour m'avoir rendu ces quatre années de recherche très agréables dans une ambiance parfois relaxée. En particulier au Professeur Diep qui, malgré la quantité de choses qu'il doit faire en même temps en jonglant avec beaucoup d'habilité il arrive à être toujours disponible et gentil. Il m'a aussi permis de continuer ma thèse pour la quatrième année en appuyant ma demande d'ATER. A Sylvie Villemin, qui avec son efficacité et sympathie a assez changé la vie d'un triste laboratoire de physique théorique. Je voulais aussi remercier le Professeur Truong et Madame Travet qui, l'un comme directeur et l'autre comme secrétaire de l'école doctorale, ont toujours supporté et pardonné, le premier avec un léger sourire et la deuxième avec la plus belle voix du monde, mes catastrophiques attitudes dans n'importe quelle occurrence bureautique. Aussi un très grand remerciement à tout le staff des maîtres de conférence du labo: Claire Pinette, Damien Foster, Laura Hernandez, Geneviève Rollet, Philippe Lecheminant, Thierry Huillet qui m'ont accompagné non seulement dans la plus part des repas mais qui m'ont surtout conseillé par rapport aux problématiques de l'enseignement. Mais surtout un super grand merci à Guy Trambly et Jean–Philippe Kownacki qui ont su comprendre, et souvent soulager, mes nombreux moment de découragement et de dépression que pendant ces années j'ai eu à intervalles réguliers.

Je remercie mes deux directeurs de thèse, François Dunlop et Christophe Oguey, qui ont eu la patience de travailler avec un personnage autant bordellique et antilogique comme moi et, non moins, de corriger tous les fautes de physique et une énormité des fautes d'anglais dans ma thèse. Surtout Christophe qui m'a conduit pendant ces années et avec sa scientificité et minimalisme a toujours eu le courage de croire dans mes capacités comme physicien et a essayé, jusqu'au dernier jour, de me faire comprendre la rigueur qu'il faut avoir pour être un bon scientifique.

En dernier (et que le proverbe soit vrai!) je remercie mes copains de mésaventures, les autres thésards de Cergy–Pontoise: Olga Lopez Acevedo (qui main-

tenant et très loin et que j'aurais aimé beaucoup avoir ici le jour de ma thèse), Daninthe Harry et Zoltán Nagy avec lesquels nous avons passé des très très bons moments ensemble et qui ont rendu ma présence à Cergy beaucoup plus agréable. Surtout un très grand merci à Zoltán qui ces dernier temps a était un copain fidèle avec sa pureté d'esprit (presque naïveté, qualité que j'apprécie fortement), sa générosité, sa maîtrise des langues (surtout l'anglais: encore merci) et, en particulier, sa forte connaissance en physique (celle que je n'ai jamais eu). De loin je dis un grand merci aux autres gens qui dans ces années sont apparus et après disparus dans le LPTM et que avec lesquels j'ai partagé non seulement le bureau mais aussi les cafés: aux deux grand informaticiens de la théorie de l'information Manuel Rubio, mon premier copain de bureau, Lahcene Mitiche, copain de cigarette qui a su me re–animer le moral d'aussi loin, et Liliana Gomez ma deuxième partageuse de bureau.

En sautant aux remerciements en dehors de la fac je voulais remercier tous les amis du pub Edward's dans lequel j'ai passé mes soirées en observant la mousse de la Guinness qui drainait dans mon verre. En particulier à Fred, Benoite et Mus (ou Moose) mes meilleurs amis français qui ont su ne pas me faire sentir trop loin de chez moi et avec lesquels j'ai avancé pas mal dans la compréhension de l'anglais (avec le chanson mes chers musiciens). Et un grand merci aussi a ma copine Lucille qui a eu la grande patience de me supporter pendant la rédaction de cet interminable manuscrit et avec laquelle j'ai passé une année incroyable.

En sortant de Paris, et de la France mes remerciements arrivent en Italie. Je remercie mon ancien professeur Orlando Ragnisco de l'université de Roma III qui a eu confiance en mes capacités, qui m'a fait parvenir la proposition de thèse que je viens de terminer ici et qui s'occupe (et préoccupe) toujours de mon future scientifique (grazie Orlando!). Merci à tous mes amis que j'ai laissé en partant et qui ont cherché continuellement à maintenir des contacts avec moi en me faisant comprendre qu'ils m'ont jamais oublié.

Le dernier merci, et aussi le plus grand, va à ma famille à laquelle je sais d'avoir manqué et qui m'a manqué énormément et c'est à eux que je dédie ce travail.

Marco Mancini

ps. Un tout dernier merci à Ferdinand Bardamu et San Antonio, mes copains de voyage.

Bibliography

[AGH] P. Atela, C. Golé, and S. Hotton. http://math.smith.edu.phyllo.

[AL92] J.E. Avron and D. Levine. *Phys. Rev. Lett.*, **69**(1):208, 1992.

[ÁLOC04] E. Álvarez-Lacalle, J. Ortín, and J. Casademunt. *Phys. Rev. Lett.*, **92**(5):54501–4, 2004.

[AV00] H. Aref and D. Vainchtein. *Phys. Fluids*, **12**, 2000.

[BCT+95] G.D. Burnett, J.J Chac, W.Y. Tam, R.M.C. de Almeida, and M. Tabor. *Phys. Rev. E*, **51**:5788, 1995.

[Ber99] V. Bergeron. *J. Phys.: Condens. Matter*, **11**:R215, 1999.

[BM98] K. Brakke and F. Morgan. *J. Geom. Anal.*, **8**(5):749–768, 1998.

[BM02] K.A. Brakke and F. Morgan. *Eur. Phys. J. E*, **9**:453–460, 2002.

[Boh93] S. Bohn. *Eur. Phys. J. E*, **11**:177–189, 1993.

[Bra92] K. Brakke. *Exp. Math.*, **1**(2):141–165, 1992.

[Bre61] F.P. Bretherton. *J. Fluid Mech.*, **10**:16, 1961.

[CDK04] I. Cantat, R. Delannay, and N. Kern. *Europhys. Lett.*, **65**:726, 2004.

[CF98] Paul Concus and Robert Finn. *Phys. Fluids*, **10**(1):39–43, 1998.

[CG03] S.J. Cox and F. Graner. *Phil. Mag.*, **83**:2573–2584, 2003.

[CG04] S.J. Cox and F. Graner. *Phys. Rev. E*, **69**:31409, 2004.

[CGV+03] S.J. Cox, F. Graner, M.F. Vaz, C. Monnereau-Pittet, and N. Pittet. *Phil. Mag.*, **83**:1393–1406, 2003.

[CR04] A. Cañete and M. Ritore. *Ind. Univ. Math. J.*, **53**(3):883–904, 2004.

[CWV02] S.J. Cox, D. Weaire, and M.F. Vaz. *Eur. phys. J. E*, **7**:311–315, 2002.

[DCM87] B.V. Derjaguin, N.V. Churaev, and V.M. Muller. *Surface Forces.* Consultants Bureau, New York, 1987.

[DFN92] B.A. Dubrovin, A.T. Fomenko, and S.P. Novikov. *Modern geometry – methods and applications. Part 1. The geometry of surfaces, transformation groups, and fields.* Springer-Verlag, Berlin, 1992. §§ 5, 8 & 15.

[dGBWQ02] P.G. de Gennes, F. Brochard-Wyart, and D. Quéré. *Gouttes, bulles, perles et ondes.* Belin, Paris, 2002.

[DWC04] W. Drenckhan, D. Weaire, and S.J. Cox. *Eur. J. Phys.*, **25**(3):429–438, 2004.

[EBdMS99] F. Elias, J.C. Bacri, H. de Mougins, and T. Spengler. *Phil. Mag. Lett.*, **79**:389–397, 1999.

[EDC+98] F. Elias, I. Drikis, A. Cebers, C. Flament, and J.C. Bacri. *Eur. Phys. J. B*, **3**, 1998. 203-209.

[EFB+97] F. Elias, C. Flament, J.C. Bacri, O. Cardoso, and F. Graner. *Phys. Rev. E*, **56**:3310, 1997.

[FAB+93] J. Foisy, M. Alfaro, J. Brock, N. Hodges, and J. Zimba. *Pacific J. Math.*, **159**(1):47–59, 1993.

[Fom90] A.T. Fomenko. *The Plateau problem.* Gordon and Breach, 1990.

[FR01] M.A. Fortes and M.E. Rosa. *J. Coll. Interf. Sci.*, **241**:205, 2001.

[FRVT04] M.A. Fortes, M.E. Rosa, M.F. Vaz, and P.I.C. Teixeira. *Eur. Phys. J. E*, **15**:395–406, 2004.

[FT01] M.A. Fortes and P.I.C. Teixeira. *Eur. Phys. J. E*, **6**:255–258, 2001.

[Fu88] T. Fu. Master's thesis, Trinity College, Dublin, 1988.

[FW92a] F.Boltom and D. Weaire. *Phil. Mag. B*, **65**:473–487, 1992.

[FW92b] F.Boltom and D. Weaire. *Phil. Mag. B*, **63**:795, 1992.

[GAG90] J.A. Glazier, M.P. Anderson, and G.S. Grest. *Phil. Mag. B*, **62**:615, 1990.

[GGS87] J.A. Glazier, S.P. Gross, and J. Stavans. *Phys. Rev. A*, **36**:306, 1987.

[GJJF01] F. Graner, Y. Jiang, E. Janiaud, and C. Flament. *Phys. Rev. E*, **63**:011402, 2001.

[Gla89] J.A. Glazier. PhD thesis, University of Chicago, 1989.

[Gla93] J.A. Glazier. *Phys. Rev. Lett.*, **70**:2170, 1993.

[GPG+95] J.A. Glazier, B. Prause, C.P. Gonatas, J.S. Leigh, and A.M. Yodh. *Phys. Rev. Lett.*, **75**:573, 1995.

[Gra02] F. Graner. Two-dimensional fluid foams at equilibrium. In *LNP 600*, pages 178–211. Springer-Verlag, Berlin Heidelberg, 2002.

[GS89] J.A. Glazier and J. Stavans. *Phys. Rev. A*, **40**:7398, 1989.

[GW92] J.A. Glazier and D. Weaire. *J. Phys.: Condens. Matter*, **4**:1867–1894, 1992.

[Hal01] T.C. Hales. 2001. lanl.arxiv.org/pdf/math.MG/9906042.

[HDPF+00] G.B. Han, A. Dussaud, B. Prunet-Foch, A.V. Neimark, and M. Vignes-Adler. *J. Non-Equilib. Thermodyn.*, **25**:325–335, 2000.

[HKKS01] S. Hilgenfeldt, A.M. Kraynik, S.A. Koehler, and H.A. Stone. *Phys. Rev. Lett.*, **86**:2685, 2001.

[HKRS04] S. Hilgenfeldt, A.M. Kraynik, D.A. Reinelt, and J.M. Sullivan. *Eur. Phys. Lett.*, **67**:484, 2004.

[HM05] A. Heppes and F. Morgan. *Phil. Mag.*, 2005. math.MG/0406031.

[HMRR00] M. Hutchings, F. Morgan, M. Ritoré, and A. Ros. *Electron. Res. Announc. Amer. Math. Soc.*, **6**:45, 2000. http://www.ugr.es/ritore/bubble/bubble.htm.

[Hut97] M. Hutchings. *J. Geom. Anal.*, **7**:285, 1997.

[IIM85] H. Imai, M. Iri, and K. Murota. *SIAM J. Comput.*, **14**:93, 1985.

[Jea84] R.V. Jean. *Mathematical Approach to Patterns and Forms in Plant Growth.* Wiley, 1984.

[Kel87] W. Thompson (Lord Kelvin). *Phil. Mag.*, **24**:503–514, 1887.

[KHS00] S.A. Koehler, S. Hilgenfeldt, and H.A. Stone. *Langmuir*, **16**:6327, 2000.

[KRvS04] A.M. Kraynik, D.A. Reinelt, and F van Swol. *Phys. Rev. Lett.*, **93**:8301–8304, 2004.

[KWM+04] N. Kern, D. Weaire, A. Martin, S. Hutzler, and S.J. Cox. *Phys. Rev. E*, **70**:41411, 2004.

[mat] http://mathworld.wolfram.com/Sphere-SphereIntersection.html.

[Mat46] E. Matzke. *Am. J. Botany*, **33**:58, 1946.

[MO03] M. Mancini and C. Oguey. *Star-triangle equivalence in two-dimensional soap froths. Phil. Mag. Lett.*, **83**:643–649, 2003.

[MO05a] M. Mancini and C. Oguey. *Equilibrium conditions and symmetries for foams in contact with solid surfaces. Col. Surf. A*, 263:33–38, 2005.

[MO05b] M. Mancini and C. Oguey. *Foams in contact with solid boundaries: Equilibrium conditions and conformal invariance. Eur. J. Phys. E*, 17:119–128, 2005.

[Mor98] F. Morgan. *Riemannian geometry : a beginner's guide*. A.K. Peters, Wellesley, MA, 1998.

[Mor00] F. Morgan. *Geometric Measure Theory: A Beginners Guide, third ed.* Academic Press Inc., San Diego, CA, 2000.

[Mou93] C. Moukarzel. *Physica A*, **199**:19, 1993.

[Mou97] C. Moukarzel. *Phys. Rev. E*, **55**:6866–6880, 1997.

[MS05] J.M. Di Meglio and T. Senden. 2005. in preparation.

[Mul56] W. W. Mullins. *J. Appl. Phys.*, **27**:900, 1956.

[MVA98] C. Monnereau and M. Vignes-Adler. *Phys. Rev. Lett.*, **80**:5228, 1998.

[Neh52] Z. Nehari. *Conformal Mapping*. New York, McGraw-Hill, 1952.

[OBS92] A. Okabe, B. Boots, and K. Sugihara. *Spatial tessellations. Concepts and Applications of Voronoi Diagrams*. Wiley, New York, 1992.

[PE96] R.K. Prudhomme and S.A. Khan (Editors). *Foams: Theory, Measurement, and Application*, volume Surf. Sci. Ser., Vol. **57**. Marcel Dekker, New York, 1996.

[PGL93] P. Peczak, Gary S. Grest, and Dov Levine. *Phys. Rev. E*, **48**:4470, 1993.

[Pie89] P. Pieranski. *Phase Transitions in Soft Condensed Matter, Vol. 211 of NATO Advanced Study Institute, Series B: Physics*. New York, 1989. Plenum.

[Pla73] J.A.F. Plateau. *Statique expérimentale et théorique des liquides soumis aux seules forces moléculaires*. Gauthier-Villars, Paris, 1873.

[RBR01] D. Reinelt, P. Boltenhagen, and N. Rivier. *Eur. Phys. J. E*, **4**:299–304, 2001.

[RP96] F. Rothen and P. Pieranski. *Phys. Rev. E*, **53**:2828–2842, 1996.

[RPRJ93] F. Rothen, P. Pieranski, N. Rivier, and A. Joyet. *Eur. J. Phys.*, **14**:227, 1993.

[RRED99] N. Rivier, D. Reinelt, F. Elias, and C. Vanden Driessche. In D. Weaire and J. Banhart, editors, *Proceedings of the International Workshop on Foams and Films, Leuven (Belgium), 5-6 March 1999*. Verlag MIT publish, 1999.

[SG89] J. Stavans and J.A. Glazier. *Phys. Rev. Lett.*, **62**:1318, 1989.

[Sir94] C. Sire. *Phys. Rev. Lett.*, **72**(3):420, 1994.

[SJG05] S.J. Cox S. Jurine and F. Graner. *Col. Surf. A*, 2005. In Press, Corrected Proof, Available online 26 February 2005.

[SMD03] Cox S.J., Vaz M.F., and Weaire D. *Eur. phys. J. E*, **11**:29–35, 2003.

[Spi79] M. Spivak. *A Comprehensive Introduction to Differential Geometry*. Number HoustonPublish or perish. Publish or perish, Houston, 1979.

[Sta90] J. Stavans. *Phys. Rev. A*, **42**:5049, 1990.

[Tay76] J.E. Taylor. *Ann. of Math.*, **1003**:489–539, 1976.

[TF05] P.I.C. Teixeira and M.A. Fortes. *J. Phys. Condens. Matter*, **17**:2327–2339, 2005.

[vDH03] A. van Doornum and S. Hilgenfeldt. 2003. preprint, private comunication.

[VF01] M.F. Vaz and M.A. Fortes. *J. Phys.: Condens. Matter*, **13**:1395–1411, 2001.

[VL01] N. Vandevalle and J.F. Lentz. *Phys. Rev. E*, **64**:21507, 2001.

[VLDB01] N. Vandevalle, J.F. Lentz, S. Dobolo, and F. Brisbois. *Phys. Rev. Lett.*, **86**:179, 2001.

[vN52] J. von Neumann. *Metal Interfaces*. American Society for Metals, Cleveland, OH, 1952. p.108.

[WB90] D. Weaire and F. Boltom. *Phys. Rev. Lett.*, **65**:3449, 1990.

[WCG02] D. Weaire, S.J. Cox, and F. Graner. *Eur. Phys. J. E*, **7**:123–7, 2002.

[Wea99] D. Weaire. *Phil. Mag. Lett.*, **79**:491–495, 1999.

[WG93] D. Weaire and J.A. Glazier. *Philos. Mag. Lett.*, **68**(6):363, 1993.

[WH99] D. Weaire and S. Hutzler. *The physics of foams*. Clarendon Press, Oxford, 1999.

[Wic02] W. Wichiramala. PhD thesis, University of Illinois, Urbana-Champaign, 2002.

[Wil96] T.J. Willmore. *Riemannian geometry*. Clarendon Press, Oxford, 1996.

[WP94] D. Weaire and R. Phelan. *Phil. Mag. Lett.*, **69**:107–110, 1994.

[WP96] D. Weaire and R. Phelan. *J. Phys.: Condens. Matter*, **8**:L37–L43, 1996.

[WR84] D. Weaire and N. Rivier. *Contemp. Phys.*, **25**:59, 1984.